

Universidad EAFIT

Contribution of the conditioning stage to the Total Harmonic Distortion in the Parametric Array Loudspeaker

Andrés Yarce Botero

Thesis to apply for the title of Master of Science in Applied Physics

Advisor

Olga Lucia Quintero. Ph.D.

Master of Science in Applied Physics

Science school

Universidad EAFIT

Medellín - Colombia

2017

Contents

| | | |
|----------|---|-----------|
| 1 | Problem Statement | 7 |
| 1.1 | On sound artistic installations | 8 |
| 1.2 | Objectives | 12 |
| 1.2.1 | General Objective | 12 |
| 1.2.2 | Specific Objectives | 12 |
| 1.3 | Theoretical background | 13 |
| 1.3.1 | Physics behind the Parametric Array Loudspeaker | 13 |
| 1.3.2 | Maths behind of Parametric Array Loudspeakers | 19 |
| 1.3.3 | About piezoelectric ultrasound transducers | 21 |
| 1.3.4 | About the health and safety uses of the Parametric Array Loudspeaker Technology | 24 |
| 2 | Acquisition of Sound from self-demodulation of Ultrasound | 26 |
| 2.1 | Acoustics | 26 |
| 2.1.1 | Directionality of Sound | 28 |
| 2.2 | On the non linearity of sound | 30 |
| 2.3 | On the linearity of sound from ultrasound | 33 |
| 3 | Signal distortion and modulation schemes | 38 |
| 3.1 | Introduction | 38 |
| 3.2 | On Total Harmonic Distortion | 40 |
| 3.3 | Effects on total harmonic distortion: Modulation techniques | 42 |
| 3.4 | On Pulse Wave Modulation | 46 |
| 4 | Loudspeaker Modelling by statistical design of experiments. | 49 |
| 4.1 | Characterization Parametric Array Loudspeaker | 51 |
| 4.2 | Experimental setup | 52 |
| 4.2.1 | Results of PAL radiation pattern | 53 |
| 4.3 | Design of experiments | 56 |
| 4.3.1 | Placket Burmann method | 59 |
| 4.3.2 | Box Behnken methodology | 62 |
| 5 | Digital filtering techniques and signal distortion analysis. | 66 |
| 5.1 | Chirp signal analysis | 66 |
| 5.1.1 | Digital filter analysis | 69 |
| 5.1.2 | Measurements of the harmonic content of a signal | 73 |
| 6 | Conclusions | 76 |
| 7 | Acknowledgements | 78 |

List of Figures

| | | |
|------|--|----|
| 1.1 | Design and construction of <i>The Soundhouse</i> | 8 |
| 1.2 | <i>The SoundHouse</i> , Marco Alunno 2015 | 9 |
| 1.3 | The Forest and the Shadows projection | 10 |
| 1.4 | <i>The Forest of the Shadows</i> , Marco Alunno 2016 | 11 |
| 1.5 | Linear velocity acoustic dependence of temperature | 14 |
| 1.6 | Deformation of a sinusoidal wave (black) into a sawtooth wave (red) due to local changes of speed during sound propagation | 14 |
| 1.7 | Common signals and harmonic contents | 15 |
| 1.8 | Audible frequency by-product [1] | 16 |
| 1.9 | Byproducts production due to the modulation of ultrasound in air | 16 |
| 1.10 | Low frequency wave generation | 17 |
| 1.11 | Complete schematic operation PAL | 18 |
| 1.12 | Constitutive equation to the KZK | 19 |
| 1.13 | Soundlazer array | 22 |
| 1.14 | Components of the PZT transducer and cone to couple the impedance [2] | 23 |
| 1.15 | Cavities configuration to modify the frequency response of the PVDF transducer [3] | 23 |
| 1.16 | Attenuation Characteristics of Sound Pressure by Distance | 24 |
| 2.1 | Conical structures used to route the sound | 28 |
| 2.2 | Commercial Sound Dome | 29 |
| 2.3 | Other techniques to enrout sound | 29 |
| 2.4 | Two-Frequency mutual interaction in a nonlinear medium | 30 |
| 2.5 | First Parametric Array Loudspeaker Yoneyama | 31 |
| 2.6 | Commercial Parametric Loudspeakers | 32 |
| 2.7 | Close difference frequency wave addition | 34 |
| 2.8 | Moiré pattern example | 35 |
| 2.9 | Monaural and Binaural beats | 35 |
| 2.10 | Graphical interpretation of a Linear and a Non linear system | 37 |
| 3.1 | Common frequency spectrum of a signal | 39 |
| 3.2 | Effect on the harmonic content of a signal caused for a Non Linear medium transformation | 39 |
| 3.3 | Frequency spectrum Audiospot AS-24 <i>The Soundhouse</i> | 41 |
| 3.4 | Frequency spectrum Soundlazer Parametric Pro amp kit <i>The Forest and the Shadows</i> | 41 |
| 3.5 | Pre-Distortion processing | 43 |
| 3.6 | Comparison between the SRAM and the SBSAM | 45 |
| 3.7 | PWM Output voltage frequency relation | 47 |
| 4.1 | Cycle of the Design of Experiment methodology | 50 |
| 4.2 | Soundlazer model SL-01 | 51 |
| 4.3 | Electronic Schematic of the Soundlazer SL-01 | 52 |
| 4.4 | Experimental setup for the radiation pattern characterization of the Loudspeaker | 53 |
| 4.5 | Soundlazer SL-01 sound field characterization | 54 |

| | | |
|------|--|----|
| 4.6 | Testing of two microphones to choose the more appropriate one | 55 |
| 4.7 | Controllable and non controllable factors for the DOE proposed | 56 |
| 4.8 | Sigmastudio [™] digital signal processing stages | 57 |
| 4.9 | Schematic Design of Experiment to measure the THD and the fundamental Intensity of the Parametric Array Loudspeaker | 58 |
| 4.10 | Precondition stage DSP | 58 |
| 4.11 | Plackett Burmann second experiment, Response THD | 61 |
| 4.12 | Plackett Burmann response for the analysis of the fundamental | 61 |
| 4.13 | Surface response plots of 3-factor Box Behnken analysis | 64 |
| 4.14 | Contour plot of surface response | 65 |
| 5.1 | Chirp Signal tested in the PAL | 67 |
| 5.2 | GUI Interface for the signal analysis | 67 |
| 5.3 | Time-dependent spectra of Chirp demodulated signal from Soundlazer PAL | 68 |
| 5.4 | Time spectra of linear chirp signal demodulated 0-4500 Hz | 69 |
| 5.5 | Software Designed Band-Pass filters | 70 |
| 5.6 | Chime signal after and before filtered | 71 |
| 5.7 | Band-Pass filter log chime signal | 72 |
| 5.8 | Periodogram power spectrum 400 Hz | 73 |
| 5.9 | THD and five first harmonics | 74 |
| 5.10 | Signal to Noise Ratio 400 Hz | 74 |
| 5.11 | Signal noise + distortion | 75 |
| 7.1 | R Code for the Plackett Burmann Design | 89 |
| 7.2 | R Code for the Box Behnken Design | 90 |
| 7.3 | Box Behnken THD response Summary R | 91 |
| 7.4 | Box Behnken Fundamental response Summary R | 91 |
| 7.5 | Harmonic Distortion 800 Hz signal self-demodulation analysis | 92 |
| 7.6 | Harmonic Distortion 1200 signal Hz self-demodulation analysis | 93 |
| 7.7 | Harmonic Distortion 1600 Hz signal self-demodulation analysis | 94 |
| 7.8 | Harmonic Distortion 2000 Hz signal self-demodulation analysis | 95 |
| 7.9 | Harmonic Distortion 2400 Hz signal self-demodulation analysis | 96 |
| 7.10 | Harmonic 3000 Hz Distortion Analysis | 97 |
| 7.11 | Harmonic 3400 Hz Distortion Analysis | 98 |

Glossary

- PAL - Parametric Array Loudspeaker: Technology that uses ultrasound modulated waves to generate directionally projected sound zones. In other documents it refers to these as well as Parametric Acoustic Arrays (PAA).
- THD - Total Harmonic Distortion: Parameter used to define the output audio signal in relation to the input. Distortion is the name given to anything that alters a real input signal in any way other than changing its magnitude.
- DSP - Digital Signal Processing: Numerical manipulation of signals to modify its content in some sense, performing a wide variety of signal processing operations.
- DFT - Discrete Fourier Transforms: Technique to obtain by decomposing a sequence of values from a signal into components of different frequencies.
- FFT - Fast Fourier Transform: Algorithm that computes the Discrete Fourier Transform.
- NLS - Non-Linear System: System in which the output is not directly proportional to the input, Systems in which the effect of the external factors is not purely additive
- THD+N - Total Harmonic Distortion + Noise: Instead of measuring individual harmonics this test measures everything added to the input signal. Everything that comes out of the unit that is not the pure test signal is measured and included: Harmonics, Hum, Noise, RFI, Buzz.
- DUT - Device Under Test: It is used to reference the system to be analyzed in the audio measurement.
- SNR - Signal to Noise Ratio: Ratio of the power of the fundamental to the power of all non-harmonic content.
- SINAD - Signal to Noise and Distortion Ratio: Measure of the quality of a signal concerning perturbations like the noise and the distortion
- PVDF - Polyvinylidene Fluoride: piezoelectric polymeric films
- PZT - Lead Zirconate Titanate: Ceramic ultrasonic transducers
- SPL - Sound Pressure Level: Sound pressure expressed as a logarithmic decibel scale, ratio between the actual pressure level and a fixed reference pressure
- RMS - Root Mean Square: Square root of the average of values over a period of the signal
- KZK - Kokhlov-Zabolotskaya-Kuznetsov: Wave equation used for modeling PAL behavior, includes diffraction, dissipation, and non-linear contribution terms
- AM - Amplitude Modulation: Technique of modulation where the waveform transmitted varies the carrier wave in proportion to amplitude (signal strength)

- DOE - Design Of Experiments: Statistical methodology for the construction of knowledge through the validation of conjectures
- PWM- Pulse Width Modulation: Technique to modulate or encode a message into a pulsating signal.
- Amplitude of signal - Amplitude refers to the voltage or current level of signals at a given frequency. In a Fourier transform, the amplitude relates to the height of the histogram in that particular frequency bin. Power can also be used to describe the level of a given frequency or an integration of amplitudes over a given frequency range.
- Fundamental Frequency - Also known as the carrier frequency, the fundamental frequency is the lowest frequency component of a periodic signal. In an ideal Fourier transform of a sine wave, only the fundamental frequency would appear. Most of the specifications below are generated using an almost perfect sine wave.
- Harmonics - Harmonics, or harmonic frequencies, are frequencies that are integer multiples of the fundamental frequency. Harmonics are often not part of the actual signal but appear due to Nyquist sampling effects and transmission line reflections.
- Spurs - Spurs, also known as device Spurs, are frequency components that appear in signals because of the electrical elements of the instrument. Some examples of spurs are interleaving anomalies in analog-to-digital converters (ADCs), leakage of oscillator clock signals, and power inserted by amplifiers.
- Noise - All voltage and frequency components that are not present in the actual or ideal signal, spurs, or harmonics, but are present in the measurement or generation of test signals, are noise. Some common causes of noise are electromagnetic fields, temperature, and ground loops. The noise floor is the maximum Fourier transform amplitude of any noise in the device's frequency range.

Chapter 1

Problem Statement

This thesis deals with the technology of Parametric Array Loudspeakers (PAL). This technology refers to the physical propagation phenomena of directional sound waves modulated over an ultrasonic carrier used to generate directionally projected sound zones. The development of this work arises because of an interest of the Ph.D. in Musical Composition Marco Alunno from the Music Department at Universidad EAFIT. In the year 2014 Marco was interested in the possibility to apply the technology of directional ultrasound speakers in acoustic artistic installations to use its properties in the composition of new pieces of music and explore new sound technologies. The idea of professor Marco was to investigate new perceptions of sound exploiting the unique characteristics that the PAL provides. The author started working with him as a research assistant in early 2015.

This phenomenon has two significant limitations. The first is a technical parameter known as Total Harmonic Distortion (THD) used to define the proportionality of the audio output of a system with the audio input. THD makes reference to the amount of harmonic content introduced to the signal. The second limitation is the inherent impossibility of reproduction of low frequencies. As a result, to reproduce perceptible low frequencies, it is necessary to use high amplitudes of the primary ultrasound wave. For artistic applications purposes and playback of music, these limitations become a turning point in the practical use of this kind of speakers.

This work focuses on these limitations in order to understand, with the specific PAL used, how the THD affects the audible perception field and how the demodulation of the ultrasound in the air affects the perceived intensity of the fundamental. Specifically, it seeks to understand how the conditioning stage of the signal in the DSP affects these parameters. In the development of this work, we put more attention to the conditioning stage of the signal intending to know what are the more active parameters that have an influence on the output characteristics of interest to be measured.

The present work is developed in one of the research lines of GRIMMAT, specifically in the area of Control and Systems (Analysis and Digital Signal Processing). This research group has experience in areas such as manipulation of signals for emotion recognition, pattern identification, Electroencephalography (EEG) signal identification, the design of filter banks, Integral Transform applied to signals, Image analysis, among others. This work contributes to some of these areas, specifically in the application of filter techniques of one-dimensional signals, audio digital

processing techniques and the hardware involved in the production of sound. All the knowledge generated from this exploration aims to contribute to the artistic endeavors of Professor Marco Alunno supporting to the lines of research in signal processing of the research group.

As complementary work, which constitutes the motivation for doing this work, and a way to explore this technology, we carried out some artistic sound installations during 2015 and 2016 and these will be briefly explained in the following section as a contextualization of this thesis research.

1.1 On sound artistic installations

Parametric Loudspeakers are one of such new technologies that make possible to direct sound as though it were a light beam. Despite the fact that this technology is going its way in the commercial sector of advertising and information in museums and libraries there are actually few examples in art. One example we could find of a piece of art using directional sound is *A=P=P=A=R=I=T=I=O=N* by conceptual Welsh artist Cerith Wyn Evans, a sculpture that features 16 shiny metal discs hanging from the ceiling and gently swaying when people pass by. Some of these reflecting discs are custom-made Audio Spotlight® speakers by Holosonics that are used by Evans to reproduce a piece by UK experimental band Throbbing Gristle [4].

Another example is the work of Professor Marco Alunno called *The Soundhouse* in 2015, a sound installation with the shape of a lighthouse that pretends to be a metaphor of light through sound [5]. The Soundhouse attempted to concretize this concept by building an art object with an explicit reference to a lighthouse with a very similar function. As a sort of spotlight, the beam of a lighthouse crops a porthole out of the darkness; likewise, the rotating head of *The Soundhouse* projects a sonic space through a sound beam and, thus, reveals a concealed acoustic world, one that is usually suffocated by the constant, transversal noise of daily life.

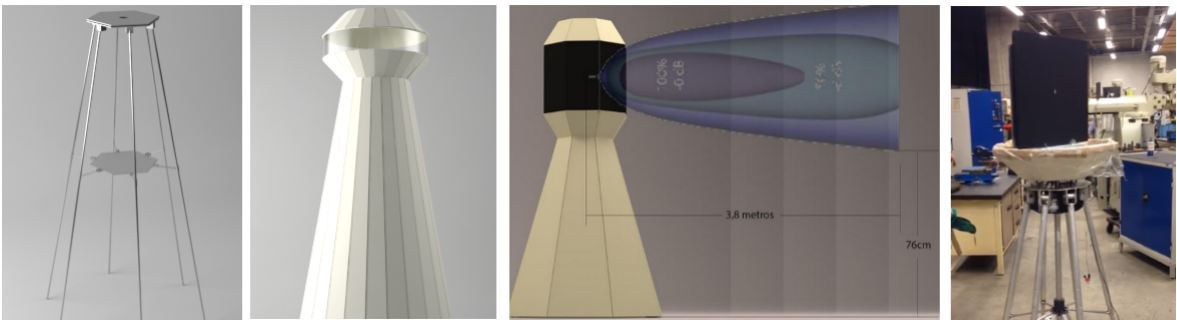


Figure 1.1: Design and construction of *The Soundhouse*

The Soundhouse installation ruminates on issues concerning sound perception and the responsible use of our sound environment. It is composed of two parts: the body and the rotating head. The body is an octagonal aluminum

stand with telescopic legs (i.e., four of which have wheels to move the installation conveniently). At the neck were placed the mechanical parts for the head's rotation: a reduction motor of 24 rpm reducer and a 20:1 speed reducer box to further slow down the rotation speed to 1.2 rpm. Ten octagonal aluminum shells that contain the loudspeaker form the head and eight rods that support the top shell. Concerning sound, the basic idea was to project an acoustic space opposed to the sound environment in which the installation was exhibited (i.e., for the prototype the contrast was urban vs. rural sounds).



Figure 1.2: *The SoundHouse*, Marco Alunno 2015

Another acoustic installation was *The Forest and the Shadows* (2016) [6], a collaborative effort between areas of Science, Engineering and Art in Universidad EAFIT. It consisted in a conceptual prototype composed of an array of microphones that record the audible sound field of a PAL to generate an interaction with a surround sound of a nature soundscape (i.e., the forest) in a visual projection. In this sound installation, the parametric speaker has again a major role emitting a reference sound to an eighth microphone array disposed opposite from it. The computer receives the signals and releases 8 sounds (i.e. emitted by two regular speakers) from each of eight different kinds of natural sounds and controls the 8 quadrants in which the video projected on the screen is divided. Each receiver acts as a trigger of various new sounds in the music composition and the image projection, allowing the interaction of the viewer with the work.

The Forest and the Shadows let the physical phenomena of sound from ultrasound interact in a multi-layer superposition of sounds and pictures aiming to be a reflection of light and sound. An array of microphones detects

several components of the demodulated sound perceived from a parametric array loudspeaker that interacts with the computer through Supercollider and Processing software introducing changes in the video and the audio profile of the room acoustic installation.

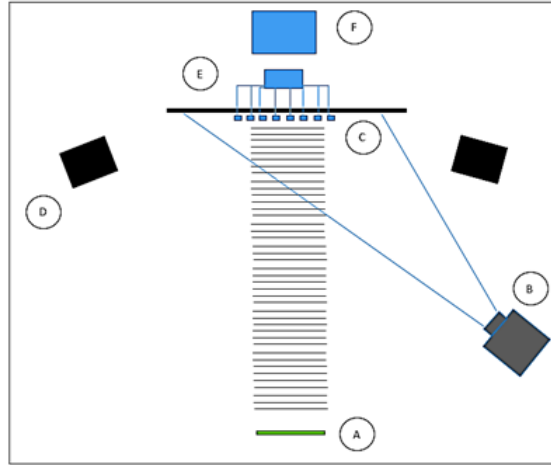
Figure 1.4 a) shows the final sound projection. Figure 1.4 b) shows the schematic operation of the sound installation. Figure 1.4 c) shows the array of microphones which detects the reference tone. The parts marked with (A), (B), (C), (D), (E) and (F), correspond to the SoundLazer SL-01 Ultrasonic Directional Loudspeaker, the Video Beam, the Array of Microphones, the Omni Directional Sound Loudspeaker, the MOTU DAC acquisition audio interface and the computer with Supercollider and Processing softwares respectively.

The software used to control the sound interaction was Supercollider, an environment, and programming language released in 1996 by James McCartney for real-time audio synthesis and algorithmic composition [7]. The SoundLazer Loudspeaker (Figure 1.4) emits a sound at a high frequency (19 kHz). The high frequency was chosen in order to minimize the frequency overlap with the frequencies of an audio composition because previously it was verified that the different banks of sounds had frequencies lower than 6 kHz. The microphones ((C) Figure 1.4) detect a sub-harmonic tone as the fundamental pitch in the range of 8 kHz; this was selected to be the pitch to be detected as a reference to the interaction. Interrupt the constant detection of the guide tone generate changes in the sound landscape emitted from the Omni-Directional Loudspeaker ((D) Figure 1.4) as in the audiovisual composition from the video Beam projection ((B) Figure 1.4).

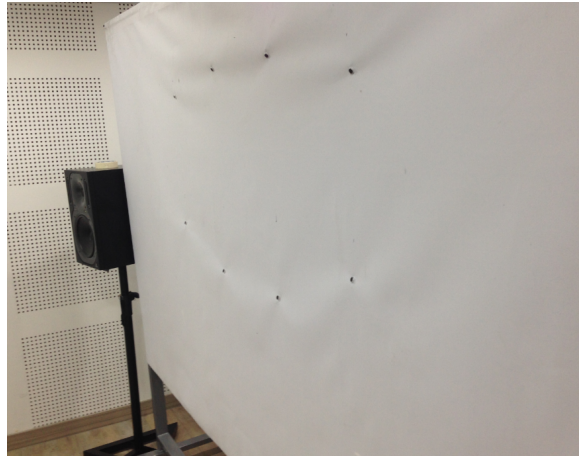


(a)

Figure 1.3: The Forest and the Shadows projection



(a) Schematic of the experimental setup



(b) Array of microphones for pitch detection of the reference tone

Figure 1.4: *The Forest of the Shadows*, Marco Alunno 2016

Proper use of PAL in art must start with investigating a whole array of different topics (i.e. non-linear acoustics, signal processing and ultrasonic transducers) to understand what this technology can offer to take advantage of its best aspects. Artistic installations that aim to make a proper use of parametric loudspeakers must start with a thorough understanding of how they work.

As follows we present the objectives of this thesis in order to contextualize the reader with the ultrasound phenomena.

1.2 Objectives

1.2.1 General Objective

Present and analyze the effects in Total Harmonic Distortion of sound produced in a directional parametric loudspeaker due to the digital processing stage and the self-demodulation process of the signal in the ultrasound field propagation through the use of a design of experiments methodology.

1.2.2 Specific Objectives

To acquire knowledge about the phenomenon of self-demodulation presented in this type of speakers due to air nonlinear behavior.

To describe modulation techniques that exist in parametric speakers and their effects on total harmonic distortion.

To design a methodology for experiments in order to verify what parameters in the pre conditioning stage are those who most have influence on the harmonic distortion of a parametric speaker.

To evaluate different digital filtering techniques to study how these contribute to the quality of sound produced by this type of speakers.

As follows a summary of the goals:

- First result section: The knowledge about the phenomenon of self-demodulation in this type of speakers due to nonlinear air behavior was acquired through a detailed state of the art literature review. In this chapter a discussion about the nature of the sound aims to clarify the nature of this kind of sound propagation, comparing it with the beating phenomena in acoustics and in optics and differing from this non linear interaction.
- Second result section: Existing modulation techniques used in parametric speakers, and their effects on total harmonic distortion are described in this chapter. This section contributes to the acquisition of the knowledge phenomena, understanding how modulation techniques affects in different proportions the harmonic distortion present in the self-demodulating beam of sound. Because the modulation scheme in our speaker was restricted to PWM, an analysis of this scheme and a discussion about the use of this speaker were made.
- Third result section: A statistical methodology for the design of experiments is presented to verify what parameters in the pre-conditioning stage are those who most have influence on the harmonic distortion and the perceived intensity of the fundamental. In this chapter the experiment is described and the characterization of the parametric loudspeaker of interest was carried out. Basically, a methodology of factor screening and a Surface Response Methodology is present to uncover the most active factors of an experiment.

- Fourth result section: As a first step to modeling the phenomenon in its linear regime of sound production from ultrasound, digital filtering techniques were studied to identify how they contribute to the quality of sound produced by this type of speakers. The analysis of different signals filtered before being reproduced by the speaker and after the self demodulation was done. In this section some measures concerning the harmonic content of a signal are shown.

1.3 Theoretical background

This theoretical framework gives basic notions of ultrasound physics: The first part shows the physical concepts that govern the phenomenon of sound generation from ultrasound. The second part describes the mathematical background used to model the phenomenon, the third part deals with the principal ultrasound transducers characteristics for this technology, the fourth part exposes the measures used to characterize the harmonic content of the signal.

1.3.1 Physics behind the Parametric Array Loudspeaker

Theories that explain the operation of this speakers are in the field of non-linear acoustics, branch of acoustics dealing with sound waves of sufficiently large amplitudes. As a first convenient approach to understand this phenomenon lets start with the acoustic wave equation:

$$\nabla^2 P(r, t) = \frac{1}{c^2} \frac{\partial^2 P(r, t)}{\partial t^2} \quad (1.1)$$

Here the amplitude of pressure of the acoustic field P , expressed in a general form, is operated by the Laplacian ∇^2 and is directly proportional to the second derivative of the same field with respect to time t and inversely proportional to the squared of the speed of sound. The way the energy propagates in space is modeled according to the reference system and the resulting shape taken by the Laplace operator (e.g. spherical, cartesian, cylindrical, etc.). The equation 1.1 is a simple wave equation form pretending that the medium is isotropic, which means that there are no variations of magnitudes (e.g. average density, temperature, and local pressure) along with all axes, and the speed of sound is assumed to be constant. In the real world, changes in density, temperature (Figure 1.5) and local pressure are present affecting the speed of sound (i.e. the sound velocity where the acoustic pressure is higher is different from the phase velocity of the wave). The term c depends on the Bulk Modulus B (i.e. which depends on pressure and temperature) and on the mass density ρ of the air by the following relation:

$$c = \sqrt{\frac{B}{\rho}} = \sqrt{\frac{\gamma RT}{M}} \quad (1.2)$$

Where γ is the adiabatic index or heat capacity ratio for the air, R is the universal gas constant. M is the average molecular mass of air and T is the absolute temperature on the Kelvin scale. It is important to know that the wave equation in this form is an idealized description of what happens when energy is propagated. This equation describes the propagation of a vibrational disturbance in a medium after a certain pressure is imposed on it. If the medium is not ideal, different characteristics affect the propagation, also if the amplitudes of the waves are high. for example Figure (1.5) shows the dependence with the temperature of the sound velocity in air:

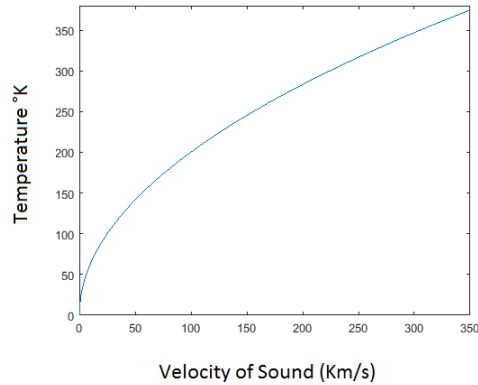


Figure 1.5: Linear velocity acoustic dependence of temperature

When the propagated wave experiences speed variations at different parts of the wave, the pattern changes progressively, the black pattern in Figure (1.6) represents a wave that is not distorted, and the red one shows a distorted wave. The points with high pressure (Crest) travel more rapidly than points with less pressure (Valleys) that displace more slowly. The profile is getting abruptly distorted seeming to a sawtooth wave profile. This is known as a self-distortion behavior of the wave pattern.

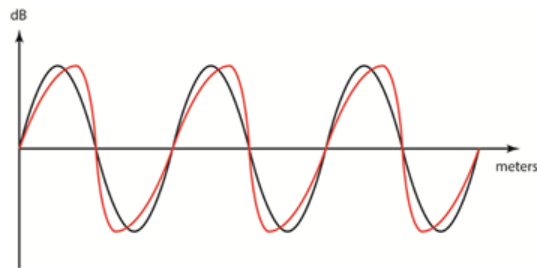


Figure 1.6: Deformation of a sinusoidal wave (black) into a sawtooth wave (red) due to local changes of speed during sound propagation

As a consequence of such non-linear behavior, harmonics start appearing as an effect of the waveform alteration of its sinusoidal shape [8]. When the wave gets distorted, the frequency profile manifests different harmonic content; the next figure shows different waves with its respective harmonic content. Notice that the ideal sine wave only has one peak in the frequency space, and the sawtooth wave has several harmonics.

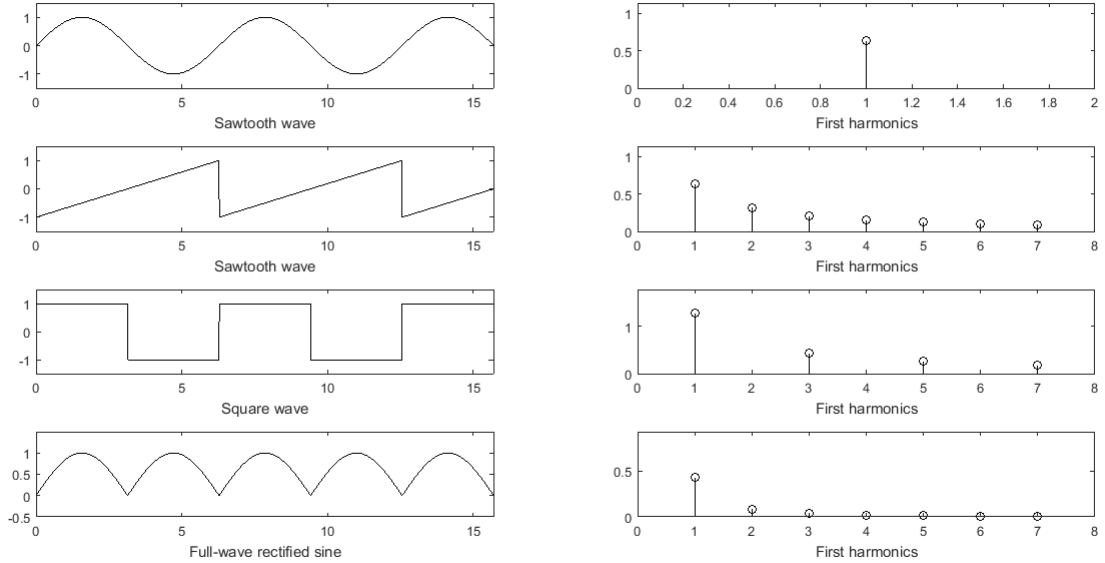


Figure 1.7: Common signals and harmonic contents

This non-linear phenomenon makes possible the generation of desired distortion components, that is practically the reason of how this technology works. The production of the audible harmonic content from the non-audible frequency range is known as a byproduct from the interaction of an Amplitude Modulated (AM) wave. AM is a modulation technique where the amplitude (signal strength) of the carrier wave is varied in proportion to the waveform transmitted. The audio waveform modifies the amplitude of the carrier wave and determines the envelope of the waveform. In the Figure (1.8) from the work of Ju et al. [1], a 1 kHz frequency component with its respective harmonic at 2 kHz is shown as a consequence of the interaction with the medium of the frequency component at 40 kHz.

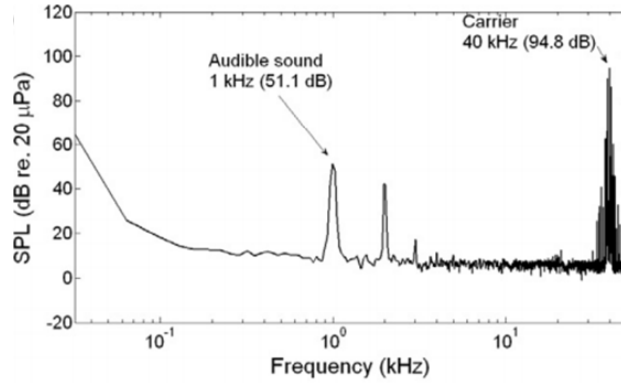
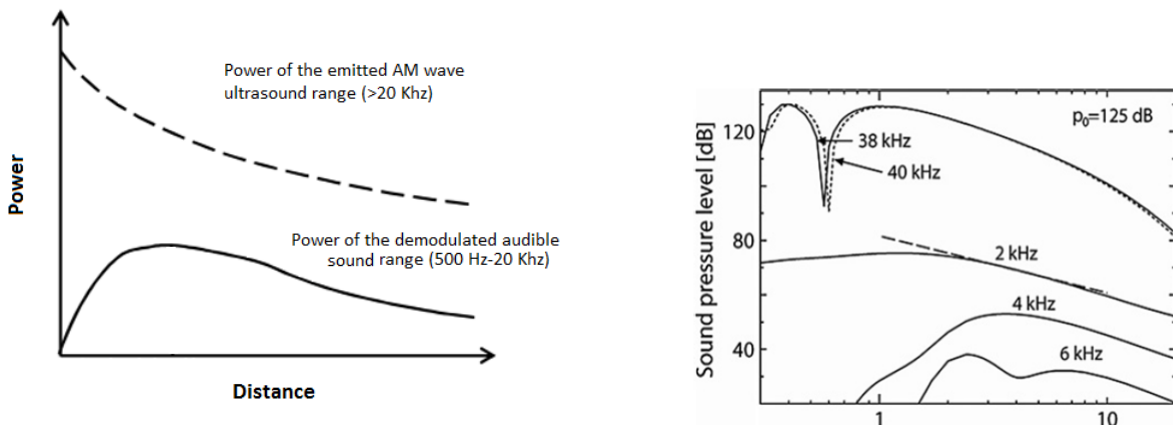


Figure 1.8: Audible frequency by-product [1]

The amplitude of the primary ultrasound wave must be higher than that in the demodulated audible wave (Figure 1.9a). Note that a high intensity is required for the ultrasound signal to generate audible sound. Figure 1.9b shows the by-products generated from two ultrasound waves of 38 kHz and 40 kHz. A frequency tone of 2 kHz is generated and two of its respective harmonics are shown. The audible intensity is much lower (1.9b). The larger the amplitude of the primary wave the more noticeable will be the audible by-product but, there is a compromise between this magnitude, the safe limit exposition to the ultrasonic wave and the distortion of the audible content perceived. By-products result from the self-demodulation due to the self-distortion of the wave because to the nonlinear behavior of air. This behavior is attributed to the self-demodulation phenomena acting as a high pass filter with a 12 dB/octave gain [9].



(a) Power of the emitted AM wave and the demodulated audible sound

(b) By products audible content [10]

Figure 1.9: Byproducts production due to the modulation of ultrasound in air

The following image (Figure 1.10) was taken from the Introductory lecture on the non-linear acoustics of Professor Vincent Tournat 2014 [11]. It shows how, from the interaction in the media, two primary high-frequency waves make possible the generation of a low-frequency wave in the path. The carrier has a much higher sound level and also decays faster than the demodulated tones. The ultrasonic waves are sent from the transducer causing the effect of sound directivity.

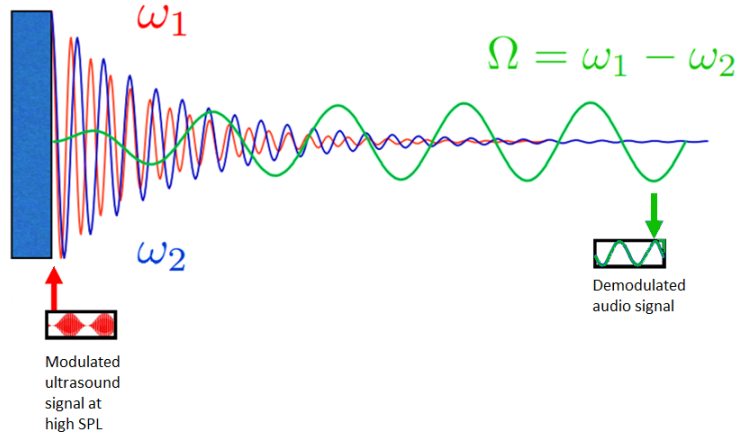


Figure 1.10: Low frequency wave generation

Let us see in detail, now, how the whole process of producing audible signals from ultrasonic carriers works.

Figure (1.11) shows two major stages, one before and one after the ultrasonic emitter (i.e. the heavy-bordered box in the diagram). The former reproduces the processing circuit and includes the DSP, the amplifier and the ultrasonic transmitter itself, while the latter describes the demodulation effect occurring in the air [12]. Once a signal in the audible range enters the DSP, it goes through a series of pre-processing steps that make it 'suitable' for being correctly demodulated. The dynamic range controller compresses and limits the input signal, and then the distortion processor reduces the level of Total Harmonic Distortion (THD) by anticipating the non-linear characteristics of the medium. Eventually, the original signal modulates the ultrasonic carrier through one of the modulation schemes. Now the new wave is ready to be amplified before being sent to the emitters.

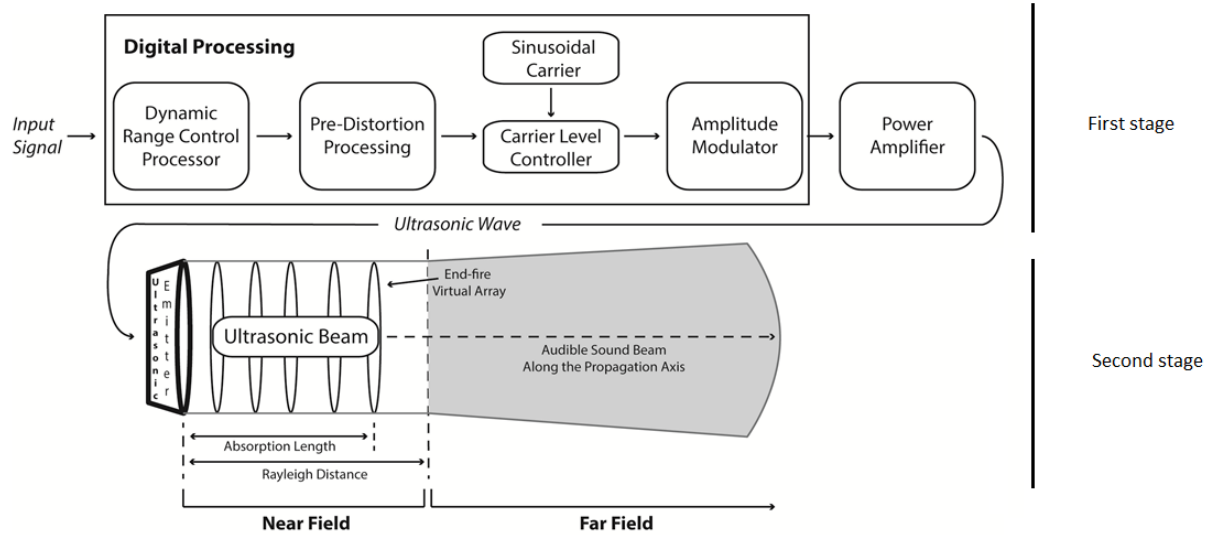


Figure 1.11: Complete schematic operation PAL

In front of the loudspeaker happens the generation of a series of virtual sound known as an end-fire array. The term end fire array comes from the antenna theory and describes a particular kind of emitters configuration used to maximize radiation along the main axis of the antenna, careful selection of the optimal numbers of elements with the appropriately related spacing creates a highly unidirectional antenna. That is how the ultrasound beam becomes the loudspeaker. The reflection of ultrasound conserves the directionality of ultrasound-modulated waves[1], this rebound of sound generates emission points which make it possible to produce the sensation that the sound is emanating from the direction where it bounces.

The propagation region is divided into two parts, the near field and the far field. The near field is defined from the transducers to the region in the propagation axis limited for the Rayleigh distance which we will explain later in the underlying physics chapter. In the near field is where the array of virtual sources is produced. In this region the intensity of the acoustic wave seems to stay constant along the propagation axis (even though the Sound Pressure Level increase in this region) contrary to the traditional non directional speakers where the intensity decrease with the ratio of the squared distance[13]. The second region of propagation is the Far field. In this region the ultrasonic wave it is being attenuated having less energy due to the absorption caused by the medium[14]. The intensity of the audible seems to propagate more as a conventional non directional speaker decreasing the intensity with the squared distance[15].

The absorption length indicates where the end-fire array terminates, while the Rayleigh distance shows how far non-linear effects of the medium are still working [13]. Within the Rayleigh range, both primary and secondary waves are produced [16]. Primary waves refer to the ultrasound modulated waves emitted, the secondary waves refer to the frequency audible wave self-demodulated. However, the former are completely absorbed before the end of the near field, whereas the latter keep propagating for a much longer stretch. An interesting effect yielded by the end-fire array

somehow contradicts what usually occurs with conventional omnidirectional loudspeakers. The average -6 dB slope per doubling distance due to a spherical expanding of the sound wave is now replaced with an increasing amplitude of the signal in the near field due to the summation of each virtual sources amplitude [17]. Moreover, while diverging from the propagation axis, the virtual sources go out of phase and act destructively. Therefore, secondary waves also manage to inherit the directional property of ultrasonic primary waves, thus giving to the demodulated beam the tightness familiar sound emitters cannot achieve.

Finally, notice that no frequency below 400 Hz will be reproduced by currently commercially available parametric loudspeakers [9]. According to Gan [12] the reason for this is the reduced volume of air molecules that the end-fire array of virtual audio sources is capable of moving. This is because the signal strength is determined by the number of the converted wavelengths within the Rayleigh distance. Whereas the large diaphragm of a conventional cone-based loudspeaker allows low audio frequencies by vibrating a wider portion of space, the intensities that low frequencies needs are not safe for human ears.

1.3.2 Maths behind of Parametric Array Loudspeakers

The equation that describes the behavior of acoustic waves like those emitted by a parametric loudspeaker is the KZK (Kokhlov-Zabolotskaya-Kuznetsov). This equation comes from relating the state equations, the continuity equation and the Euler equation for a differential test volume including the consideration of non-linear medium interaction.

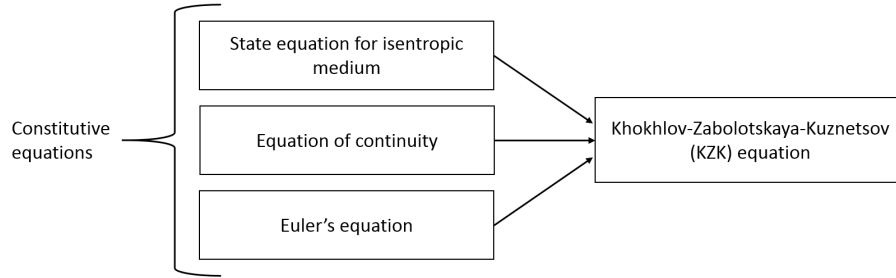


Figure 1.12: Constitutive equation to the KZK

KZK equation looks like:

$$\frac{d^2 P}{dz dt'} = \frac{c_o}{2} \nabla_T^2 P + \frac{\delta}{2c_o^3} \frac{\partial^3 P}{\partial t'^3} + \frac{\beta}{2\rho_o c_o^3} \frac{\partial^2 P^2}{\partial t'^2} + \sum_v \frac{c_v'}{c_o^2} \frac{\partial^2 P^2}{\partial t'^2} e^{-(t-t')/t_v} \quad (1.3)$$

Where P is the acoustic pressure, z the coordinate along the propagation axis, t is the delay time ($t' = t - z/c_o$), ρ_o the density of the medium of propagation, c_o is the speed of sound and β is the coefficient of non-linearity. The right hand side of KZK equation is composed of four terms: the first expresses the parabolic diffraction, the second the

dissipation, the third the non-linear contribution and the fourth is the term that makes reference to the relaxation effect of the medium. ∇_T^2 Is the Laplacian operator that operates in the plane perpendicular to the axis of propagation z ($\nabla_T^2 = \partial^2/\partial x^2 + \partial^2/\partial y^2$).

In general, when the wave cannot be considered plane and is necessary to take account the diffraction effect, considering that this could be seen as a “Transversal diffusion” of the field, the process which the energy scapes in the perpendicular direction of the wave acoustic propagation [18]. A relaxation time t_v characterizes each relaxation process v (where $v = 1, 2, \dots$) and a small manifestation of the increase of the speed of the sound c_v' ; the atmosphere can be modeled as a thermoviscous fluid with two relaxation processes [19]. Since KZK is derived under the parabolic approximation, we have to pay attention to its applicability; the paraxial region that is within 20 degrees from the z -axis restricts the upper limit of beam angle [17]. The dissipation term was introduced later by Kuznetsov who added the sound diffusivity δ to the originally lossless KZ equation. δ is related to the thermo-viscosity absorption of the medium and is defined by the following expression:

$$\delta = \frac{1}{\rho_o} \left(\frac{4}{3} \mu_s + \mu_B \right) + \frac{k}{p_o} \left(\frac{1}{c_v} - \frac{1}{c_p} \right) \quad (1.4)$$

where μ_s is the shear viscosity, μ_B is the bulk viscosity, k is thermal conductivity, c_v and c_p are specific heat at constant volume and pressure respectively. There is no explicit analytical solution of the KZK, although numerical methods such as frequency domain, time domain or time-frequency algorithm can be used to solve it [20]. This equation is a good approximation for directional sound beams for points near the axis. Also was mentioned that the usual method to solve it in an analytical way is called the quasi-linear approach [21], where two solutions are proposed. One relates the linear field that propagates setting the nonlinear coefficient β to zero and the other describes the nonlinear contribution solution found with the linear ultrasonic field as a source. In this method, two components make up the resulting acoustic field:

$$P = P_1 + P_2 \quad (1.5)$$

where the resulting pressure field assumed is P , P_1 is the solution to the ultrasonic field for the linear part including the absorption term of the KZK equation and the equation of the standard wave equation in their respective coordinates:

$$P_1 = \frac{c_o}{2} \nabla_T^2 P + \frac{\delta}{2c_o^3} \frac{\partial^3 P}{\partial t'^3} \quad (1.6)$$

And P_2 is the field due to the non-linear interaction. The result from the reference [22] solved with the result of P_1 is:

$$P_2 = \frac{\beta}{2\rho_o c_o^4} \frac{\partial^2}{\partial t^2} \iint_{00}^{x\infty} P_1^2(x', r', t - \frac{r'^2}{2c_o(x-x')}) \frac{r' dr' dx'}{(x-x')} \quad (1.7)$$

It is assumed that the ultrasound signal emitted has the form:

$$P_1(0, r, t) = P_0 E(t) \sin(\omega_o t) \quad (1.8)$$

where the term P_0 is the intensity of the ultrasound carrier, and $E(t)$ is the envelope function which modulates the carrier. Introducing the equation ((1.7)) in equation ((1.6)) and making the assumption for the far field $x \gg L$, and forgetting the high-frequency term that result from the self-demodulation mechanism of the air in the process is found the Berkay equation [22]:

$$P_d = \frac{\beta P_0^2 a}{16\pi\rho_0 c_0^4 z \alpha_T} \frac{\partial^2}{\partial t^2} E^2(\tau) \quad (1.9)$$

where P_0 is the acoustic pressure, β is the nonlinear coefficient, and a is the effective source area cross-section, ρ_0 is the density of the medium of propagation, c_0 is the speed of sound, z is the axial distance from the source, α_T is the coefficient of absorption and $E(t)$ is the envelope function.

In the case of Parametric Acoustic Arrays α_T is a combined absorption coefficient that determines the extent of the nonlinear interaction

$$\alpha_T = \alpha_a + \alpha_b + \alpha_- \quad (1.10)$$

where α_a and α_b are the absorption coefficient of the primary frequencies and α_- is the absorption coefficient of the difference frequency wave. Due to the much smaller absorption coefficient of the difference frequency wave compared to the ultrasonic waves, the overall absorption coefficient can be approximated by $\alpha_T = 2\alpha_a = 2\alpha$. The absorption length indicates a significant drop in the pressure level of the high-frequency waves, so it is considered the end of the non-linear interaction. It is the reciprocal term of the absorption coefficient α_T

$$L_\alpha = 1/\alpha_T = 1/2\alpha \quad (1.11)$$

The Rayleigh distance $z_o = \frac{s}{\lambda} = \frac{\pi f_c r^2}{c_0}$ describes the transition from the near-field to the far-field. Parameter s is the area of the source and r the effective radius and λ is the wavelength of the mean frequency (f_c) of the two primary waves [13].

The Berkay equation (1.9) establishes that the demodulated signal is proportional to the second time derivative of the squared envelope and it has been accepted as the most used acoustic model of preprocessing methods for PALs [23]. The characteristics of the self-modulated wave depend on the primary waves, the audible level is proportional to the square of the ultrasonic level, for every doubling the ultrasonic level, the audible sound is quadrupled [22]. From this equation could be also deduced that low frequencies need more ultrasound to be generated. The second derivative in time creates a natural equalization curve of 12db/octave , which means that for each octave decrease in frequency, the required level of ultrasound quadruple.

1.3.3 About piezoelectric ultrasound transducers

One transducer can be considered as a band pass filter with a defined bandwidth which is sensitive to a particular range of frequencies. PAL uses two kinds of transducers: ceramic ultrasonic transducers (i.e lead zirconate titanate (PZT)) discovered by the Japanese research group of E. Sawaguchi [24] and the piezoelectric polymeric films (i.e polyvinylidene fluoride PVDF) created in 1969 by H. Kawai [24]. The transducers are typically arranged in a honeycomb configuration (Figure 1.13) because the directivity at higher frequencies requires closer spacing of

individual speakers [25]. In fact, by maximizing space occupancy, the distance among the propagation axes of each transducer is reduced and thus is the aliasing effect due to the interference among the wavefronts that each transducer generates [16]. On the other hand, piezoelectric films such as PVDF conveniently provide a continuous vibrating surface, but also have the drawback of making harder to attain well-ordered modes of vibration [26][27].

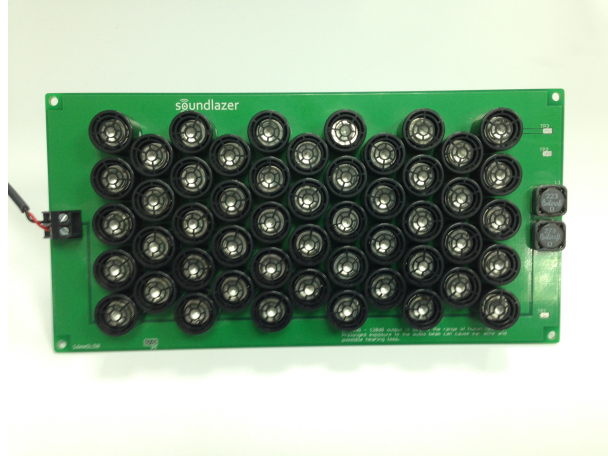


Figure 1.13: Soundlazer array

When a potential difference is applied to piezoelectric ceramics, mechanical distortion is generated according to the voltage and frequency. On the other hand when a vibration is applied to this materials there appears a difference in voltage, this phenomenon is known as the piezoelectric effect. The piezoelectric effect is the ability of certain materials to generate an electric charge in response to applied mechanical stress. It is a reversible effect, and it means that these materials exhibit the converse piezoelectric effect, the generation of stress when an electric field is applied. The transducer sound output reaches 105-120 dB (30 cm distance) when a voltage of 10-20 V_{rms} is applied [28]. The resultant pressure wave can be modelled as a convolution between the input signal and the impulse response of the transducer which has a defined bandwidth.

The figure 1.14 shows the components of a piezoelectric transducer. The piezoelectric ceramic element is a two-layer wafer of poled PZT material arranged in such a way that it bends from concave to convex as the AC is applied. The total resonance of one of these transducers depends on the resonance properties of the piezoelectric material, the radiating cone, and the air cavity. The cone or horn structure acts as a coupler impedance needed to match the high impedance of the dense material PZT to the much lower impedance of the low density of the air. This transducer has a relatively wide-band, typically about 5 kHz depending on the choice of resonance frequencies.

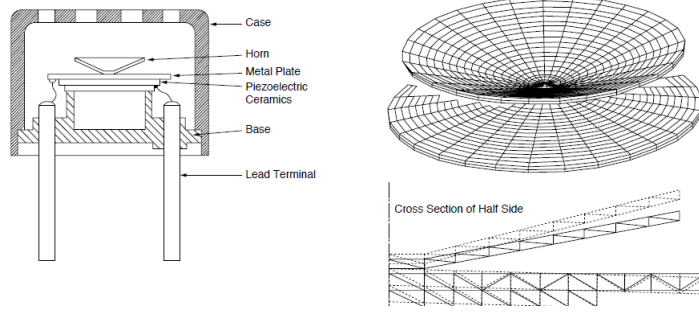


Figure 1.14: Components of the PZT transducer and cone to couple the impedance [2]

The piezo film such as polyvinylidene offer promising prospects as broadband emitter and have a high intrinsic efficiency due to their better impedance match between the thin diaphragm foil layer and the air [29]. The PVDF arise to reduce the high cost of the piezo-emitters, but the resonance frequency is less, reason why they are used on structures with cavities and pressure to achieve stretches and thereby increase the frequency of which these arrangements are excited. The Figure 1.15 shows a schematic of the PVDF.

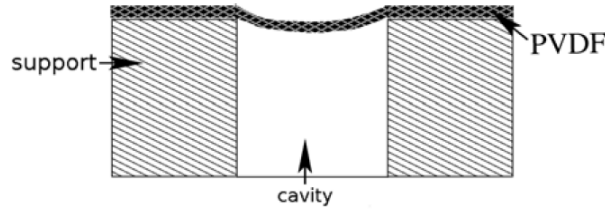


Figure 1.15: Cavities configuration to modify the frequency response of the PVDF transducer [3]

The matching of acoustic impedances of the piezoelectric ceramics and the air becomes necessary. The specific acoustic impedance of the piezoelectric ceramics and air is $2.6 \times 10^7 \text{ Kg/m}^2\text{s}$ and the specific acoustic impedance of air is $4.3 \times 10^2 \text{ Kg/m}^2\text{s}$. The difference of 5 orders of magnitude causes a significant loss on the vibration radiation surface of the piezoelectric radiating ceramic. Bonding performs this matching of impedances with a unique material the piezoelectric ceramics or using an inductance in parallel to the array also works for match the electrical impedance.

The attenuation is caused by diffusion loss on a spherical surface due to diffraction phenomena and absorption loss. The medium absorbs that energy. Figure 1.16 shows the wave attenuation behavior, it is possible to see that the higher the frequency of the ultrasonic wave, the more the attenuation rate and the shorter the distance the wave reaches.

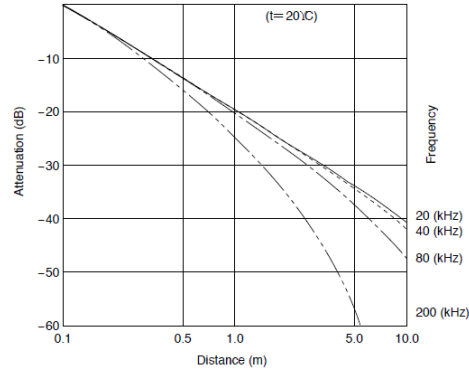


Figure 1.16: Attenuation Characteristics of Sound Pressure by Distance

Attenuation is a strong function of humidity at these frequencies. Since a large area and the short wavelengths needed are not generally compatible requirements, an array of small elements is generally used [8].

1.3.4 About the health and safety uses of the Parametric Array Loudspeaker Technology

These loudspeakers must be guaranteed not to have any health issues for people. The work of Soomin Lee et. al [30, 31] seems to be the principal reference regarding experiments designed to evaluate some physiological consequences from the exposition to the acoustic radiation from the piezo transducer array. This experiments used a design of experiments methodology over a group of people which were analyzed with different physiological functions like Electroencephalogram EEG Electrooculogram EOG, Blood pressure. The same autor has articles in which the topic of the research is the safety use of the PAL in the near and the far field. For the far field he concludes that the physiological burden of the sound of the of parametric speakers set at 2.6 m from the subjects was lower than that of the general speaker. For the near field he concludes that the physiological burden increase in progress with time but compared with an ordinary loudspeaker the result does not not differ significantly.

The work of Jammet [32] recommended that the limits of continuous occupational ultrasound exposure be set at 110 dB, and 100 dB for exposure to the general public. The recommended limits for exposure to airborne ultrasound have increased over the years, as more has been understood the associated risks [33]. In the review of Wiernicky [34] they explain the evolution for exposure standards since the 1960s, which have been generally in the region of 110-120 dB for maximum exposure limits for ultrasound greater than 20 kHz. More recently, the Occupational Safety and Health Administration (OSHA) recommended a limit of 115 dB for continuous exposure [33, 35].

Woon Sen Gan, affirms that there is no report that describes the cause-and-effect relationship between hearing loss and exposure of the ear to high-frequency ultrasound. He argues that the human skin reflects almost 99% of the ultrasound energy due to the high impedance mismatch between air and the skin, the body part that suffers more with that kind of ultrasound radiation are the eardrums [17]

There is another use for this loudspeakers: the military industry. The LRAD is a non-lethal weapon that directs the acoustic energy for crowd control to disperse protests[36] using 145 dB tone at distances more than 300 m causing headache and panic. It is evident that prolonged exposure to high-intensity acoustic waves in the human causes feelings of discomfort. One of the necessities to make a contribution in the PAL is to reduce the carrier ultrasound to a safe pressure level without compromising the performance of parametric sound.

Hypersound Audio System has a paper that affirms that the system has an excellent safety behavior in normal hearing subjects under standard conditions [37]. The ultrasonic radiation with low frequency has more harmful effects in the human body than the high-frequency ultrasounds, the most accepted frequency for the carrier wave is 30-70 kHz

The PAL device SoundLazer SL-01 generates an uncomfortable feeling if the PAL is completely directed to the ear cannal, and if the exposure is prolonged. There is a health standard safe limit of 120 dB of exposure to ultrasounds [17] that makes impractical this situation. This thesis was developed under safe conditions considerations, also the experimental set up and the sound installations.

Chapter 2

Acquisition of Sound from self-demodulation of Ultrasound

The current work is focused on the sound propagation technique using ultrasonic fields. This technology is based on the phenomenon that occurs when two ultrasonic waves with different frequencies radiate in the same propagation medium. The small wavelength of the ultrasonic waves generates a beam with a low divergence within all point of the absorption length recover the audible field due to a phenomena known as self-demodulation [38][22]. The nonlinear interaction of the two primary waves generates a spectral component at the frequency difference along the beams. At the same time, spectral components including the sum and difference of the two primary frequencies are produced by the nonlinear interaction of the two ultrasonic waves. All emission points are known as virtual sources and are explained by the scattering effect originated from the nonlinear interaction of the modulated ultrasonic wave with the air [39].

This chapter addresses the problem of understanding the phenomena of sound production from the ultrasound. We will start with the historical background of the field of Acoustics emphasizing in the directionality property through the development of different technologies until we get the subject that competes the Parametric Array Loudspeakers (Section 2.1). Section 2.2 explains the nature of sound as a non-linear interaction which generates audible sound that propagates linearly. Section 2.3 explains the relationship that the phenomenon has with others linear phenomena such as beats in acoustics and moiré patterns in optics and how it is interpreted to be the linear propagation audible from the ultrasound.

2.1 Acoustics

There is a personal interest of understanding a subject knowing its historical background; it permits me to appropriate a piece of knowledge in a more solid way. Along the history the interdisciplinary science that deals with the study of the mechanical wave known as Sound, Acoustics, has been consolidating. From the early Greek concepts of the world existed ideas of what was sound and how it behaves[40]. The knowledge about the different characteristics of sound waves like for example the sound velocity in various media, how they spread, what happens when it changes of media, and the temperature and pressure dependence of they when are transmitted has been

generated and refined for years. Table 2.1 shows a review of some advances in the Acoustic area [41, 42]:

| | |
|--|---|
| Marco Vitruvio (.- 15 A.D) | Sound waves travel in three dimensions. |
| Quintiliano (35-100 A.D) | Demonstrate the resonance of a string in the air. |
| Leonardo Da Vinci (1452- 1519 A.D) | “Sympathetic Resonance” Velocity of sound must have a defined value. |
| Marin Mersenne (1588- 1648 A.D) | “Air motion generated by musical sound is oscillatory in nature and sound travel with a finite speed” L’Harmonie Universelle, Father of the modern acoustics. |
| Galileo Galilei (1564 - 1642 A.D) | "Waves are produced by the vibrations of a sonorous body, which spread through the air, bringing to the tympanum of the ear a stimulus which the mind interprets as sound". |
| Pierre Gassendi (1582 - 1655 A.D) | Demonstrates that sound velocity was independent of the pitch. |
| Robert Boyle (1626 - 1691 A.D) | Proved that air is necessary for the production or emission of sound. |
| Robert Hooke (1635 - 1703 A.D) | Basis of vibration and elasticity theory . |
| Joseph Saveour (1653 - 1713 A.D) | Suggests the acoustic term for the science of sound. They appear in his work for the first time the terms "node" "disturbance" "Harmonics". |
| Francisco Mario Grimaldi(1653 - 1713 A.D) | Generates a connection between different physical phenomena from other areas with sound. “Phsycomathesis de lumine, coloribus er ride”. |
| Newton (1642 - 1726 A.D) | Newton considered an isothermal medium, Dependence of the temperature for the sound velocity. |
| Richard Helsham (1680 - 1758 A.D) | Exponential Horn. First experience related to the directionality of the sound: Source energy loading. |
| Giovanni Ludovico Bianoni (1701 - 1773 A.D) Charles Marie de la condamine (1701 - 1774 A.D) | Influence of the temperature on the velocity of sound. |
| Simon Ohm(1789 - 1854 A.D) | Developed the analogy between electricity and acoustics. |
| Hermann F.L Von Helmholtz(1821 - 1894 A.D) | Theory of resonators, Combination, and sensations of tones. |
| Lord Rayleigh (1845 - 1919 A.D) | Formulation of the wave equation. Theory of sound. |
| James P Joules (1818 - 1889 A.D) | Magnetorestrictive effect. The genesis of ultrasonics. |
| Robert Williams Wood (1868 - 1955 A.D) Paul Langevin (1872 - 1946 A.D) | Counter surveillance acoustic techniques Piezoelectric effect. |
| Karl D Kryter (1914-2013 A.D) | Physiological effects of noise in humans. |
| Sir James Lighthill(1924 - 1998 A.D) | Foundations of Aeroacoustics. |

Table 2.1: Acoustic chronological progress

The ability of human beings to develop techniques that focus and direct sound to specific locations is ancient. With the evolution of the knowledge about the sound appears the directionality concept. In the next section, the directionality sound history and the different ways of doing it is illustrated.

2.1.1 Directionality of Sound

For instance, the natural gesture of cupping hands around one's mouth to prevent the sound of the voice from being diffused is a clear example of our intuitive understanding that sound needs to be guided in order to arrive at a particular target. The first reference of it could be traced in the work of Irish physician Helsham (1682–1738) [42] with his study of the so-called exponential horn, a waveguide structure that allows sound amplification because its exponential geometry which acts concentrating more energy in the source causing a directional propagation of its output. These were the first notions of the directional property of sound explained later by John William Strutt more recognized as Lord Rayleigh (1845-1919) who treated the problem of source loading. Arthur Gordon Webster (1863-1923) contributed to the theory of horns equations [43][42] describing the mathematical relationship between the geometry of the source and the directional propagation of sound.

Sound can be directed using parabolic geometries [44]. Figure (2.1) shows some examples of conical structures used to route the sound:



(a) Sound mirror at Denge, England

(b) Acoustic Shell, Medellín, Colombia

Figure 2.1: Conical structures used to route the sound

The left image in Figure (2.1a) is an acoustic mirror in the south-east coast of England at Denge; these structures were used in the Second world war as early warning devices to detect incoming enemy aircraft by listening for the sound of their engines over long distances [45]. Figure 2.1b shows a conical shape sculptures used to transmit sound from one shell to the other in a public park in Medellín, Colombia as an interactive installation to engage visitors in the hands-on learning of the laws of physics. Figure (2.2) below is a commercial conical loudspeaker of the company Soundtube®



Figure 2.2: Commercial Sound Dome

Other ways to route the sound are the wave guides[46] Figure (2.3a), the electrostatic flat panel speakers [47] and Headphones. Headphones are the most optimal way to transmit the sound concerning energy loss because of the proximity to the ear canal. Sound can also be directed using the physical arrangement and disposal of the sources [48][49] like the line arrays shown in Figure (2.3b) commonly used in concerts where the phase distribution of the arrangement allows to direct the loudness to the crowd.



(a) Sound wave guide



(b) Line array loudspeaker

Figure 2.3: Other techniques to enroute sound

Another technique in the category of sound directionality perception is through the use of microwaves. The Microwaves do not generate sound perception in the traditional way through the ear canal transmission. The thermoelastic effect produces the sound perception directly in the brain, effect interpreted as an audible sensory stimulus known as Frey effect [50]. It is worth commenting that this technique seems not to be very investigated and the information found was not so much, also having a conspiratorial character.

2.2 On the non linearity of sound

The history of parametric speakers starts with some observations made by Helmholtz at the end of the XIX century [8] . The German physicist realized that transmission of acoustic pressure in air is not linear, so much so that given two frequencies, more frequencies are generated that are the sum and the difference of the originals as it is shown in Figure 2.4. The non-linear interaction of the medium over acoustic vibrations when they propagate is of paramount importance for the existence of parametric speakers, as it is the main condition for them to work. Works of Helmholtz for example “The sensation of tones” of 1863 constitutes the physiological basis for the theory of music. Other studies about non-linearity in air were carried on after Helmholtz [26] which mainly investigated the distortion generated during sound propagation and the effect this impresses on the shape of the wave.

In 1963, Westervelt [51], in his article of parametric arrays suggests that it is possible to generate emitters and receivers in some configuration in order to generate virtual sources of emission. Westervelt found that when two primary wave frequencies f_1 and f_2 are fully confined beams, the angle at which the sound intensity of the difference frequency $f = f_1 - f_2$ is reduced by one-half ($-3dB$) is approximately $\theta_h = \sqrt{\frac{2\alpha_t}{k}}$ where α_t is the total sound absorption coefficient of the primary waves and k is the wave number of the difference frequency. Interestingly the directivity of a parametric source is thus independent of the source aperture what happens in an omnidirectional speaker.

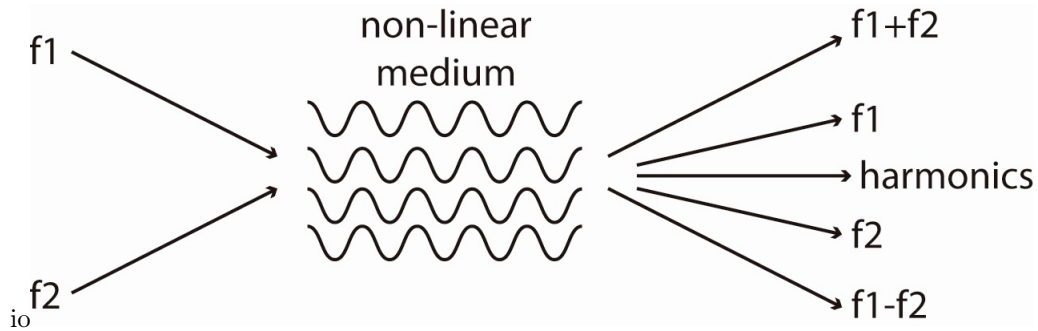


Figure 2.4: Two-Frequency mutual interaction in a nonlinear medium

Two years later Berkta in 1965 [39] proposed the to understand how the primary ultrasonic waves and the secondary audible waves are related which will be explained in later sections. In 1975, Mary Beth Bennett and Dr Blackstock [52] presented their results demonstrating for the first time the possibility to generate a parametric array in the air, the previous work only conceived this kind of emissions for applications under water. Subsequently in 1982 Yoneyama [53] developed the first directional speaker (2.5) accompanied by a high THD. In his work he implemented an analog modulation scheme of the carrier called Double Side Band Amplitude Modulation DSB AM based on the Berkta envelope proposal.



Figure 2.5: First Parametric Array Loudspeaker Yoneyama

In 1984 Kamakura [54] proposed a modulation scheme named Square Root Modulation Amplitude SRAM. By this way, he achieved to reduce the THD compared with the conventional DSB-AM but with a high implementation cost and energy consumption. At this time the works about parametric array speaker began to include the powerful tool called the Digital Signal Processing DSP and at the ends of the 90s and beginnings of this century arise the work of Joseph Pompei [55] and Elwood Norris [8]. Both have several numbers of patents and claims to be the creators of the first commercial PAL with a low THD (less than 5%). Nowadays they have recognized directional audio companies, Audio Spotlight by Holosonics [56] and Hypersound of Turtle Beach Corporation [55]. Hypersound has developed electrostatic ultrasonic speakers whereas Holosonics relies on its customized piezoelectric transducers. Also Hypersound devices have lower perceived distortion than Holosonics who delivers high bandwidth [25]. Another company that exist is the Finnish company Pamphonics [57] and from Slovenia the company Acouspade [58]. In the last years they have been generating different businesses, and ventures related to directional audio applications. It is important to report a company that was born from a crowd-funding Kickstarter campaign and is called Sound-lazer [59]. The latter is important because it allowed the low-cost accessibility from this technology. In the near environment at the level of Colombia only the work of Cadavid was found in Medellín [60].



(a) Hypersound



(b) Holosonics



(c) Soundlazer SL-01

Figure 2.6: Commercial Parametric Loudspeakers

The most recent research papers in the topics of steerable PALs [61, 16], propose to control the sound beam of the loudspeaker having control over each transducer separately like in the line arrays, controlling the phase the lobe can be directed at specific targets with no orienting the speaker. Other areas of recent research are modeling and numerical simulation of the acoustic field from a PAL [62, 63, 11], improvement of the limitations like the total harmonic distortion and low frequency reproduction [9], diverse applications for security, defense and gadgets [64, 65], reviews[49, 17, 66], safety issues[31, 30, 17]. The directional property of this technology has also been found useful in different areas like Non-Destructive Testing (NDT),[15, 67], Active Noise Control (ANC)[68, 69, 70, 71], Multi translation systems [72, 73], artistic installations [74] and advertising. The use of museums and other spaces for control of quiet areas are still the most important area of applications.

The next table resume chronologically the major contributions on the topic of audio directional using ultrasound. This table does a survey in the directional sound ultrasound technology.

| Date | Milestones |
|-----------|--|
| 1856 | Hermann von Helmholtz, “Ueber Combinationstöne.” |
| 1934 | A.L. Thuras, R.T. Jenkins, and H.T. O’Neil, “Extraneous Frequencies Generated in Air Carrying Intense Sound Waves.” |
| 1940 | L.J. Black, “A Physical Analysis of Distortion Produced by the Non-Linearity of the Medium.” |
| 1963 | Peter Westervelt, “Parametric Acoustic Array.” |
| 1965 | Hasan Orhan Berkay, “Possible Exploitation of Non-Linear Acoustics in Underwater Transmitting Applications.” |
| 1974 | Mary Beth Bennett and David T. Blackstock. “Parametric Array in Air.” |
| 1983 | Masahide Yoneyama, Jun-ichiroh Fujimoto, Yu Kawamo, and Shoichi Sasabe, “The Audio Spotlight: An application of nonlinear interaction of sound waves to a new type of loudspeaker design.” |
| 1984 | Tomoo Kamakura, Masahide Yoneyama, and Kazuo Ikegaya, “Development of Parametric Loudspeaker for Practical Use.” |
| 1999 | Joseph Pompei, “The Use of Airborne Ultrasonics for Generating Audible Sound Beams,” Audio Engineering Society, convention |
| 2001/2002 | James J. Croft and Joseph O. Norris, “Theory, History and the Advancement of Parametric Loudspeakers,” American Technology Corporation, Hypersonic Sound White Paper. |
| 2012 | Applied Acoustics, 73 (12), Woon-Seng Gan, Jun Yang and Tamoo Kamakura (eds.) |

Table 2.2: Chronologically advance in Parametric Array Loudspeakers

The contribution of this thesis aims to be framed in the study of harmonic distortion focusing on the conditioning part of the signal. This thesis generate a knowledge in the subject of characterization of audio equipments and be able to be a reference in the near environment for future works

2.3 On the linearity of sound from ultrasound

Could be a misconception on understanding the nature of the phenomenon of the production of sound from an ultrasound source. The confusion lies in the interpretation of this phenomenon solely regarding a linear interference process, instead to a scattering process due to the nonlinear interaction with the air. As a linear interference process we find, for example, the beating phenomena. Beats are the interference pattern that appears with the superposition of two fields that have slightly different frequencies understood as amplitude fluctuation. The non-linear interaction of the ultrasound waves with the media is the the characteristic that generates the possibility of transmission of sound from ultrasound, it constitutes the nature of the audible sound perception from the non-audible modulated ultrasound fields.

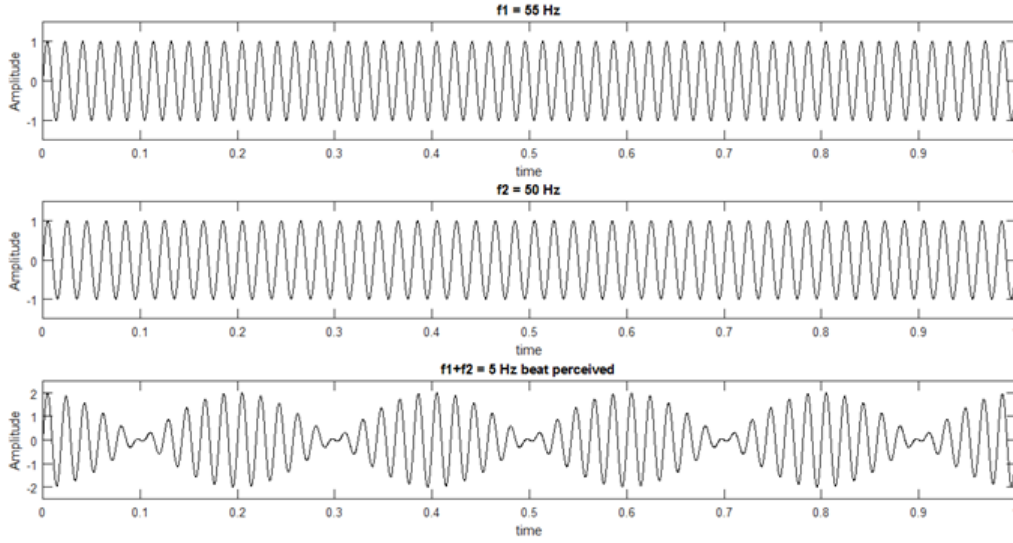


Figure 2.7: Close difference frequency wave addition

As an example Figure (2.7) shows two waves of slightly different frequencies, $f_1 = 50$ Hz and $f_2 = 55$ Hz. These waves add up to generating a third wave which has an envelope frequency correspond to the difference of the frequency of both previous waves f_3 of 5 Hz. A beat is the difference frequency between the mixed tones is acoustically perceived as modulation in loudness. Beats are regular binary pulses underlying the music [75]. In nature sustained pure tones are rare, sustained tones are proper of machinery and motors reason why the beat phenomena was hardly noticed, was just at the beginnings of the last century where its understanding was formalized.

A phenomenon could be appreciated in the area of optics that have a similar nature is the Moiré pattern Figure (2.8). They occur when there are two different arrays of strips that are separated by various distances between lines and are superimposed or also when the collections of strips have changed in the angle between them [76]. Our eyes appreciate a visual pattern generated by the constructive interference from this. It is reasonable to think in the first stage in a linear phenomenon of destructive or constructive interference waves for the generation of new sounds from the ultrasound waves. What is usually called an optical beat is the sinusoidal behavior of the intensity of two overlapping and coherent fields.

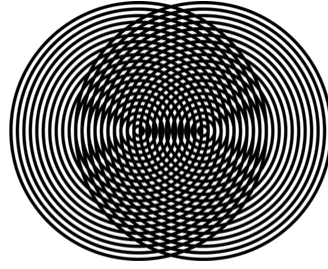


Figure 2.8: Moiré pattern example

Two kinds of beats perception exist, the monaural or acoustic, and the binaural beats or psychoacoustic [77]. Monaural are when one ear can just perceive the two slightly different frequency waves, Binaural beats require the combined action of both ears and the interpretation from the brain. The German physicist Heinrich Wilhelm Dove discovered Binaural Beats technology in 1839 but as late as 1915 they were considered a trivial special case of monaural beats [75].

In the case of the binaural beats, the brain is the one that acts as a mixer, in the monaural the mix is made in the medium (Figure (2.9)). The phenomenon of the binaural beats differs from the monaural beating by the amplitude modulation that beat at the rate of the difference between the two audio signals produces [78]. In both cases the amplitudes are larger in the modulation difference frequency than in high-frequency same case modulation.

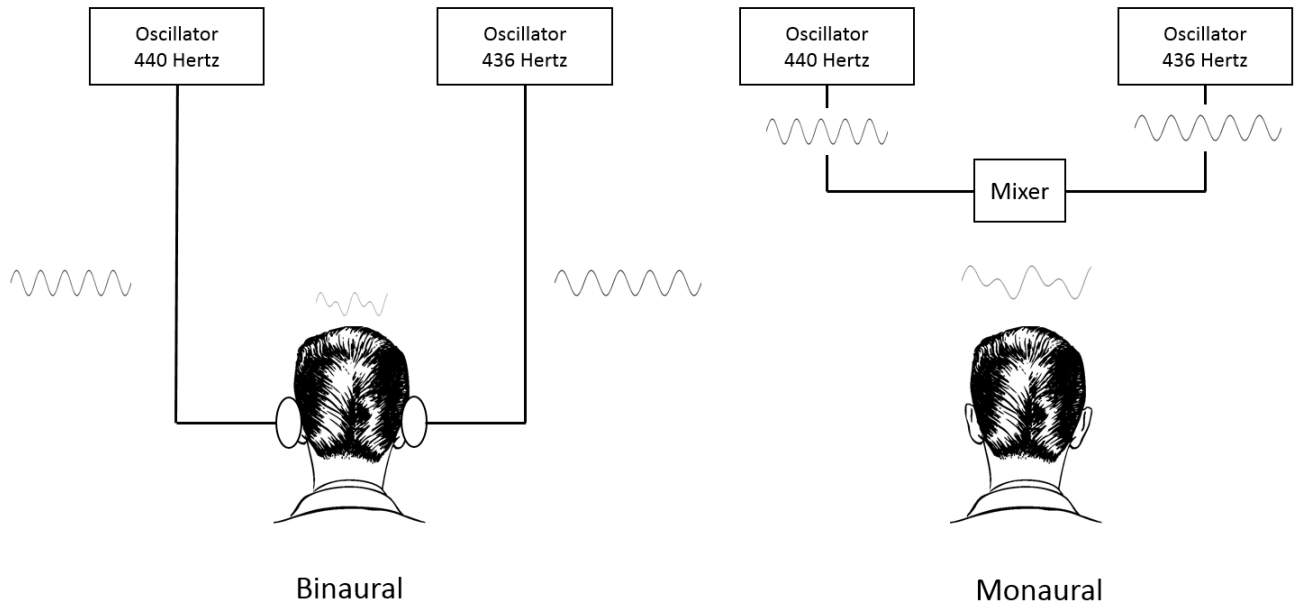


Figure 2.9: Monaural and Binaural beats

In the HSS White Paper of Norris [8], the authors affirm that the beating phenomena already exist in the ultrasound generation of sound but are not the principal reason of the audible sound in the commercial parametric speakers. In fact, creating sound from beatings is limited because it only generates recognizable sounds with the difference of frequencies that are from 1kHz to 9kHz. When two primary tones are summed or combined, they alternately reinforce or annihilate each other. If one tone has a frequency f_1 and the second has a frequency f_2 the resulting signal has frequency $f_1 + f_2$. When two different tones of slightly frequencies sound, the beat tone is perceived. When the frequency difference increases the beating sound rough until the distinct tones are heard [8]. The best results of beating sound perception phenomena were from pointing the transducer at each emphasizing that they use a tube between to amplify the weak difference frequency signals.

From beating is possible to find a lower tone but its intensity is small to have a practical use. Also, the ear only can detect beat frequencies in a certain range of frequencies and a higher beat frequency the sound is perceived like a continuous tone with a slight warble. Oster's paper [75] mentions that binaural beats only form if the two tones are separated by less than 30 Hz at most. It is important to say that beatings are not an audio signal itself, they are a rate at which two signals of higher frequency go in and out of phase, a clear example of linear superposition. Beating is not the cause of the production of sound from ultrasound in this kind of speakers. This sound nature is more related to a non-linear phenomenon resulting from the medium in the propagation. The interaction of the air with the ultrasound carrier that creates components of audible sound during the propagation is known as self-demodulation [20].

One of the first references on the nature of how the directional ultrasound speaker works were from John William Strutt, more known as Lord Rayleigh. He considered the possibility of the scattering of sound waves from regions in which both density and compressibility were assumed to be different from the values obtained in the rest of the medium [39, 79]. He assumed these scattered waves as small quantities that propagate in a linear way. In the paper of Berkay, the concept of the "Huygens wavelets" was necessarily valid. He used this concept to elucidate the sound created at all points in the proper volume due to the interaction of sound waves.

This idea is consistent with our actual understanding of the phenomena which we agreed after discussing: there is a nonlinear interaction of the emitted ultrasound propagating that produces sound due to the nonlinear air characteristics, and from this phenomenon, a linear frequency audible sound field appears. This nonlinearity exist as a perturbation in the speed of sound as a function of local air pressure or density[33]. Next picture (Figure (2.10)) shows a graphical explanation to understand the difference between these two systems, the Linear and the Non-Linear. The following graph illustrates a way to understand the interaction of the non-linear properties of the medium to produce the distortion of the traveling waves causing energy demodulation in the form of harmonics.

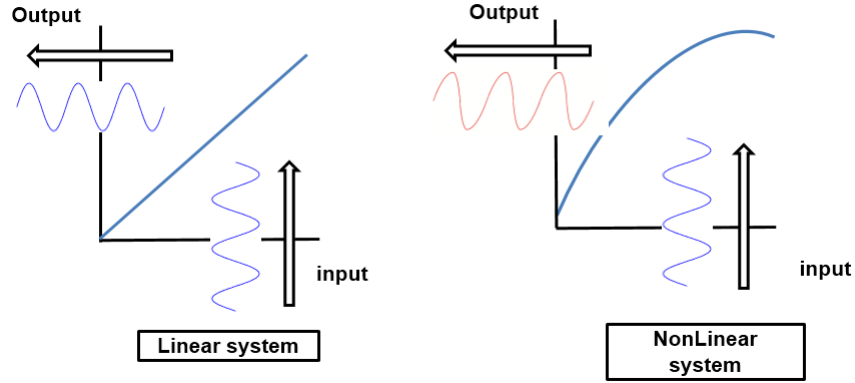


Figure 2.10: Graphical interpretation of a Linear and a Non linear system

As conclusion, nonlinear behaviors are always operative in real life, but absorption and dispersion effects are usually greater than those of self-distortion. However, the opposite occurs in the ultrasonic range, so that, a signal previously amplitude-modulated with an ultrasonic carrier generates by self-distortion an audible signal with the directional property that shorter wavelengths have over longer wavelengths waves. This interaction with the air has two main consequences which are disadvantageous for the quality of sound: Limitation of reproducibility of low frequencies, and harmonic content generated in the self-demodulation process.

The first limitation is inherent to the generation of sound from ultrasound in air, the self-demodulation acts as a high pass filtering effect. Shi proposes a method to produce bass perception with the missing fundamental technique [9], a psychoacoustic bass sound perception. It is a way that works to hear a low pitch due to the brain interpretation patterns that are present. This pitch is known as the missing fundamental or a virtual pitch. The other limitation is the high distortion levels presented in the audible sound demodulated.

The knowledge acquired about the phenomenon of self-demodulation due to nonlinear air behavior was acquired through a review of state of the art, the historical background in acoustics and the discussion generated about the nature of sound from the ultrasound. The analysis aims to clarify the nature of this kind of sound propagation, comparing it with the linear interference of beatings in acoustics and in optics, which seems to generate confusion when the PAL phenomenon is trying to be explained. As a new knowledge acquired, we have learned about the Binaural and Monaural Tones and the nonlinear mechanism of sound production. In the next chapter, a description of the different modulation techniques is made to understand the preprocessing stage existing in most of the PALs that makes it possible anticipate the distortion generated in order to control it. Also, the THD parameter is explained, the modulation techniques that PAL use to reduce the harmonic distortion in the preprocessing stage are briefly described and the modulation scheme of our test speaker is analyzed.

Chapter 3

Signal distortion and modulation schemes

The interest of this thesis is focused on the conditioning stage of the signal because the modulation scheme integrated in the PAL that we had was a pulse width modulation PWM that was generated in a posterior stage to the DSP. This fact limited the research on this topic and, because of that in the next chapter the most common modulation schemes are briefly explained and the PWM is analyzed in terms of the contribution in harmonic content, and the cause of such a distortion.

3.1 Introduction

The Fourier transform is a graphical representation of all frequency components that appear in a signal over a given period. The x-axis of a Fourier transform is in units of frequency. The y-axis of a Fourier transform shows the amplitude of the signal at a given frequency. The signals that we recorded of the audio field demodulated usually have the form shown in Figure 3.1. An unique fundamental frequency is not just perceived, it has a remaining amount of harmonics and other characteristics that affects the quality of the sound and are visualized using the Fourier transform of the signal.

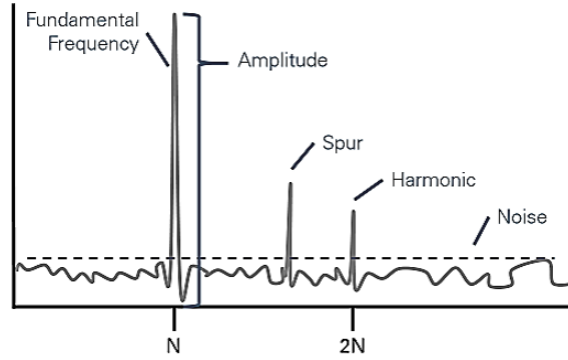


Figure 3.1: Common frequency spectrum of a signal

A signal is a formal description of a phenomenon that evolves over time or a defined space [80]. As a symptom of nonlinearity, the output of a system exhibits distortions. Encyclopedia Britannica describes the distortion as any change in the signal that alters the basic waveform or the relationship between various frequency components that is usually a degradation of the signal [81]. The most common forms of distortion are unwanted elements or artifacts added to the original signal or non-linear device adds in the form of harmonics of the original frequencies (Figure 3.2).

As a direct consequence of what Helmholtz initially envisioned, it is precisely the non-linear behavior of the medium the responsible for the demodulation within the audible range of a signal carried on by an ultrasonic frequency. The non-linear medium changes the wave pattern having an effect in the apparition of different amplitudes in the frequency spectrum, that correspond to harmonics or sub-harmonics of the fundamental tone emitted.

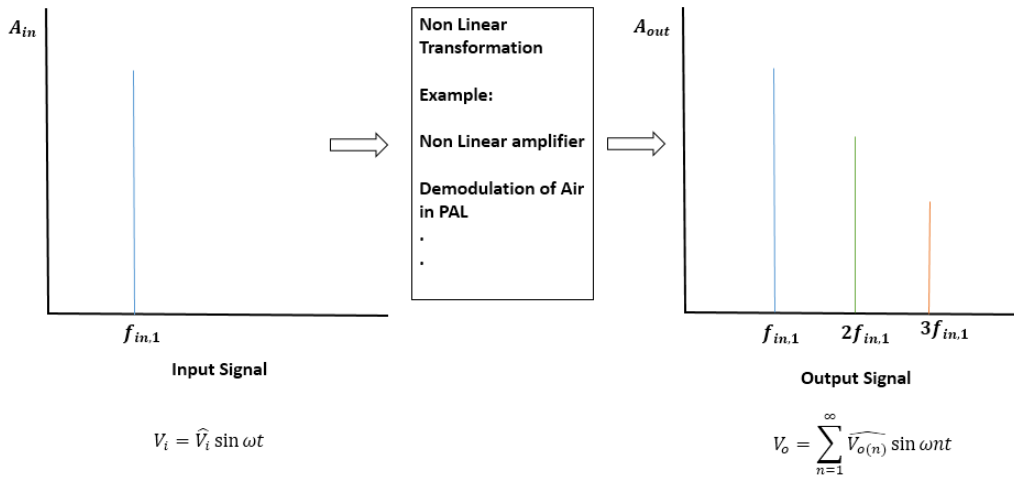


Figure 3.2: Effect on the harmonic content of a signal caused for a Non Linear medium transformation

When the input signal of the system is a sine-wave signal of frequency f_o , the harmonic distortion correspond to components of the output signal at frequencies which are integer multiples of f_o . When a system is excited with an input signal made of two sine waves having different frequencies f_1 and f_2 , the Intermodulation distortion correspond to the components that have frequency values that are linear combinations of f_1 and f_2 such as $f_1 - f_2$, $f_1 + f_2$, $2f_1 - f_2$ and other combinations. If the system produces at least one of these two effects, it is considered to be nonlinear [81]. When the resulting signal is demodulated what we hear is neither the modulated carrier wave nor the additive frequency because they are both beyond the limit of our acoustic perception. What we hear is the difference frequency.

3.2 On Total Harmonic Distortion

The Total Harmonic Distortion THD is a parameter used to define the output audio signal in relation to the input. It is a measure of unwanted signals. Harmonics are undesired extra energy at multiples of the fundamental frequency, therefore they cause unwanted consequences on power systems that can lead to inefficiency and damages of many electric components [82]. In power systems, lower THD means reduction in peak currents, heating, and emissions. We can distinguish between two types of distortion: One can be considered an intra-sideband distortion and the other inter-sideband distortion [29]. The intra-side band distortion is caused by different frequency components that subtract each other within a particular sideband, but its impact is negligible. Inter-Sideband distortion is the interaction between the frequency components of two distinct sidebands. The latter distortion needs to be actively reduced because it adds more distortion to the demodulated signal. Total Harmonic distortion is used to measure the quantity of distortion that exists in the secondary field generated by the primary ultrasonic field and is given by the next expression [83]:

$$THD = \sqrt{\frac{T_2^2 + T_3^2 + \dots T_{n-1}^2 + T_n^2}{T_1^2 + T_2^2 + T_3^2 + \dots T_{n-1}^2 + T_n^2}} \times 100\% \quad (3.1)$$

Where T_i represent the i_{th} amplitude of the i_{th} secondary sound harmonic. Usually this measure is taken just till the second harmonic and in other words, it measure the performance of the system

$$THD = \sqrt{\frac{T_2^2}{T_1^2 + T_2^2}} \times 100\% \quad (3.2)$$

Figures (3.3) and (3.4) show a comparison between the frequency spectrum for two kinds of PAL, the Audiospot AS-24, the PAL used in *The Soundhouse* and the Soundlazer 50 PZT transducer used in *The Forest and the Shadows* at 1 kHz test tones. These measurements were made with an AKG C451 B condenser microphone, a Fireface 800 audio interface and the iZotope's RX spectrum analyzer plugin for Logic Pro. This measurement let us comprehend

visually the behavior of the phenomenon at the first stages

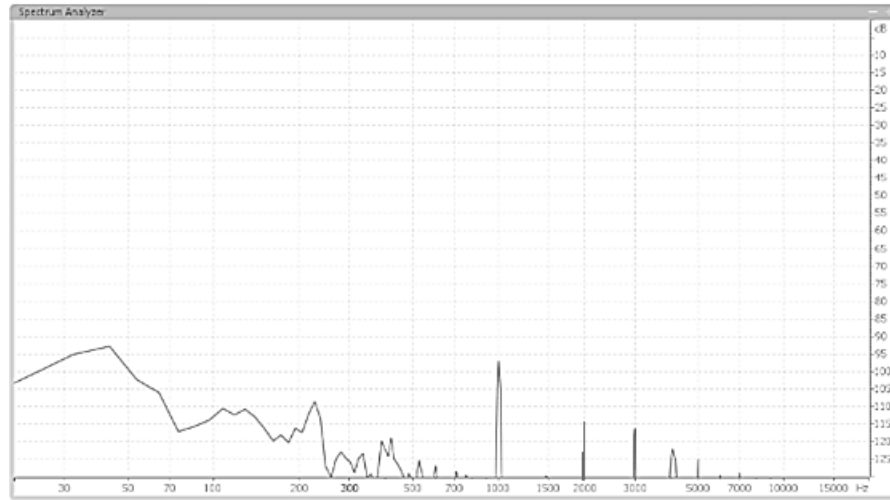


Figure 3.3: Frequency spectrum Audiospot AS-24 *The Soundhouse*

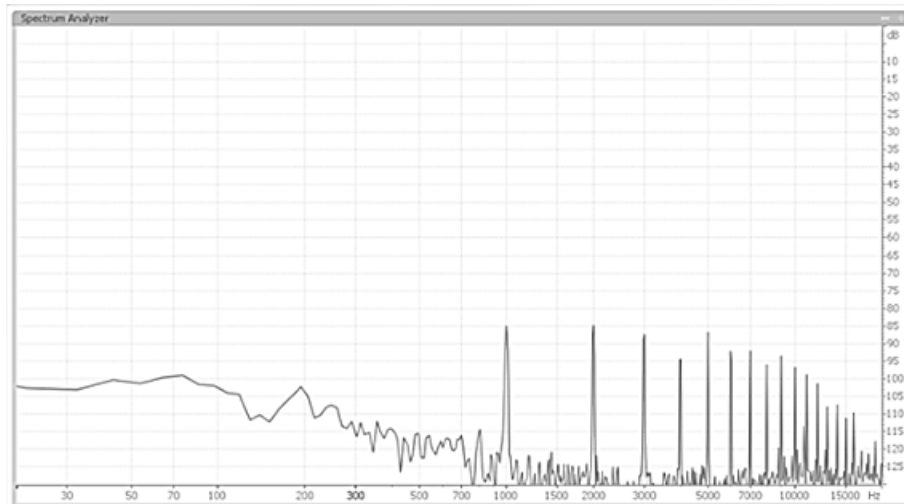


Figure 3.4: Frequency spectrum Soundlazer Parametric Pro amp kit *The Forest and the Shadows*

With these first two measures we had a first idea of the THD for the loudspeakers. From this first frequency spectrum, of the self demodulated waves, we could understand the visual appreciation of two signals with different quantities of harmonic distortion, a characteristic that affects the sound quality from this loudspeakers. In the case of the Audiospoligh (Figure 3.3) was approximately 30% and for the case of the Soundlazer (Figure 3.4) was of 80 %. It is possible to observe in the frequency spectrum for the 1 kHz test tones emitted and recorded for the two types of speakers how the Audiospotligh presents less harmonic content than the speaker of the Soundlazer brand. The values in the low frequencies correspond to ambient noises such as air conditioning, the nearby freeway as background

noise.

Another parameter usually provided in audio equipments is the THD+N (Total Harmonic Distortion + Noise) which instead of measuring individual harmonics, it measures everything added to the input signal, everything that comes out the unit that isn't the test signal is measured and included: harmonics, hum, noise, RFI, buzz, etc. Distortion analyzers make this measurement by removing the fundamental, using a notch filter and measuring what is left using a bandwidth filter, typically 22 kHz, 30 kHz, 80 kHz. It is important to know that there are different ways to evaluate the distortion of a signal, for example another measure is the SNR Signal to Noise Ratio that compares the level of the desired signal to the level of the background noise

$$SNR = \frac{P_{signal}}{P_{noise}} \quad (3.3)$$

and the SINAD, which is a measure of the quality of a signal from a communication device defined as:

$$SINAD = \frac{P_{signal} + P_{noise} + P_{distortion}}{P_{noise} + P_{distortion}} \quad (3.4)$$

where P is the average power of the signal, noise and distortion components. Unlike SNR, a SINAD reading can never be less than 1. THD is the measure which is commonly studied in the literature of PALs and we think it is important to introduce more distortion measures that take more in account other characteristic con the signals.

There has been a variety of preprocessing methods developed to reduce the harmonic distortion implemented in the DSP stage of this loudspeaker. Precompensation is the technique of anticipating the transformation that experience the ultrasound modulated wave to generate audible sound due to the demodulation applying inverse transformations in the input to the speaker array waiting that the output be near to the inputs with no transformations. Nowadays the precompensation stage and the conditioning stage of the signal are made in Digital Signal Processors DSP where a mathematical manipulation is made to condition it.

3.3 Effects on total harmonic distortion: Modulation techniques

The most common solution suggested in the literature to reduce the undesirable characteristics of the output is oriented to the digital signal processing modulation stage. Most of the works concerning about the THD are focused on the modulation stage of the signal and several corrections and modulation schemes are being proposed over the years. Anticipate the distorted behavior of the signal distorted by the non-linear medium it is what the preprocessing stage is focused.

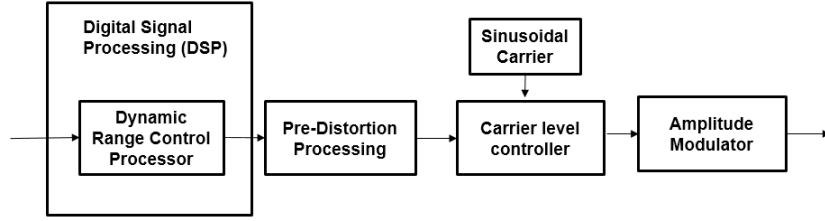


Figure 3.5: Pre-Distortion processing

Berkday equation (1.9) is a good approximation for directional sound beams for points near the axis. From this equation depart the modulation schemes that are commonly used in PALs. The Berkday equation shows the dependency of the demodulated audio signal pressure on the envelope of the amplitude modulated signal. In this model, the equation of the ultrasonic signal is assumed to be an AM-modulated waveform of the form

$$P_1(0, r, t) = P_0 E(t) \sin(\omega_c t) \quad (3.5)$$

where P_1 is the amplitude of the carrier signal, $E(\tau)$ is the modulating envelope and ω_c is the carrier angular frequency. From equation 1.9 is possible to illustrate the characteristics of the self-demodulated wave. The self-demodulated wave depends on the primary waves, the audible level being proportional to the square of the ultrasonic level. Because of the square term, the system becomes more efficient as the ultrasonic level is increased. For every doubling the ultrasonic level, the audible sound is quadrupled. The audible level is proportional to the square of the area of the array. From this equation also could be deduced that low frequencies need more ultrasound to generate them. The second derivative in time creates a natural equalization curve of 12 db/octave, which means that for each octave decreases in frequency, the required level of ultrasound quadruples.

The modulation schemes used commonly in PALs which are based on the Berkdays equation to reduce THD are as follows:

- Double Side Band Amplitude Modulation (DSB-AM):

Standard AM is called DSB-AM to distinguish it from other more sophisticated modulation methods also based on AM. This technique was used by Yoneyama in 1983 with an analog signal modulation hardware for the first parametric acoustic array [53]. The output expression of this modulation envelope is $E(t) = 1 + mg(t)$ where $g(t)$ is the input signal, and m is the modulation index. The modulation ultrasonic carrier is $\sin(\omega_0 \tau)$.

When there is a high m , a high THD incurs, for this reason a balance must be maintained aiming to produce

an acceptable sound pressure level at the expense of increase distortion[12]. In the opposite sense, a small value of the m index is used to decrease the amount of THD, but it is not useful for practical applications because the sound pressure level (SPL) decreases. They realized that the second harmonic had a similar amplitude to the fundamental signal what it means it has a high THD [19]. The resulting modulated wave is

$$A_c[1 + m \cdot g(t)] \cdot \cos(\omega_c t + \varphi) \quad (3.6)$$

where A_c is the amplitude and φ is the phase of the carrier. The interpretation of the modulation index m may be that it is the fraction of the carrier varies [84], if m is 0.5, the carrier amplitude varies by 50 % above and below its original value. If m is 1.0, then it varies by 100%. The information modulates the envelope of the carrier signal: The stronger the carrier modulated, the more power is put input the side-bands. The modulation index m is the indicator of how strongly carrier is modulated: if the modulation index increases the efficiency and gain will increase but also the distortion increases

- Square Root Amplitude Modulation (SRT-AM):

The output expression of this modulation envelope is $E(t) = \sqrt{1 + mg(t)}$. This method produces a THD lower than the SSB but requires a larger bandwidth to reproduce the infinite harmonics generated by the square root operation. An additional double integration in the output signal can be carried out before the square root operation. This integration process can be regarded as a form of equalization to achieve a demodulated signal with uniform response. Ideally, SRAM leads to a demodulated signal free of distortion but what makes it not to have a completely free distortion from this technique is the band limitation of the piezo transducers. SRAM produces the ideal modulation envelope that leads to a distortion free demodulated signal if and only if the ultrasonic emitter has infinite bandwidth.

- Single Side Band Amplitude Modulation (SBS-AM):

This method is similar to the DSBAM but only requires half of the bandwidth of it because instead of using the whole spectrum it uses a filter to select either the lower or the upper sideband. SSB method has been studied since 1991 and is primarily a quadrature modulation method. DSBAM produces an envelope that is similar to the one in the SRAM method, however, for multiple primary waves there occur multiple envelope errors. Figure 3.6 shows a comparison between the SRAM and the SBSAM envelope at 1 kHz. In time domain both envelopes are similar, but in the frequency spectrum, the changes are evident. The spectrum of SRAM contains many harmonics, and the SBSAM includes only the fundamental frequency (40kHz) and the upper side band (41kHz). The lower or upper sideband choice results in the lower side band (LSB) and upper side band (USB) modulation, respectively. There are two approaches to eliminate one of the sidebands. One is the filter method, and the other is the phasing method. The process usually used in the SBSAM for the Parametric speakers involved a Hilbert transform which makes possible to use the phasing approach. This modulation shifts the message signal to another central frequency without creating pairs of frequency components $X(f - f_o)$ and $X(f + f_o)$ where f_o is the central frequency and f the value that shifts the upper and lower frequency). Ideal Hilbert transform is useful to describe the complex envelope of a real modulated carrier signal. This transform has the effect of moving the negative frequency component $+ 90^\circ$ and the positive parts -90° .

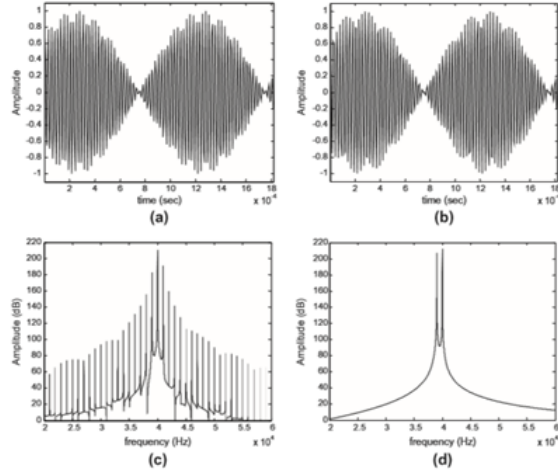


Figure 3.6: Comparison between the SRAM and the SBSAM

- Recursive Single Side Band Amplitude Modulation (RSS-BAM):

This method consists of the SSB modulator and the non-linear demodulator (NLD). The role of the NLD is to calculate the square of the envelope, which models the nonlinear acoustic propagation in the air by assuming that the second time derivative effect in the Berktays model can be entirely compensated. This blocks are combined with a distortion model (DM) and subtracted from the original input $g(t) = g_o(t)$ to obtain the distortion $d_i(t)$ at the output of the i th stage, where $i = 1, 2, \dots, q$. Each DM stage progressively reduces the distortion, and higher reduction is achieved by cascading several DM stages [17]. This method approximates the envelope as the SRAM method and avoids the errors introduced by multiple signals but, due to the high complexity of its recursive nature, a high-speed processor must be used to achieve real-time performance.

- Modified Amplitude Modulation (MAM):

See Tan et al. method [20]. This method employs an orthogonal amplitude modulation which has the flexibility of controlling the amount of THD with different complexity of the primary signals and adjusting the bandwidth requirements. This method also has a lower complexity than the recursive SSB AM. Table 3.1 summarizes the advantages and disadvantages of the modulation schemes studied

There are different recent proposals regarding modulation schemes. For example, the modified amplitude AM I, AM II and AM III in the work of Tan et. al. [85]. In every modulation method, a key affecting factor is the modulation index. A higher modulation index leads to a larger sound pressure level but also more severe distortion.

| Modulation Scheme | Advantages | Disadvantages |
|--|--|---|
| DSB Double Side Band Amplitude Modulation - 1983 Yoneyama | Employed to evaluate the performance of PAL. Easy implementation | High THD at high modulation index |
| SRB AM Root Square Band Amplitude Modulation - 1984 Kamakura | Lower THD than DSB achieved | Large bandwidth transducers |
| SSB AM Single Side Band Amplitude Modulation - 1984 Kamakura | Similar envelope to SRB AM with half the bandwidth and less power consumptions | Envelope occurs in case of multiple primary waves or broadband signals |
| RSSB Recursive Single Side Band Amplitude Modulation 2003 Croft, Norris | THD is progressively reduced by each recursion stage | High speed processor must be employed to achieve real time performance. High complexity |
| MAM Modified Amplitude Modulation - 2010 Tan, Gan | Scale bandwidth to an appropriate values | Complex implementation |

Table 3.1: Modulation schemes used in Parametric Array Loudspeakers

The more recent recursive method for PAL preprocessing reduces the amount of distortion to considerably with respect to the other techniques but there is a compromise between the cost of implementation and the effective distortion reduction and fundamental intensity self-demodulated. A careful selection of modulation index contributes to a good design of a PAL.[86]. The limitation on the research in terms of modulation schemes was the fact that the PAL has a fixed PWM modulation scheme, we had to focus on another stage of the signal and study the characteristics of this modulation method and the way it affects the THD of the self-demodulated signal.

3.4 On Pulse Wave Modulation

Other technique of modulation to encode the audio information in a ultrasonic carrier in PALs is the Pulse Width Modulation PWM (Figure (3.7)). This technique is mainly used to control the power supplied to electrical devices but is sometimes used to the modulation of information in audio and telecommunication. PWM encodes a non-constant envelope signal into a train of two levels pulses with varying widths. What the PWM does is to control the width of the pulse, generating a constant perception of voltage at the output of the load, the ripples are corrected by a smoothing filter. However, a conventional PWM modulated signal contains a large amount of distortion that cannot be removed by the reconstruction filter in a satisfactory manner [87]. The PWM technique combined with the PAL was reported by Miura [28] and the disadvantage of the PWM modulation is the introduction of harmonic distortion but on other hand it's easy to make prototypes because there are numerous integrated circuits available in the market [63]. The modulation of a signal using the PWM technique is shown in Figure (3.7).

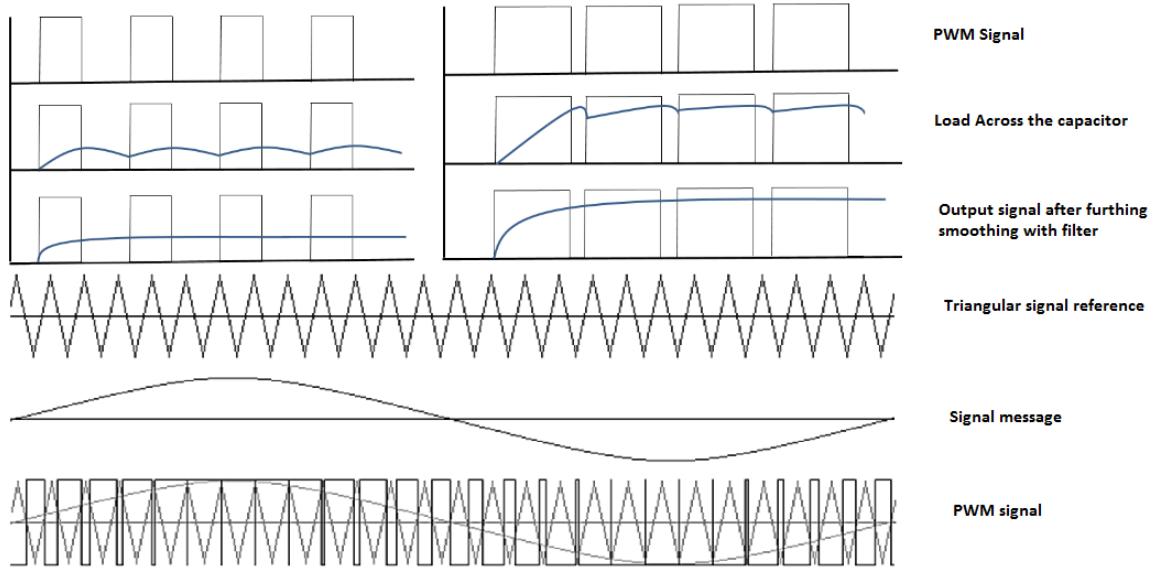


Figure 3.7: PWM Output voltage frequency relation

What basically happens is that the signal with the message is constantly compared to a reference triangular signal. If the value of the message is less than the value of the triangular signal, the value of the pulse assigned is low, if it is higher than the reference it is assigned high. The complete PWM method can be expressed in analytical way to determine sinusoidal harmonic components as follows

$$f(t) = f(x, y) = \frac{A_{00}}{2} + \sum_{n=1}^{\infty} (A_{0n} \cos(ny) + B_{0n} \sin(ny)) + \sum_{m=1}^{\infty} (A_{m0} \cos(mx) + B_{m0} \sin(mx)) + \sum_{m=1}^{\infty} \sum_{n=-\infty}^{\infty} (A_{mn} \cos(mx + ny) + B_{mn} \sin(mx + ny)) \quad (3.7)$$

where

$$A_{mn} + jB_{mn} = \frac{1}{2\pi^2} \int_{-\pi}^{\pi} \int_{-\pi}^{\pi} f(x, y) e^{j(mx+ny)} dx dy \quad (3.8)$$

Where it is assumed the existence of two temporal variables, $x(t) = \omega_c t + \theta_c$ for the carrier and $y(t) = \omega_o t + \theta_o$ for the message, each one of the signals assumed periodic and independent. This is the output of the most known method to determine the harmonic component of a PWM signal originally developed by Bowes and Bird [88]. With this representation for all PWM algorithms the process of determining the magnitudes of various harmonics [89] becomes the process to evaluate the double Fourier integral for the output of the signal composed by the carrier and the message. Each of the summations in equation 3.7 represent a harmonic. The first summation represents the low frequency message signal and contains harmonics of base band of low frequency, The second summation corresponds

to the harmonics of the carrier which are relatively high. The third summation represent the set of all possible frequencies formed from addition and subtraction of the harmonics of the waveform modulator and the message waveform and its baseband harmonics [90]. As a consequence of the modulation process PWM the output presents multiple harmonics of the carrier and multiples harmonics known as lateral band harmonics that are grouped around the Frequency of the carrier signal [90].

In the loudspeaker used for the experiments, the stage of modulation of the audible signal over the ultrasonic was made in a stage after the DSP just before injecting the signal to the piezotransducers using PWM technique to encode the audio in the ultrasound carrier. PWM for modulation is a more practical solution in terms of implementation but in terms of distortion is not a good solution to be used in parametric arrays because the high content of harmonics that this technique inherently have. All these harmonics combined with the harmonics produced by the self-demodulation process generate the harmonic spectrum content that a PAL that uses PWM modulation has. A confirmation of this will be shown in the last results chapter where a chirp signal recorded from the PWM parametric speaker shows a high harmonic content.

Next chapter introduces the contribution subjected to the PWM limitation of the conditioning stage of the signal to characterize the PAL.

Chapter 4

Loudspeaker Modelling by statistical design of experiments.

Loudspeaker mathematical modelling is an interesting problem that can't be tackled analytically. In this contribution statistical Design Of Experiments (DOE) is conducted to obtain empirical models to correlate with the theoretical behavior of this kind of loudspeakers.

The Parametric Array Loudspeaker (PAL) to be studied is intended to be used in artistic sound installation reason why the quality of the sound sought was a parameter of great importance thinking about the comfort of the viewer. there are two principal limitations in the production of sound from ultrasound which contribute to the perceived audio quality: Total Harmonic Distortion (THD) and the inherent impossibility of low frequencies reproduction [91]. Both are the response variables of the DOE proposed. DOE is a systematic, rigorous approach to engineering problem-solving that applies principles and techniques at the data collection stage so as to ensure the generation of valid, defensible, and supportable engineering conclusions, carried out under the constraint of a minimal quantity of experiments, time, and money [92]. Figure 4.1 illustrates DOE as a cyclic scientific methodology to generate knowledge through hypothesis validation and problem modeling [93]

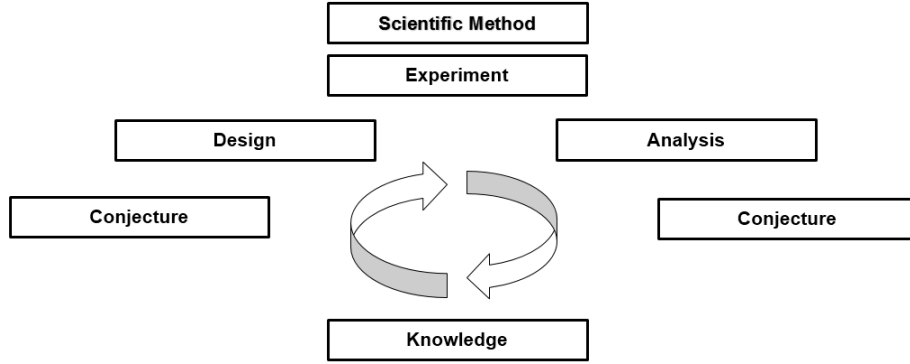


Figure 4.1: Cycle of the Design of Experiment methodology

There are a few and recent works interested in the characterization of a PALs to understand the variables involved in the production of the acoustic field from to use them in diverse applications, but works with a design of experiments of PAL of this type have not been very reported. The work of Calicchia for example presents the analysis of the pressure field generated by the commercial PAL AS8 Audio Spotlight as a function of the distance from the microphone and can be found in [15]. They characterize the near to the far acoustic fields specifically for non-destructive detection of detachments in panel paintings. In this work the author didn't consider interaction between the independent variables and performed the analysis changing one variable every time (OVAT).

Another similar recent work is the work of Non-Destructive Testing (NDT) found in [67] where they mentioned some aspects that are taken into account during their research work, not seeming to have a particular DOE methodology. They take into account variables or factors that are involved in the metrological characteristics of the PAL, but they don't report an analytical characterization of the loudspeaker. The Work of Ju and Kim [1] is also about the characteristics of a PAL; they studied the directivity and attenuation characteristics of the parametric loudspeaker in the near field where they desired to use it. In the near field, the ultrasonic carrier coexists with the generated audible sound influencing performance measurements. On the other hand, we refer the work of Ikefuji [91] because the interest it shows in the quality of sound from a PAL, proposing a method for reducing harmonic distortion at high frequencies emphasizing power at the lower frequency.

Several works about experiments for analyze the behavior of PALs have been carried but at the time we have seen small amount of works using the methodology of statistical design of experiments. The work of Ji et al [94] is a study of the parameters effects on a PAL, they examine the performance with different apertures and modulation schemes with the developed acoustic filter carried out in their study, they used more a comparative ullustration between the theoretical model and the results of their experiments. Kohel et al. says that a subjective evaluation of loudspeakers is a difficult and time-consuming task, the parameters to be controlled are numerous and the results are very often context-dependent [95], in his paper he shows a design of experiment based in three paired compared experiences and made a multivariate analysis to see whether the preference scores were affected by the loudspeaker. Bai et al.

used a systematic design procedure for a Cross-talk Cancellation System. they use a Taguchi method, an experiment design procedure well suited to multivariate optimization[96].

In Section 4.1, the characterization of the PAL Soundlazer SL-01 was done in terms of the radiation pattern and electronic configuration. Section 4.2 is more about the considerations for the experimental setup. Section 4.3 is about the Design of Experiments methodology proposed and the Section 4.4 and 4.5 are about the Plackett Burman and Box Behnken designs respectively. Unlike the works mentioned about the characterization of loudspeakers we propose a methodology based on experimental statistical design which allowed us to discriminate the most active factors by being interested in a fixed study answer responses.

4.1 Characterization Parametric Array Loudspeaker

The parametric loudspeaker available for the experiments of the thesis was the SoundLazer SL-01 4.2. The first step was to know the system, A Soundlazer SL-01 was dismantled and electronic diagrams were drawn. Individual components were studied to find out signal transformations through the different stages.



Figure 4.2: Soundlazer model SL-01

This PAL has two operation options, one the standard mode audio input, and the other the test reference control signal (an irritating sound). In the standard control input mode the loudspeaker is operational and is waiting for the input. Figure 4.3 shows the electronics schematic inside it. TP red boxes in the figure indicate the test points used to study different stages of the signal in the circuitry.

The digital signal processor chip is the Analog Devices Adau 1701. It has an internal clock of 250 Mhz, a wordlength of 28-56-bit and makes 50 MIPS. Some characteristics of the conversion stages are 2 ADCs stages with an SNR of 100 dB. The THD + N is of -83 dB (0.007 %). It has 4 DACs with SNR of 104 dB and THD + N of -90 dB (0.003 %). Adau 1701 is a fully programmable DSP. Digital Signal Processing includes different capabilities that

are usually possible to deal with it like equalization, cross-over, bass enhancement, multiband dynamics processing, delay compensation, speaker compensation and stereo image widening

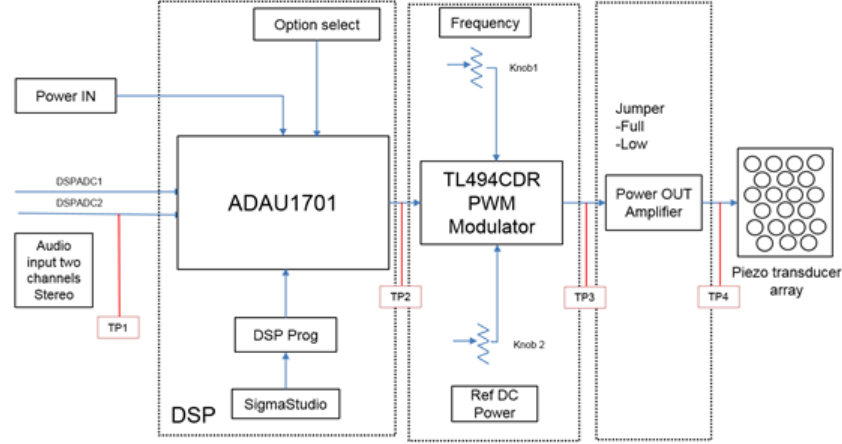


Figure 4.3: Electronic Schematic of the Soundlazer SL-01

The Device Under Test (DUT) uses the TL 494CDR PWM Modulator, a single chip that incorporates all the functions required in the construction of a pulse-width-modulation (PWM) control circuit. When we learned about this speaker we were hooked because they it offers a fully programable open source hardware. While the signal conditioning stage could be modified in the DSP, the PWM stage before the piezospeaker output conditions the scheme modulation, thus other modulation schemes were not tested and the interest of this work was directed towards the stage of conditioning of the signal. 39 PZT transducers connected in a parallel circuit compose the array of transducers (the DUT). The central frequency of each one is of 40 kHz with a bandwidth of 3-4.5 kHz.

4.2 Experimental setup

The experimental setup was mounted in an appropriate indoor space for these measures. Although was not an ideally insulated, phono-absorbent material panels were disposed to cover the room walls. The experiments were performed in the evening hours helped to achieve an ambient sound level for the test of 51 (dB). We took care in positioning the speaker at a large height (2 m) to avoid issues concerning sound reflections on the floor, and we made sure that not highly reflecting materials were present in front of the sound beam. The data acquisition card used was a U-PHORIA UMC202HD Audio Interface with MIDAS Mic Preamplifiers and USB 2.0. This card has a 24-bit/ resolution and up to 192 kHz sampling rate, and a 48 V phantom power.

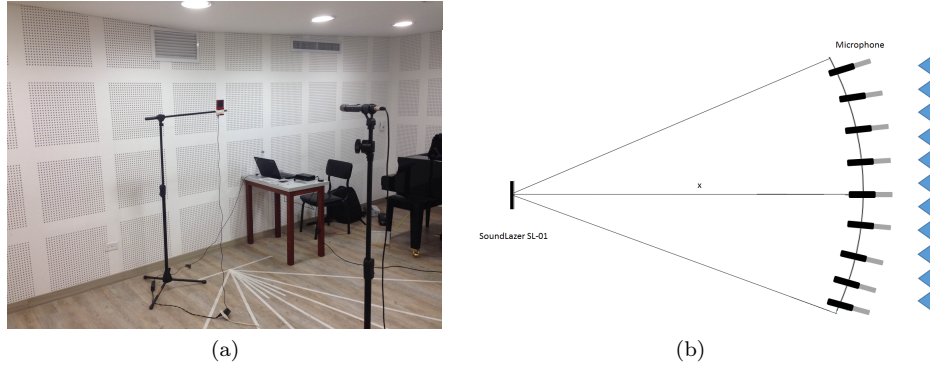


Figure 4.4: Experimental setup for the radiation pattern characterization of the Loudspeaker

4.2.1 Results of PAL radiation pattern

Figure (4.5) shows the PAL radiation pattern achieved at each one of its axes. The average distance intended to be used in the sound installations were 3 meters. Here we can notice the directionality of the speaker of 30 degrees at 3 m (i.e, a fall in 12 dB aprox for the highest intensity and fifteen degrees from the zero axes) were assumed as a good value to be taken into account of the design of the Soundscapes. It is also possible to have a notion of the frequency response from here. Notice how the low frequencies had a weak response to the same condition of the experiment and at the high frequencies response was higher.

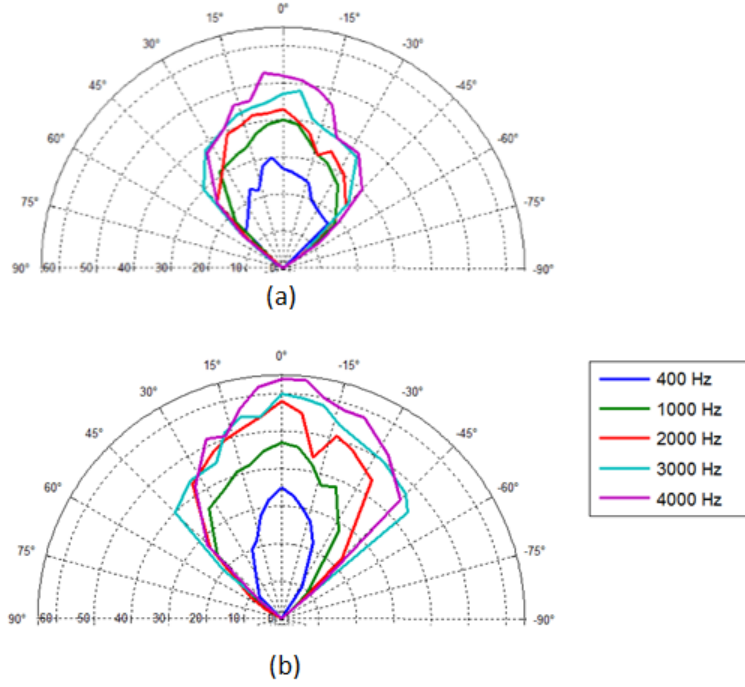
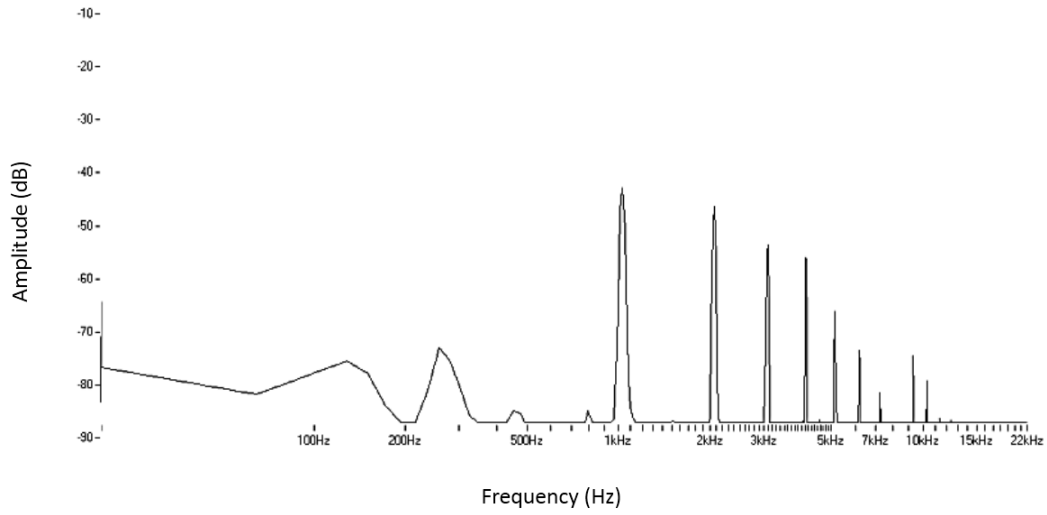
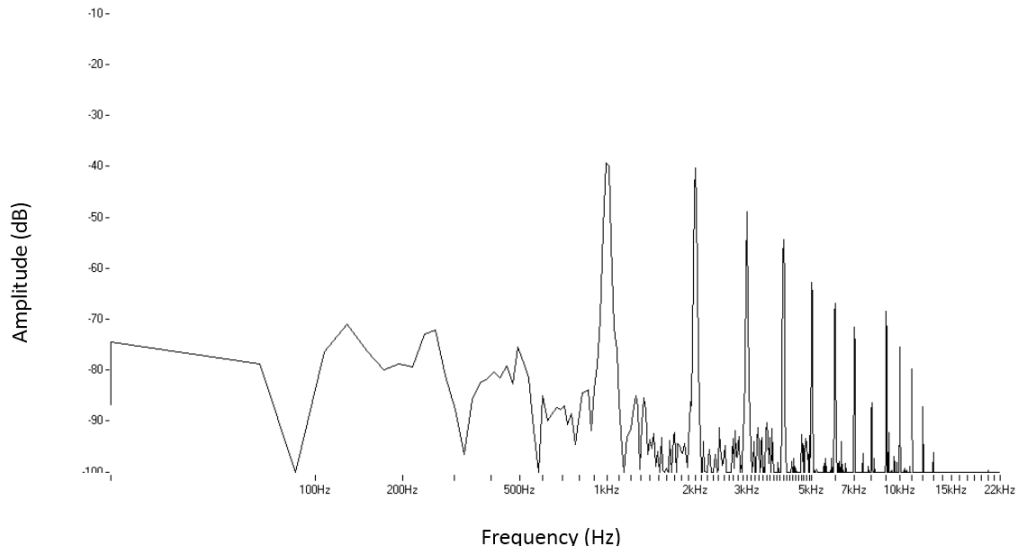


Figure 4.5: Soundlazer SL-01 sound field characterization

Two different microphones were tested to select the best option to take the measurements (Figure 4.6) to acquire knowledge about the level of noise of the audio recording devices. Figure 4.6a shows the AKG C1000S microphone which shows less noise level than the microphone Shure SM58 (Figure 4.6b). From these measurements we select the first microphone to make the recording in the experiments. The work of Ju [1] makes a detailed description of various frequent problems that happen with the microphones during the characterization of PALs. The first situation that they studied were the spurious signals generated by the non-linear distortions inside the microphone; they used a dome-shaped physical filter to suppress the ultrasound and the spurious noise. Another concern that they addressed was how the incidence angle affects the measurements between the microphone and the ultrasound propagation axis. They confirmed that the incidence angle had a negligible influence on the measured audible sound pressure.



(a) AKG C1000S Condenser Mic



(b) Shure SM58

Figure 4.6: Testing of two microphones to choose the more appropriate one

Once the speaker was physically described in section 4.1 and the experimental setup considerations were explained in 4.2, the section 4.3 will deal with the design of experiments performed to discriminate the most relevant factors of the pre-conditioning stage.

4.3 Design of experiments

First step in the DOE was to identify the factors that are involved in the experiment (Figure 4.7). As we see in the figure we have factors that we can control and also factors that we can't. These factors were chosen to represent the stages that we have often read in the literature about the preconditioning stage or dynamic control stage[17].

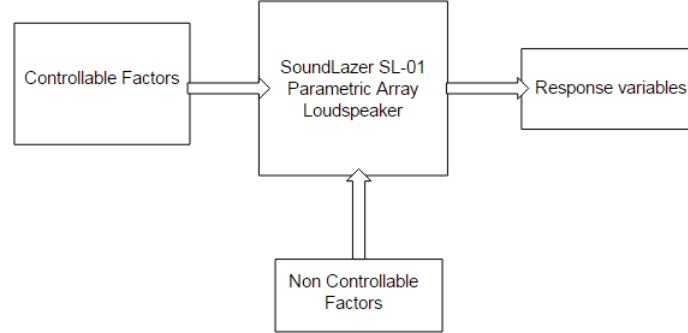


Figure 4.7: Controllable and non controllable factors for the DOE proposed

The controllable factors are the variables that are possible to vary, they are:

- Frequency tone
- Mixer
- Volume
- Gain
- Bandpass
- Compressor

The non-controllable factors are the variables that are not possible to vary:

- Background noise
- Temperature
- Pressure humidity

and the responses variables of interest are:

- Sound Pressure Level
- Total Harmonic Distortion

Figure (4.8) represents the stages in the conditioning stage chosen for the experiment. The audio signal is received from the input stimuli in stereo mode, the mixer block combines the two signals that come from the stereo input to produce a single mono signal. This block controls the intensity of each channel to be combined into one; the intensity

is controlled in db. The compressor is a signal processing operation that reduces the volume of low sound or amplifies quiet sounds by narrowing or compressing an audio signal dynamic range. The limiter is similar to the compressor with a different degree and perceived effect. It is used to prevent the input signal from clipping. The filter block represents a low pass and high pass filter that were put in series acting as a band pass filter. The frequency band that most PALs are well designed to work with is the range of the human voice (400-4000 Hz).

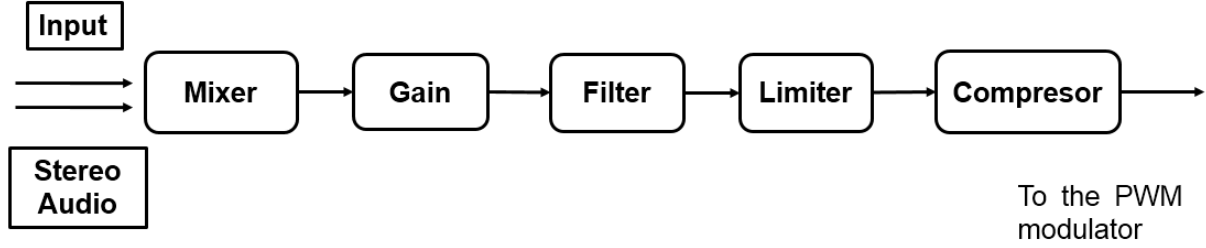


Figure 4.8: Sigmastudio TM digital signal processing stages

The software that allows the user to configure the firmware of the DSP chip inside the PAL is SigmaStudioTM, a graphical flow programming environment. After selecting the type of DSP and the inputs and outputs it is ready to run the code and change the PAL configuration. Figure (4.9) shows the general assembly of the experiment. The signal generator was implemented with a software function generator for a mobile device, (different software resources were used for the signal generation, signals apps for mobile devices are economical current alternative for experimentation). The distance between the PAL and the microphone was established for the experiment at 1 meter. For the DUT the Rayleigh distance was approximately 60 cm ($z_o = \frac{s}{\lambda} = \frac{\pi f_e r^2}{c_0}$) knowing that the wavelength of the primary waves is about 8 mm and the surface emission area about 4800 mm²

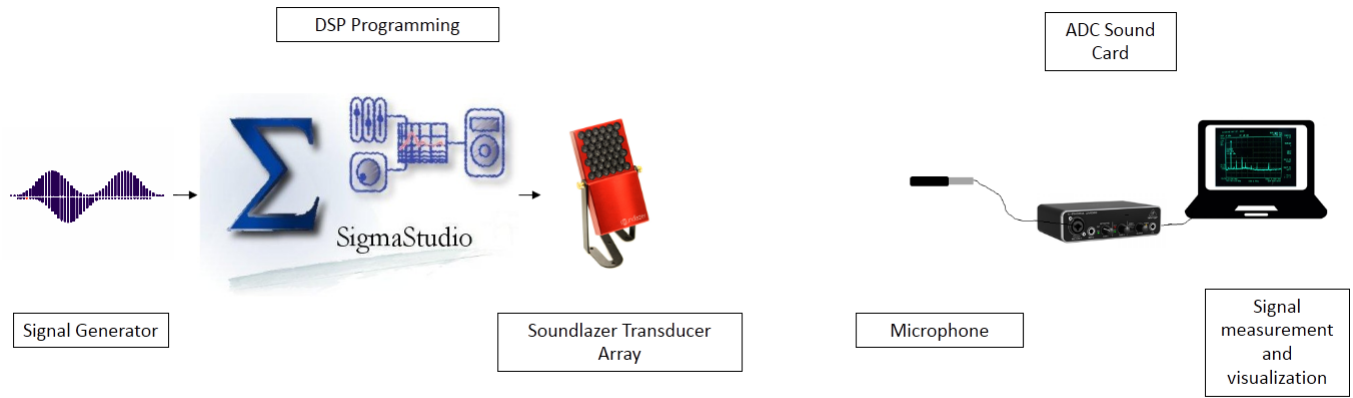


Figure 4.9: Schematic Design of Experiment to measure the THD and the fundamental Intensity of the Parametric Array Loudspeaker

Figure (4.10) shows the conditioning stage taken in account for the design of experiments represent in the graphical blocks in the software SigmaStudio™. In this figure two signals enter in the stereo input and in get mix in the first block. From here a gain stage connects the mixed signal to a high pass and low pass filter that combine to become a band pass to enter then to the compressor and limiter and from there get out to the DSP stage to enter the PWM stage before being emitted by the piezospeakers.

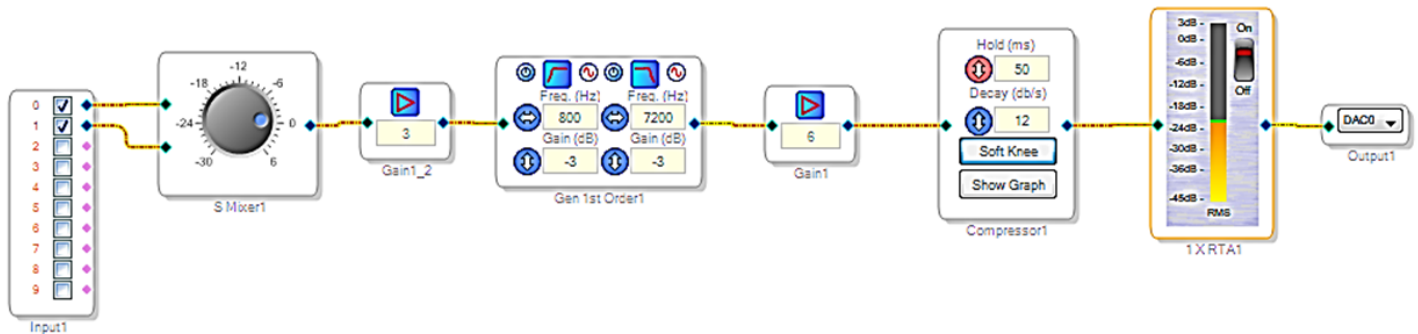


Figure 4.10: Precondition stage DSP

Table (4.1) shows the experimental conditions for the DOE. The ambient noise level was measured before each

test, trying to have the same condition always. The USB Behringer sound card was used with the software Audacity and the one spectrum analyzer software. The microphone, as we mention in the noise floor tests, was the AKG1000S.

| Characteristic | Value |
|------------------------|---|
| Ambient noise level | 51 (dB) |
| Sound Card | U-Phoria IMC202HD Behringer USB Audio Interface |
| Quantization | 24 bits |
| Parametric Loudspeaker | Soundlazer SL-01 |
| Microphone | AKG1000S |

Table 4.1: Experimental Conditions

Once the factors of interest were chosen, and we agreed on how to measure them and in what range of values each factor changes, the DOE methodology was proposed in order to determine, from the factors which we have control, which ones cause the most harmonic distortion, and which cause the perceived fundamental to be small. In the next section the two methodologies used, the Plackett Burmann and the Box Behnken are shown. This two methodologies are used in a joint way since the first allows to reduce a large number of factors to a few and the second leaves us model the output response from the most active factors

4.3.1 Plackett Burmann method

The number of factors involved in this experiment were chosen 11 (Table 4.2), and due to a full factorial design need too much experimental runs a screening design known as Plackett Burmann was proposed as an initial step to identify what were the most relevant factors because of their remarkable properties. This design works as a starting point and it is intended to be used with a more detailed design of experiments from the results it gives [97]. This kind of DOE was presented in 1946 by Robin L. Plackett and J.P Burman when they were investigating the dependence of some measured quantity on a significant number of independent variables or factors. Next Table (4.2) presents the selected factors for analyzing with Plackett Burmann design. It shows the summary of the factors that are possible to change over an established range in the conditioning stage of the signal in the DSP.

| | | Factor | Level - | Level + | Unit |
|-----|---|----------------------------|---------|---------|------|
| x1 | A | Sound Pressure Level | 50 | 100 | % |
| x2 | B | Frequency | 440 | 2500 | Hz |
| x3 | C | S Mixer 1 | 0 | 3 | dB |
| x4 | D | Gain 1 | 1 | 5 | |
| x5 | E | High Pass Filter Frequency | 300 | 500 | Hz |
| x6 | F | High Pass Filter Gain | 0 | -10 | dB |
| x7 | G | Low Pass Filter Frequency | 500 | 2500 | Hz |
| x8 | H | Low Pass Filter Gain | 0 | -10 | dB |
| x9 | I | Gain 2 | 1 | 3 | |
| x10 | J | Output Level | -20 | 0 | mS |
| x11 | K | Compressor Decay | 1 | 20 | dB/S |

Table 4.2: Design of experiments without the Chime stage

Table 4.3 shows the Hadamard matrix that we use to organized the experiments generated with linearly independent columns in a cyclical substitution with a generator particular pattern row composed by the sequence of + and - levels. These patterns are provided by the literature and software packages to design the run experiments for a different number of factors. Placket-Burman designs utilize two levels of each factor, the higher level (+) and the lower level (-). These levels were determined knowing the interval range that the factors change and making a first qualitative experiment with Marco to identify the most pleasant sound interval. For the 11 factors we had, the Hadamard Matrix for the Placket-Burman had 12 runs. In the right columns the output responses from each runs are reported. The response value of the THD is due to the relation of the harmonics measured. The fundamental and harmonics are measured in decibel relative to full scale (dBFS).

| | A | B | C | D | E | F | G | H | I | J | K | Fundamental | 1st Harmonic | 2nd Harmonic | THD % |
|----|----|----|----|----|----|----|----|----|----|----|----|-------------|--------------|--------------|-------|
| 1 | 1 | 1 | 1 | 1 | 1 | 1 | 1 | 1 | 1 | 1 | 1 | -51 | -60 | -56 | 77,17 |
| 2 | -1 | 1 | -1 | 1 | 1 | 1 | -1 | -1 | -1 | 1 | -1 | -59 | -78 | -97 | 47,62 |
| 3 | -1 | -1 | 1 | -1 | 1 | 1 | 1 | -1 | -1 | -1 | 1 | -66 | -78 | -100 | 54,32 |
| 4 | 1 | -1 | -1 | 1 | -1 | 1 | 1 | 1 | -1 | -1 | -1 | -57 | -77 | -100 | 47,16 |
| 5 | -1 | 1 | -1 | -1 | 1 | -1 | 1 | 1 | 1 | -1 | -1 | -62 | -81 | -100 | 44,72 |
| 6 | -1 | -1 | 1 | -1 | -1 | 1 | -1 | 1 | 1 | 1 | -1 | -47 | -56 | -83 | 66,48 |
| 7 | -1 | -1 | -1 | 1 | -1 | -1 | 1 | -1 | 1 | 1 | 1 | -62 | -58 | -58 | 84,23 |
| 8 | 1 | -1 | -1 | -1 | 1 | -1 | -1 | 1 | -1 | 1 | 1 | -47 | -49 | -82 | 71,42 |
| 9 | 1 | 1 | -1 | -1 | -1 | 1 | -1 | -1 | 1 | -1 | 1 | -62 | -75 | -88 | 58,94 |
| 10 | 1 | 1 | 1 | -1 | -1 | -1 | 1 | -1 | -1 | 1 | -1 | -43 | -50 | -68 | 72,13 |
| 11 | -1 | 1 | 1 | 1 | -1 | -1 | -1 | 1 | -1 | -1 | 1 | -57 | -73 | -100 | 53,17 |
| 12 | 1 | -1 | 1 | 1 | 1 | -1 | -1 | -1 | 1 | -1 | -1 | -44 | -60 | -65 | 67,18 |

Table 4.3: Hadamard matrix for PB DOE

The Placket Burman DOE was analyzed using the software R (codes in annex). The package BsMD was used to run the probability model that tell that the more relevant factor for the THD and the Fundamental Output. The

graphic below (Figure 4.11) is known as a bayes plot, it represent the posterior probability chart that the bayesian analysis of the R packet provides.

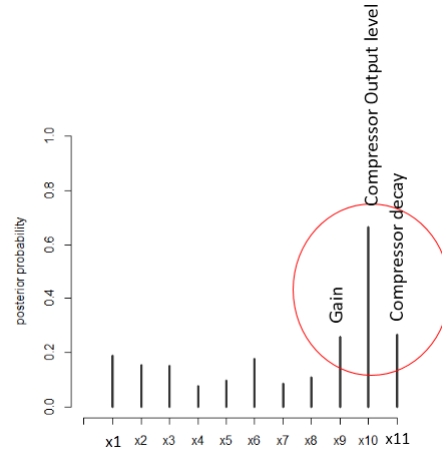


Figure 4.11: Plackett Burmann second experiment, Response THD

From Figure 4.11 we can determine the most important factors that affect the THD. This means that, from all 11 factors varied, Gain (x9), the Compressor Decay (x10), and the output-Level (x11) are the most influential.

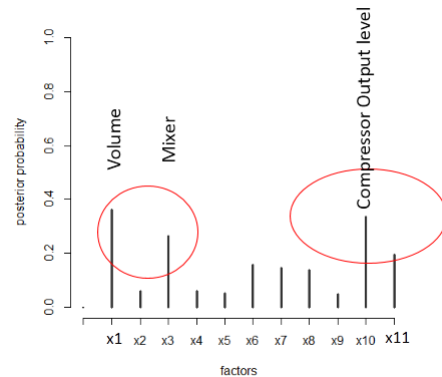


Figure 4.12: Plackett Burmann response for the analysis of the fundamental

From Figure 4.12 we can conclude that the main factors that minimize the fundamental analysis are the Volume (x1), the Mixer (x2), and the Compressor Decay (x3).

Plackett Burman DOE works well screening out the factors that are more active and influence more the behavior of the desired outputs. Because the arrangement on the Plackett Burmann have a complicated alias structure, the

Lenth's and normal plot are inappropriate [97]. The Bayesian analysis calculates a marginal posterior probability for different models loaded with the packet. Once the active factors are known, a more detailed analysis in terms of main effects and interaction can be carried out.

4.3.2 Box Behnken methodology

Once the three more relevant factor were obtained using the screening methodology we proceed to use the methodology Box-Behnken. This DOE gives the idea of the local shape of the response surface. Box-Behnken designs are independent quadratic designs. It means it does not contain an embedded factorial or fractional factorial design. These designs require fewer treatment combinations than other cases of central composite design in cases involving 3 or 4 factors. In this design, the treatment combinations are in the midpoints of the edges of the process space and at the centre. Table 4.4 shows the aleatoric run order in the first column, the following columns are the level of the factors that are being varied, and in the last column the values of the response for the THD.

| Run (Aleatoric) | Gain | Outputlevel | Compressor decay | THD Value % |
|-----------------|------|-------------|------------------|-------------|
| 15 | -1 | -1 | 0 | 34.25 |
| 6 | 1 | -1 | 0 | 45.92 |
| 1 | -1 | 1 | 0 | 41.2 |
| 8 | 1 | 1 | 0 | 50.2 |
| 9 | -1 | 0 | -1 | 37.77 |
| 10 | 1 | 0 | -1 | 31.48 |
| 11 | -1 | 0 | 1 | 76.55 |
| 13 | 1 | 0 | 1 | 91.04 |
| 5 | 0 | -1 | -1 | 17.7 |
| 4 | 0 | 1 | -1 | 29.17 |
| 14 | 0 | 1 | 1 | 78.23 |
| 12 | 0 | -1 | 1 | 86.65 |
| 2 | 0 | 0 | 0 | 51.24 |
| 3 | 0 | 0 | 0 | 49.3 |
| 7 | 0 | 0 | 0 | 53.51 |

Table 4.4: Box Behnken experimental design for the THD

This design of experiment give us an idea of the local shape of the response surface and all the regressions were made under the second order model. The equation of the surface is generated from the BB design. For the THD:

$$X_1 = \text{Gain } X_2 = \text{Output Level } X_3 = \text{Compressor decay } Y_1 = \text{THD}$$

$$Y_1 = 51,35 + 3,6X_1 + 3,89X_2 + 27,04X_3 - 0,66X_1X_2 + 5,19X_1X_3 - 0,76X_2X_3 - 1,09X_1^2 - 7,36X_2^2 + 8,95X_3^2 \quad (4.1)$$

Table 4.4 shows the aleatoric run order in the first column, the following columns are the level of the factors that are being varied, and in the last column the values of the response for the Fundamental test tone intensity.

| Run | Volumen | Mixer | Compressor decay | Fundamental Intensity value (dB) |
|-----|---------|-------|------------------|----------------------------------|
| 9 | -1 | -1 | 0 | -65 |
| 4 | 1 | -1 | 0 | -64 |
| 1 | -1 | 1 | 0 | -65 |
| 8 | 1 | 1 | 0 | -63 |
| 15 | -1 | 0 | -1 | -72 |
| 10 | 1 | 0 | -1 | -71 |
| 11 | -1 | 0 | 1 | -61 |
| 13 | 1 | 0 | 1 | -62 |
| 14 | 0 | -1 | -1 | -72 |
| 6 | 0 | 1 | -1 | -73 |
| 12 | 0 | 1 | 1 | -62 |
| 5 | 0 | -1 | 1 | -61 |
| 2 | 0 | 0 | 0 | -65 |
| 7 | 0 | 0 | 0 | -65 |
| 3 | 0 | 0 | 0 | -65 |

Table 4.5: Box Behnken experimental design matrix for the analysis of the fundamental

Equation of the responses generated from the BB design for the fundamental intensity:

X_1 = Volume, X_2 = Mixer, X_3 = Compressor decay, Y_2 = Fundamental Intensity

$$Y_2 = -65,33 + 0,375X_1 + 0,125X_2 + 5,25X_3 + 0,25X_1X_2 - 0,5X_1X_3 + 0,5X_2X_3 + 0,79X_1^2 + 0,29X_2^2 - 1,95X_3^2 \quad (4.2)$$

Figure (4.13) shows each of the output responses of the interaction between two factors per plot. It is possible to affirm that for a high THD, as well as for the fundamental tone perceived, the most active factor is the Compressor decay and also for the Fundamental tone perceived this same factor is responsible of this situation. And at this time we remember the following sentence from [17] "By compressing the dynamic range of the input speech or musical signal with a constant gain, the reproduced sound can be perceived clearly without noticeable distortion".

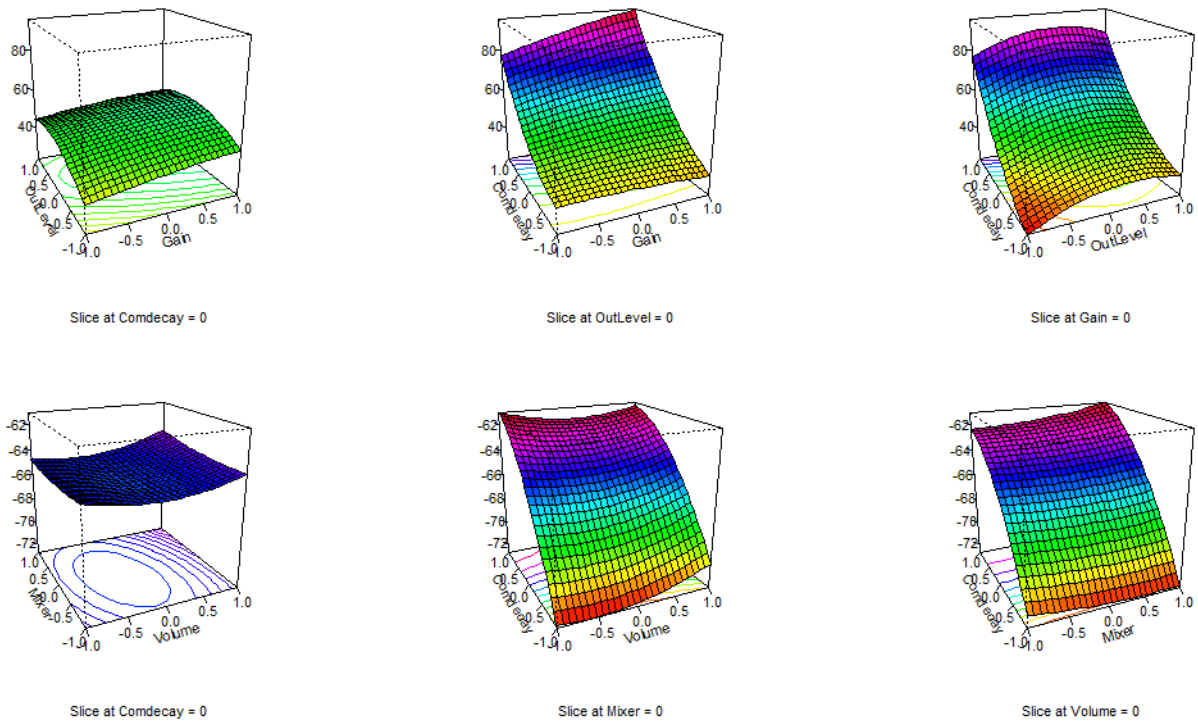


Figure 4.13: Surface response plots of 3-factor Box Behnken analysis

The contour plot of the equation 4.1 and 4.2 represent the second order model which is the basis of surface response for a slide at a constant value for one of the two responses. This second order equation contains linear terms, cross product terms and second order terms for each of the X_k . Next we have the contour plot of the response contrasting pairs of factors. This charts lets to know the direction of ascent and the location of probable maxima. At the end of the document in the section appendices there is a summary of the DOE outputs.

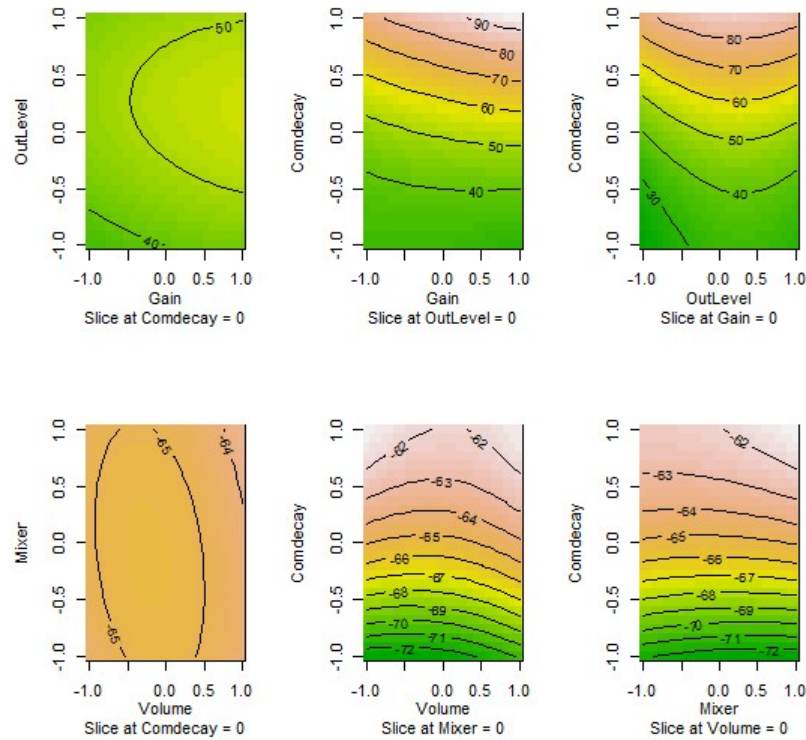


Figure 4.14: Contour plot of surface response

With the development of this chapter the DOE methodology was explored allowing us to acquire a capacity to model a phenomenon or, as in this case, to verify what factors affect the process the most. With the Plackett Burman methodology was possible to screen out the more active factors and, from them we can modelate the surface response with the Box Behnken deciding what were the most active factor of the experiment. As a future consideration it would be important to be able to have some degree of control over the factors of the environment (e.g temperature and humidity of the room). A methodology of this type can be useful to characterize processes where the factors that intervene are many and a factorial design becomes impractical because of the high number of runs involved

Chapter 5

Digital filtering techniques and signal distortion analysis.

In chapter 2 we addressed the non linear and linear phenomena around the topic of study. In the literature review, we noticed that in the last years there is an interest in modeling PALs using Volterra adaptive filters [98, 99, 100, 23]. What this technique looks for is to linearize the phenomena in certain approximate regions using this particular filter structure that is configurated through iterations. The weight coefficients of the filter are update until the error approaches to a minimum established [101, 102]. This approach is very interesting because it is possible to generate a model of a nonlinear system without having to deal with the numerical approaches to the KZK equation. In future work we want to apply this approach to the problem but at this time we will just develop some experience in the treatment and analysis of a signal.

As an initial step to approach the problem in this way, the purpose of this last results chapter is to learn about basic digital filters to achieve sufficient experience in this subject and gain the ability to analyze the total harmonic distortion of a signal. The region of interest to design our filters was the region of the human speech (300-4000 Hz) because from the literature of PALs we know the response in frequency of this loudspeaker is not flat in a broad frequency range and in most of the cases the attention is focused in this region. To study the signal, we build a GUI to analyze the signal and describe the linearity of the phenomena in some regions. Finally, in this chapter we find the analyzes in terms of harmonic distortion carried out on the signals in the range of frequencies of interest.

5.1 Chirp signal analysis

The work of Masunaga [103] studies the harmonic distortion on PALs using a time stretched logarithmic pulse. From this work we had the idea to test this speaker using a chime signal. A chirp is a signal in which the frequency increases (Up-Chirp) or decreases (Down-Chirp). We expect from it use to have a broad image of the behavior of the

PAL of the demodulated signal to understand not just for a pure tone, but also how the harmonics start appearing during the change of the signal.

We use a linear and a logarithmic chirp signals as input to the speaker. The chirp range from 20 Hz to 12000 Hz in 60 seconds and we expect to see lines corresponding to the multiple harmonics of the fundamental chime. The following spectrograms show the two chirp signals selected to filter and test the speaker, one being a linear chirp and the other a logarithmic chirp.

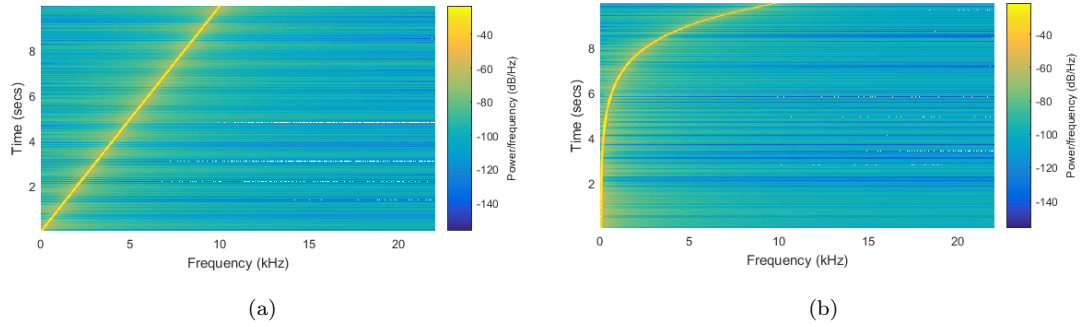


Figure 5.1: Chirp Signal tested in the PAL

Thus we decided to use the knowledge in DSP to develop a Graphical User Interface GUI in Matlab to filtering and analyze the signals. This GUI allows to load a sound and visualize it in the frequency and time domain. It shows the spectrogram and the peridogram and also generates filters using the filter design and filter visualization toolbox. Figure 5.2 below shows a screenshot of the GUI developed

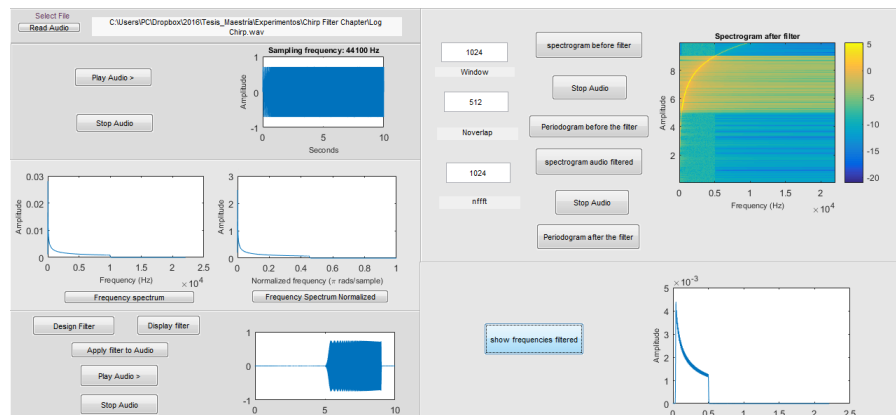


Figure 5.2: GUI Interface for the signal analysis

The use of this GUI is simple. First, the file in a .wav extension must be selected. From here it is possible to listen

and visualize the sound in the frequency spectrums. A filter must be designed assigning what kind of filter, the order, the magnitude of the response and the frequency ranges. The filter designed must be exported to the workspace and from there the sound could be filtered and visualized in the time domain. Signals can be also visualized in their spectrogram where it is possible to assign values to characteristics like the window length, the size of the overlap of windows and the number of bins to the FFT.

The spectrograms in Figures 5.3 and 5.4 are evidence that the place where the measurements were taken was not ideal, yet it was possible to extract some information. The vertical lines at constant frequencies are stronger in the near field. This kind of high frequency intensity is proper of electronic noise from the measurement equipment. The intensities in non harmonic areas and disordered patterns marked in red probably are recordings of some sounds of musical instruments because the place where they were taken is a room for musical rehearsals and wasn't completely insulated

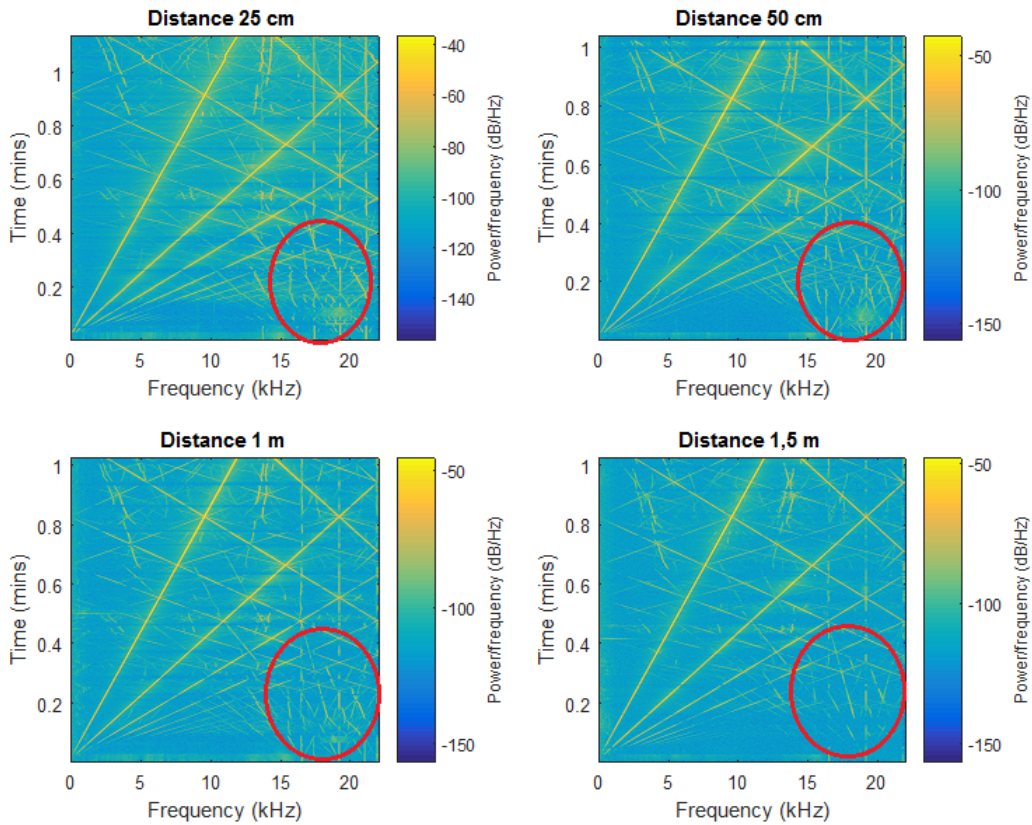


Figure 5.3: Time-dependent spectra of Chirp demodulated signal from Soundlazer PAL

The analysis of the demodulated signal through the spectrogram gives a good overview of the harmonics behavior in a broad frequency range. This analysis lets us know the reason of some subharmonics viewed in the periodogram of the signal. An aliasing phenomenon causes the reflection of the chime signal when it reaches 22 kHz which is the

Nyquist frequency for the signals sampled at 44010 Hz of this experiments.

Figure 5.4 is a nice graphic. These are some spectrograms of the linear chirp signal for the range 100 Hz and 5000 Hz recorded at 1 and 2 meters of distance. It let us see how the high harmonics corresponding to the fundamental demodulation, appear to be descending in frequency contrary to minor harmonics. From this analysis and knowing the harmonic content analytic expression of the PWM technique (eq. 3.7), we can conclude that these harmonics at high frequencies that decrease in frequency with time, are base-band harmonics (marked in red Figure 5.4) from the fundamental frequency harmonic of the PWM carrier demodulated.

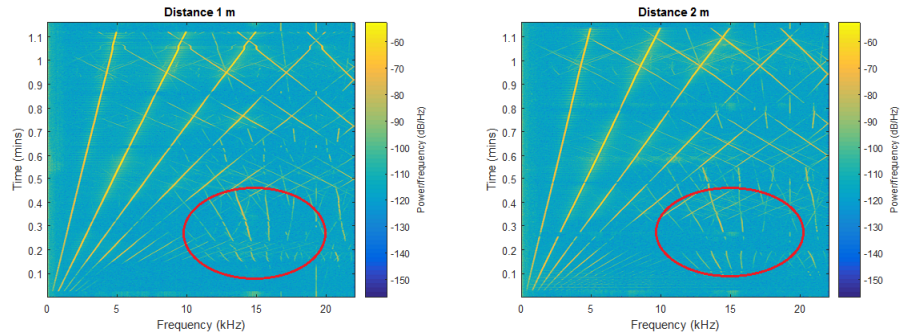


Figure 5.4: Time spectra of linear chirp signal demodulated 0-4500 Hz

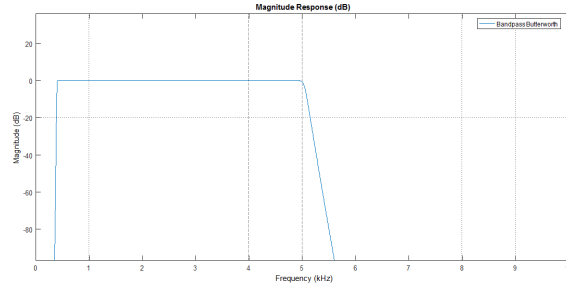
This initial section results let us understand a broad overview of the harmonic behavior over the audible range. In the next section we took this chirp signals and applied different filters to them to understand how they behave before and after the self-demodulation stage.

5.1.1 Digital filter analysis

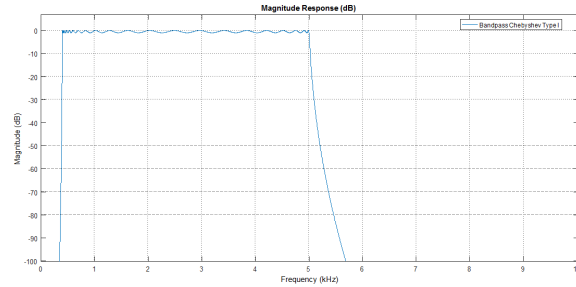
The work of Kim et al. [104] propose a method focused on a modified preprocessing digital signal processing stage to compensate for phase and amplitude mismatch caused for the preprocessing technique they used. This linearization technique gives us a reference of the interest of digital filter in audible sound production by ultrasound. From this work, we had a reference to study digital filters for this purpose. The test signals were filtered using a Low-Pass IIR Butterworth filter, a Low-Pass Chebyshev IIR Filter, a Low-Pass Equiripple FIR, and with this same configuration a Band-Pass frequency response filter to the same chirp test signals. The chirp signals were filtered and introduced to the audio input of the speaker to were then recorded at a distance of 1 m. The passband and stopband for each filter were selected equal, having a transition band always of 50 Hz. The magnitude response was set to 80 dB for all the filtering experiments.

Some difference is noticeable with the filters applied. The order of FIR direct form filter was higher than the order

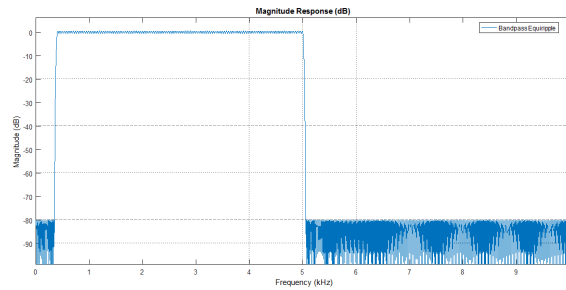
of the IIR Filter, (in the design filter option the order filter was set to its minimum filter order, for this configuration: Chevychev Type I Order: 44, Butterworth Order: 166, Direct FIR equiripple Order 2232). FIR filters have high computational requirements, but are however stable. In this characterization, the implementation of the filter doesn't require too much computational cost, because all the analysis was done offline. Difference between the two IIR filters was also noticeable. Butterworth filter has a sharper slope than the Chevy filter; this is noticeable at the end of the pass region: how a small trace appears longer in the Chevychev than the Butterworth filter. In the Chevychev filter the attenuation is slower. Figure 5.5 below shows the frequency response of the different filters designed.



(a) Bandpass Butterworth IIR filter



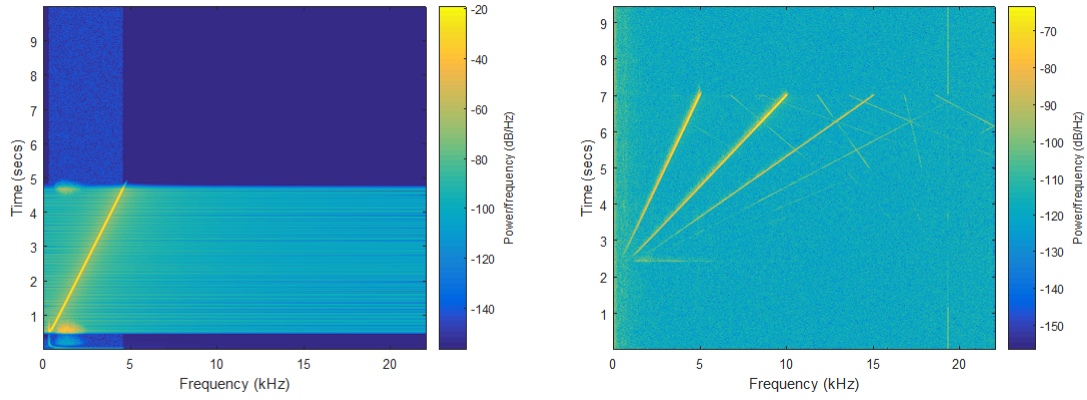
(b) Bandpass Chevychev IIR filter



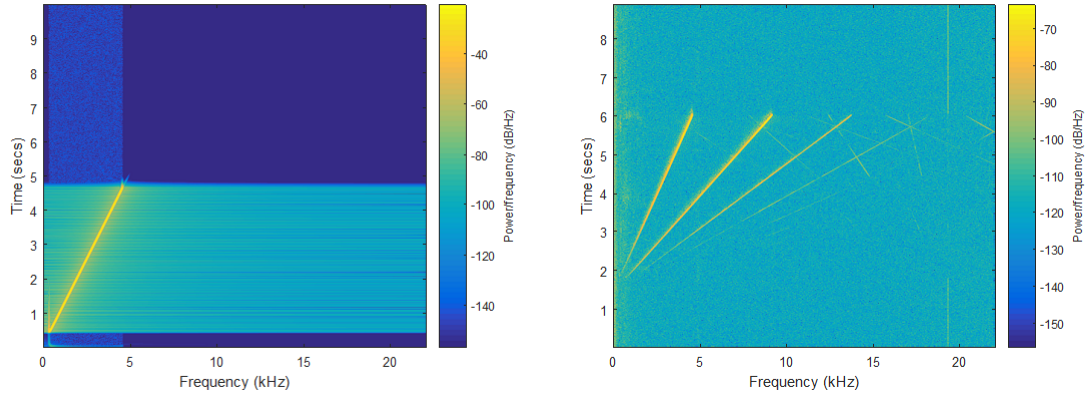
(c) Band-pass direct form FIR

Figure 5.5: Software Designed Band-Pass filters

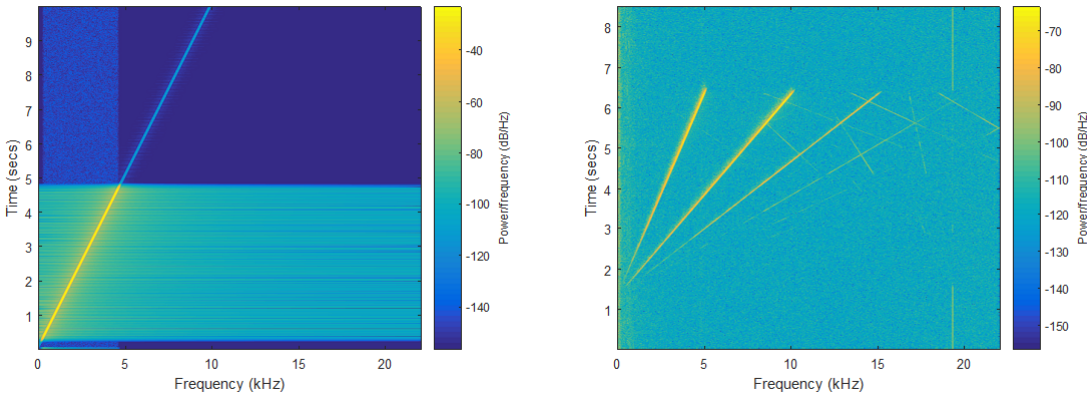
In Figure 5.6 the spectrograms of the chirp signals filtered before and after being emmitted for the band-pass filters case are shown:



(a) Bandpass Butterworth IIR filter chirp signal filtered before being input the PAL (b) Bandpass Butterworth IIR filter after air wave self de-modulation



(c) Bandpass Chebychev IIR filter chirp signal filtered before being input the PAL (d) Bandpass Chebychev IIR filter after air wave self de-modulation



(e) Band-pass direct form FIR chirp signal filtered before being input the PAL (f) Band-pass direct form FIR after air wave self demodulation

Figure 5.6: Chime signal after and before filtered

In the filtered images (Figures 5.6a 5.6c 5.6e), the ripple of the filter generates a trace in the spectrogram in the area in which the energy of the signal it is being filtered. Also, a square is noticeable in all the graphics in a faint blue; This is attributed to the gain that the filter has in the frequency region that blocks. The spectrogram of the signal demodulated (Figures 5.6b 5.6d 5.6f) shows the fundamental and the harmonics caused by the non linear interaction of the air.

From this graphics it is evident that the speaker has a smaller low-frequency response, as we have talked through the document. Notice that the intensities how are less for low frequencies compared to the high values. The signal its being introduced to the speaker at the same amplitude at whole frequency range of the chirp signals. The self-demodulation due the air diminishes the low-frequency intensity what is something we knew before: the PAL phenomenon has the inherent disadvantage of having a small low-frequency response.

Figure (5.7) below shows an example of this same practice of filtering to the log chime signal for a FIR filter designed. the output response of the demodulated field for the log chime signal let see the corresponding harmonics, and because the low pass filter the frequencies above 5 kHz were recorderd frequency due to the aliasing caused by the nyquist frequency. The self demodulated signals recorded are less noisy than the complete chirp signals because the filter eliminates the frequencies in the no pass range. Also the surround environment was more quiet

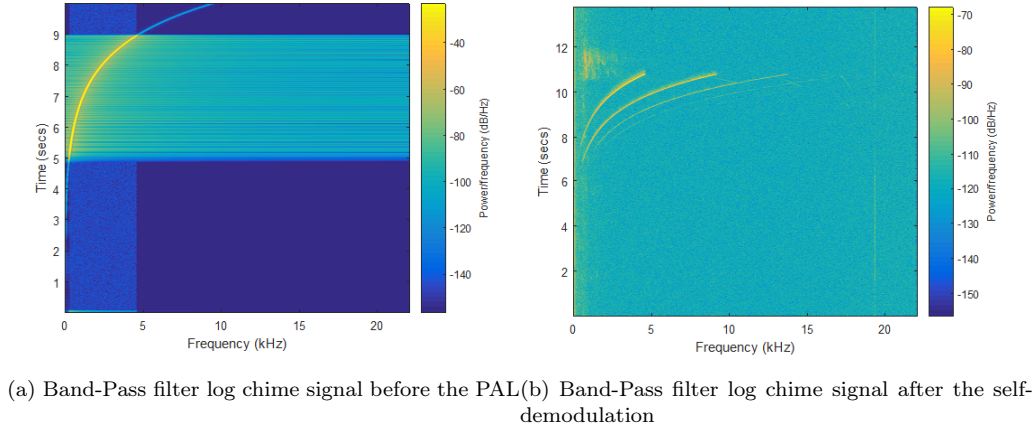


Figure 5.7: Band-Pass filter log chime signal

There exist some magnitude fluctuation or ripples evident in the filter response and we can make the filter transition region more narrow using additional coefficients however we cannot eliminate the pass band ripple. That ripple is known as Gibb's phenomenon [105] and manifests inself a function with an instantaneous discontinuity. The strength of IIR comes from their flexibility. IIR filter requires fewer coefficients that a FIR for the same set of specifications, which is why they are used when the sharp cutoff is needed, but the price to pay is that it can become unstable. In the appendices of this thesis the same analysis for the same kind of filters designed but for the low pass case.

5.1.2 Measurements of the harmonic content of a signal

The last part of this chapter is about the methodology developed for visualize the frequency spectrum of the signal and other values relates to the distortion of the signal like the THD, the SNR and the SINAD.

An script was done for visualizing and calculating some of the quantities of interest related to harmonic distortion integrated into the GUI. The next figures show the graphics that this script provides. The code in Matlab detects the most intense tone as the fundamental, and from it measures harmonics frequency and intensity values.

A sinusoidal single tone input is a well-established way to test speakers. Testing the distortion with more complex tones such as dialogues or speech is difficult because determining the content to measure is difficult, as there are several class of criteria by which to determine what should be used as the test signal. Figure (5.8) shows for example the periodogram power spectrum of a signal of 400 Hz. The strongest signal that could be identified in this chart is established as the fundamental tone and from it the harmonic are chosen as the powers multiple integers of this harmonics of that tone.

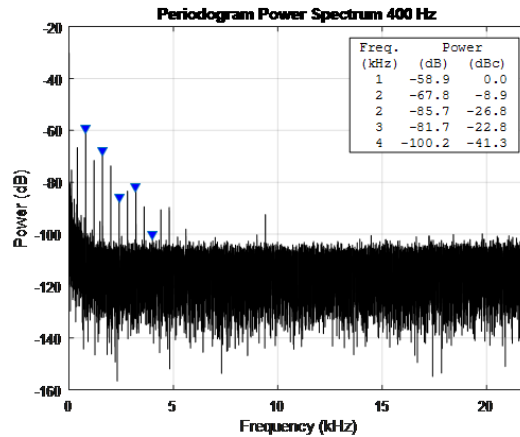


Figure 5.8: Periodogram power spectrum 400 Hz

For acoustic specifications, the value of THD is measured for a 1 kHz tone and at a given intensity value. Measurements of the THD depend on the equipment specification, the amount of THD and how it is recording. These values of the harmonic content also depend on the way the measures were made. The measures of THD were performed using some functions from the Signal Processing toolbox of Matlab, organized in a script that calculates several values such as the THD, the THD+N and the SINAD. Figure 5.9 shows the measure of the THD as the ratio of the RMS value of the fundamental signal to the mean value of the root-sum-square. THD of an ADC is also generally specified with the signal close to full-scale, although it can be specified at any level.

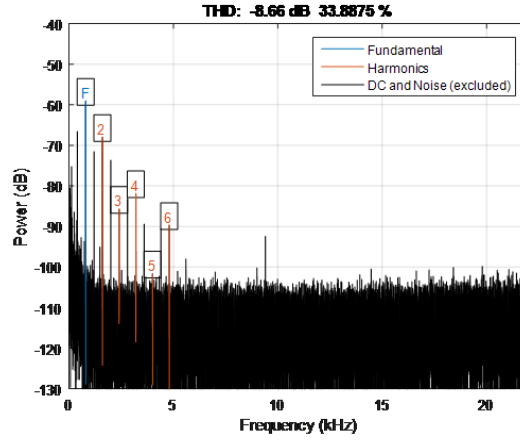


Figure 5.9: THD and five first harmonics

Figure (5.10) shows in blue the fundamental which respect the algorithm calculate and from the first five harmonics the measures.

The THD +N is the ratio between the RMS value of the fundamental signal to the mean value of the root-sum-squared of its harmonics plus all noise componentes (excluding dc).

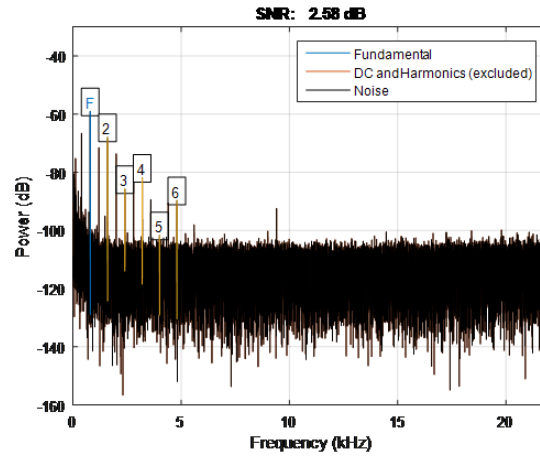


Figure 5.10: Signal to Noise Ratio 400 Hz

And finally in Figure 5.11, we show the measure of $SINAD = THD + N$

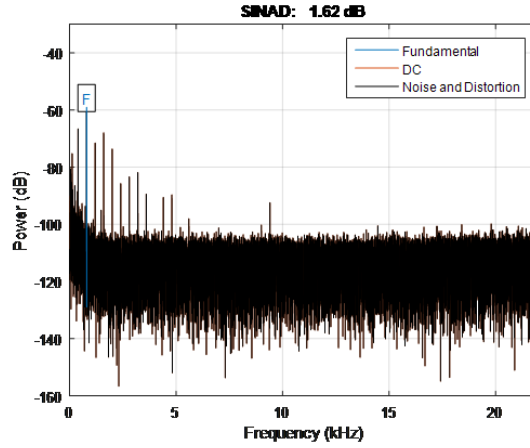


Figure 5.11: Signal noise + distortion

At the end of the document can be found other Figures obtained for tones (800 Hz Figure 7.5, 1200 Hz Figure 7.6, 1600 Hz Figure 7.7, 2000 Hz 7.8 Figure, 2400 Hz Figure 7.9, 3000 Hz Figure 7.10, 3400 Hz Figure 7.11) and the measurements related to the distortion in the section appendices. From these Figures we can visualize and quantify the distortion of tones in the range of human voice which is the range that these speakers are intended to work. Note that in some of these cases how the second harmonic for the input signal is higher than the fundamental then the distortion of this speaker is too high for some frequencies (In the appendices is possible to see other test tones and associated graphics)

From the first section of this chapter we were posible to understand the self demodulation phenomena in a broad frequency range using chirp signals and then, with the use of a GUI, we explore different filtering techniques and the self demodulated signals recorded from the PAL. With the development of the last section we develop the capacity to precess digital signals and to extract the analysis of the harmonic content. This capacity will be important in future work for model non linear systems through adaptive filters such as the Volterra filtering techniques.

Chapter 6

Conclusions

Two main issues prevent parametric loudspeakers from being extendedly employed in art, especially in music: 1) a hard-to-control harmonic distortion and 2) a narrow frequency bandwidth. PAL cannot reproduce frequencies below, at best, 300 Hz which mean that they are designed for speech reproduction (between 300 and 3400 Hz), but not so much for music with a broad range of frequencies. Algorithms implemented in commercially available loudspeakers can dramatically improve sound quality, but there is still much work to be done on THD and bass reproduction before this technology can be appealing for a broad range of artistic purposes.

The knowledge about the phenomenon of self-demodulation in this type of speakers due to nonlinear air behavior was acquired. It is important to emphasize here that the transversality of this research that makes it possible to share knowledge between different disciplines to create synergies that stimulate research. This research led us to discuss the nature of the physical phenomenon of the self-demodulation of amplitude modulated ultrasound fields illustrating the relationship with other areas such as Optics and the Beating phenomena in Acoustics. The understanding of the phenomenon let us understand the nature of the propagation of this sound emitter what enabled us to propose the acoustic and visual installation "The Forest and the Shadows" at "Paisajemed, Universidad EAFIT 2016" and the sound installation "The Sound House (2015)". As a conclusion, the phenomenon of ultrasonic sound generation is due to a non-linear interaction of the medium producing a linear propagation of audible sound.

We describe the different modulation existing techniques and their effects on total harmonic distortion on PALs. Nowadays, this modulation stage is made in a digital way using DSPs. Distortion of the self-demodulated signal depends heavily on the preprocessing techniques. One limitation, as a drawback of the research, was that this "fully programmable" (i.e., advertising with which the product is sold) speaker only was able to modify the signal stage of the dynamic range of condition because the signal carrier modulation was fixed as a PWM modulation dedicated.

As a consequence of this restriction, we decided to study through the DOE the conditioning stage of the signal. It is still the preprocessing stage where the attention is focused on reducing the THD of these loudspeakers. Different proposals that reduce the distortion complicate the system with some new technique especially those that have a recursive nature to reduce harmonic distortion. The analysis performed in section 3.4 told us why the PWM is not a good option to generate sound from ultrasound, illustrating why this method for modulating ultrasound, already

inherently has a great harmonic contribution. PWM modulation is an economical way to make a functional prototype that illustrates this physical phenomenon, but for sound quality purposes it is suggested modulation schemes such as SSB for its simplicity of implementation and its cost-of-implementation versus harmonic distortion.

A statistical methodology for the design of experiments was shown to verify what factors in the pre-conditioning stage are those who most have an influence on the harmonic distortion and the fundamental intensity perceived on a parametric speaker. It has been demonstrated to be useful for the detection of factors to build a model.

Initial Plackett-Burman design works screening out three factors for each one of the outputs of interest measured, and from that, we decided to run a three factors Box Bencksen design for three levels to determine the more relevant factor and the model surface. A second order equation was returned from the methodology proposed for each one of the responses. This methodology allows being a starting point for the characterization of acoustic equipment where large numbers of variables. It seems a little obvious that the result of the fundamental analysis is proportional to a factor like volume, although it does not seem a great discovery it can tell us somehow that the methodology adopted has some consistency. We propose to validate this model for future works on parametric speakers of better sound quality, as they also have the possibility of varying the modulation schemes.

In the fourth section results, we explored digital filtering techniques and implemented different measures to improve the quality of sound focused on harmonic distortion. In this section, a GUI in Matlab was designed to design filters and, visualize and analyze the filtered signals before and after the parametric loudspeaker device. In the visualizations obtained from the records we can visualize the harmonics corresponding to the base band of a PWM modulation. From some particular frequencies, the harmonic content was measured and analyzed. The Soundlazer PAL has a high harmonic distortion level. With the development of this research and acquisition of this technology we can conclude that for sound artistic installations, the Soundlazer SL-01 is not a good choice. This technology is still being developed and it is currently seen as a curious gadget, but the quality is still not good enough for high-quality definition music applications.

Chapter 7

Acknowledgements

Thanks to the gods I believe

I want to thank Professor Marco Alunno for giving me the opportunity to develop this research work within his research project I learned a lot from his perseverance, curiosity, punctuality and discipline to execute a project.

To Olga Lucia Quintero for the constant support she gives me. I admire her passion for generating around her an ecosystem of people who are passionate about learning. I thank you for helping me stay strong in times when I was emotionally down and for the orientation and advice she gives me.

To Daniel Sierra For his advice and constructive criticism during this process, I thank him for saying me things without filters, I enjoyed and learned in the discussions with him.

To my mother for not letting me fall for being the most special person I have, To my father for always being there supporting me and his financial help to finish this master. To my grandmothers for their support and their lunches. To my sister and to my uncles for their support and advice.

To my friends and colleagues in the GRIMMAT: “Tabla” Because the dependence we all generate with him in the group, a support for all. Paniagua, whenever someone needs advice in the group he goes to him, because of the experience that he transmits to the others. Leo “Lyx”, Anything I needed and asked him always gave me some time, thank you. Martin, thanks for the discussions generated. David “Orto” Because I bothered him countless times to lend me his audio card and to give me advice with working with audio signals.

To Luciano Angel because he introduced me to Marco Alunno’s research problem. I give thanks to the Science School of EAFIT University for being my alma mater and support me.

To the music department of the Universidad EAFIT for having provided spaces and equipment for the development of the experiments. To Lucho and Jair from the physics laboratories department, are those people without whom the department does not work.

To friends who gave me an inn when I lived outside the city and went daily to the University, how much I value

having left so many nights to stay overnight. To friends during life, each one has contributed in my personal formation to some degree in many ways.

Bibliography

- [1] Hyeon Sick Ju and Yang-Hann Kim. Near-field characteristics of the parametric loudspeaker using ultrasonic transducers. *Applied Acoustics*, 71(9):793 – 800, 2010.
- [2] Murata Manufacturing Co. Ltda. Application manual, ultrasonic sensors. 2009.
- [3] A. Ritty. Directional loudspeaker using a parametric array. *Acta Polytechnica Vol. 46 No. 4*, 2006.
- [4] Cerith Wyn Evans. Apparition. centre pompidou. *Video Reference*: <https://www.youtube.com/watch?v=78qrZY6HA4o>, 2014.
- [5] Marco Alunno. Andrés Yarce Botero. Directional landscapes: Using parametric loudspeakers for sound reproduction in art. *Journal of new music research*, 2016.
- [6] Marco Alunno. The forest and the shadows. Medellín, Universidad EAFIT, 12 2016.
- [7] J. Mc. Cartney. Supercollider: A new real time synthesis language. *Proceedings International music conference (ICMC 96)*, 1996.
- [8] Joseph O Norris James J. Croft. Theory, history and the advancement of parametric loudspeakers. *HSS Hypersonic Sound, American Technology Corporation ATC*, 2002.
- [9] Chuang Shi, Hao Mu, and Woon-Seng Gan. A psychoacoustical preprocessing technique for technique for virtual bass enhancement of the parametric loudspeaker. *ICASSP(2013)*, 2013. Digital Signal Processing Laboratory, School of Electrical and Electronic Engineering, Nanyang Technological University, Singapore.
- [10] Yoshiro Kumamoto Kenichi Aoki, Tomoo Kamakura. A parametric loudspeaker- applied examples. *Electrics and Communication in Japan, Part 3, Vol.77*, 1994.
- [11] Vincent Tournat. Introductory lecture on nonlinear acoustics. In *Research cientist at CNRS. Laboratoire d Acoustique de LuUniversity du Mayne*, 2014.
- [12] Woon-Seng Gan. Ee-Leng Tan. and Sen M Kuo. Audio projection: Directional sound and its application in immersive communication. *IEEE SIGNAL PROCESSING MAGAZINE*, 2011.
- [13] F. Farias and W. Abdulla. On rayleigh distance and absorption length of parametric loudspeakers. In *2015 Asia-Pacific Signal and Information Processing Association Annual Summit and Conference (APSIPA)*, pages 1262–1265, Dec 2015.
- [14] Chuang Shi and Yoshinobu Kajikawa. A convolution model for computing the far-field directivity of a parametric loudspeaker array. *The Journal of the Acoustical Society of America*, 137(2):777–784, 2015.
- [15] Paola Calicchia, Sara De Simone, Lucilla Di Marcoberardino, and Jacques Marchal. Near- to far-field characterization of a parametric loudspeaker and its application in non-destructive detection of detachments in panel paintings. *Applied Acoustics*, 73(12):1296 – 1302, 2012. Parametric Acoustic Array: Theory, Advancement and Applications.

- [16] Chuang Shi, Hideyuki Nomura, Tomoo Kamakura, and Woon-Seng Gan. Development of a steerable stereophonic parametric loudspeaker. *978-616-361-823-8 © 2014 APSIPA*, 2014.
- [17] Woon-Seng Gan, Jun Yang, and Tomoo Kamakura. A review of parametric acoustic array in air. *Applied Acoustics*, 73(12):1211 – 1219, 2012. Parametric Acoustic Array: Theory, Advancement and Applications.
- [18] Ivan Felis. Estudio y análisis del efecto paramétrico en aire y de los efectos de interponer una capa de material tras el transductor. Master’s thesis, Universitat Politècnica de Valencia, 2012.
- [19] Peifeng Ji. Ee-Leng Tan. Woon-Seng Gan. A comparative analysis of preprocessing methods for the parametric loudspeaker based on the khokhlov-zabolotskaya-kuznetsov equation for speech reproduction. *IEEE Transactions On Audio, Speech, and language processing*, 19(4), 2011.
- [20] Jing Tian Jun Yang and Woon Seng Gan. Parametric loudspeaker: From theory to applications. *ICSV21, Beijing, China, 13-17 July 2014 1 The 21st International Congress on Sound and Vibration ICSV21, Beijing, China*, 2014. Institute of Acoustics, Chinese Academy of Sciences, Beijing, China 100190.
- [21] G.B. Airy. The astronomer royal on a difficulty in the problem of sound. *Philosophical magazine and journal of science*, 1849.
- [22] Michalakis A. Averkiou, YangSub Lee, and Mark F. Hamilton. Selfdemodulation of amplitude and frequency modulated pulses in a thermoviscous fluid. *The Journal of the Acoustical Society of America*, 94(5):2876–2883, 1993.
- [23] C. Shi and Y. Kajikawa. Ultrasound-to-ultrasound volterra filter identification of the parametric array loudspeaker. In *2015 IEEE International Conference on Digital Signal Processing (DSP)*, pages 1–4, July 2015.
- [24] Kenji Uchino. *Advanced Piezoelectric materials*. Woodhead publishing, 2010.
- [25] Jon Datorro. Speaker arrays: Audio & ultrasonic. Technical report, Stanford University, 2016.
- [26] A.L.Thuras. R.T.Jenkins. H.T. Oneil. Extraneous frequencies generated in air carrying instense sound waves. *J.A.S.A*, 1935.
- [27] Limei X. Jianfang. Dagui. Design and characterization of a pvdf ultrasonic acoustic transducer applied in audio beam loudspeaker. *Proceedings of the IEEE International Conference on Mechatronics & Automation, Niagara Falls. Canada*, 2005.
- [28] Kazunori Miura. Ultrasonic directive speaker: 50+ piezo transducers generate sudible sound beam. *Readers Project, Elektor*, 2011.
- [29] Kleiner Mendel Barbagallo Mathias. Modulation and demodulation of steerable ultrasound beams for audio transmission and rendering. *Proceedings of the 11th Conference on digital audio effects, Espoo, Finland*, 2008.
- [30] Soomin Lee. Yoshihiro Shimomura. Tetsuo Kastura. Physiological response at short distance from a parametric speaker. *Journal at Physiological Anthropology. BioMed Central*, 2012.
- [31] Yoshihiro Shimomura. Soomin Lee, Tomoko Tawatari. The effects of parametric speaker sound on salivary hormones and a subjective evaluation. *Graduate School of engineering, Chiba University, Japan*, 2010.
- [32] Jammet HP. et al. Interim guidelines on limits of human exposure to airborne ultrasound. *Health Physics Volume 46(4)*, 969-974, 1984.
- [33] Joseph Pompei. *Sound From Ultrasound: The Parametric Array as an Audilble Sound Source*. PhD thesis, Massachusetts Institute of Technology, 2002.
- [34] Karoly WJ Wiernicki C. Ultrasound: Biological effects and industrial hygiene concerns. american industrial hygiene association journal. *1985, Volume 46(9)*, 488-496, 1985.

- [35] Alan G Madsen Martin L. Lendhart, Douglas G Richard. An assesment of airborne ultrasound risk from the audiospotlighth. *BiosonX Inc, Richmond, VA*, 2002.
- [36] Roman Vinokur. Acoustic noise as a non lethal weapon. *Wieland Associates, California, Sound and vibrations*, 2004.
- [37] Ritvik P. Mentha Sara L. Mattson Brian A. Kappus Robin L. Seitzman. Safety of the hypersound audio system in subjects with normal hearing. *Audiology research, Volume 5, pp 136*, 2015.
- [38] Dong Weiguo et al. Self demodulation of acoustic waves in air. *International congress of sound and vibration*, 2003.
- [39] H.O. Berkday. Possible exploitation of non linear acoustics in underwater transmitting applications. *J. Sound Vib. Vol 2 435-461*, 196 5.
- [40] Paolo Callichia et al. An overview of the development of the acoustic. *International Journal of Conservation Science, Rome, Italy- Vol. 4, pp. 621-632.*, 2013.
- [41] Robert T. Beyer. *Sounds of our time, two hundred years in acoustics*. AIP Press, Springer, 1998.
- [42] Daniel R. Raichel. *The science and applications of acoustics*. Springer, 2006.
- [43] Arthur Gordon Webster. Acoustical impedance, and the theory of horns and of the phonograph. *Proceedings of the National Academy of Sciences of the United States of America*, 5(7):285–282, 1919.
- [44] Dix Gordon R. Development and comparison of highly directional loudspeakers. *Brigham Young University, Master thesis submitted*, 2016.
- [45] Raviv Ganchrow. Perspectives of sound-space: The story of acoustic defense. *Leonardo Music Journal*, 2009.
- [46] Alejandro Costa Joaquin Castillo. Guia de ondas acústicas (bocinas): Generalidades. *Cátedra fundamentos de acústica y electroacústica*, 2012. Universidad Tecnológica Nacional, Facultad regional Córdoba.
- [47] Masahiro Sato Katsuhiko Tsumori Tetsuya Kurosaki Shigeki Kato. Development of flat panel speaker for personal computers. *Fujitsu Technical Journal No.14*, 2000.
- [48] Ferdinando Olivieri et al. Theoretical and experimental comparative analysis of beamforming methods for loudspeaker arrays under given performance constraints. *Elsevier, Journal of Sound And Vibrations*, pages 302–324, 2015.
- [49] Jussi Kuutti Juhana Leiwo and Raimo E. Sepponen. Local control of audio environment: A review of methods and applications. *Open technologies ISSN 2227-7080*, 2014.
- [50] James C. LIN. Further studies on the microwave auditory effect. *IEEE transaction on microwave theory and techniques*, MTT-25(11):938–943, 1977.
- [51] Westervelt PJ. Parametric acoustic array. *J Acoust Soc America*, 1963.
- [52] Mary Beth Bennett and David T. Blackstock. Parametric array in air. *The Journal of the Acoustical Society of America*, 57(3):562–568, 1975.
- [53] Masahide Yoneyama, Jun-chiroh Fujimoto, Yu Kawamo, and Shoichi Sasabe. The audio spotlight: An application of nonlinear interaction of sound waves to a new type of loudspeaker design. *The Journal of the Acoustical Society of America*, 73(5):1532–1536, 1983.
- [54] T. Kamakura et al. Development of parametric loudspeaker for practical use. *Proceedings of the 10th International Symposium on Non Linear Acoustics*, 1984.
- [55] Elwood Norris. Turtle beach corporation. Technical report, <http://corp.turtlebeach.com/>, 1996.

- [56] Joseph Pompei. Holosonics. Technical report, <http://www.holosonics.com/>., 2002.
- [57] Panphonics. Panphonics company. Technical report, <http://www.panphonics.com/> ., 2005.
- [58] Ultasonic Acouspade. ultrasonic-audio.com/products/acouspade. 2008.
- [59] Richard. Soundlazer parametric array loudspeakers. <http://www.soundlazer.com/>.
- [60] Jose Miguel Cadavid Tobon. Dispositivo de reproducción ultra-direccional de audio basado en las propiedades no lineales del aire. *Universidad de San Buenaventura, Medellín, Facultad de Ingenierías. Ingeniería de Sonido*, 2013.
- [61] Chuang Shi, Yoshinobu Kajikawa, and Woon-Seng Gan. Generating dual beams from a single steerable parametric loudspeaker. *Applied Acoustics*, 99:43 – 50, 2015.
- [62] Yoshinobu Kajikawa Chuang Shi and Woon-Seng Gan. An overview of directivity control methods of the parametric array loudspeaker. *APSIPA Transactions on Signal and Information Processing*, 3, e20, 2014.
- [63] P. Bratoszewski, J. Cichowski, and A. Czyzewski. Examining acoustic emission of engineered ultrasound loudspeakers. In *Signal Processing: Algorithms, Architectures, Arrangements, and Applications (SPA), 2014*, pages 60–65, Sept 2014.
- [64] Ferdinand Fuhrmann and Clemens Amon. Evaluation of a transaural audio system using parametric loudspeaker arrays. *Austrian Acoustic Association, Congress of Alps-Adria*, 2014. ISBN: 978-3-200-03921-6.
- [65] Camilo J. Taylor Alex Burka. Pedestrian collision warning for septa buses. *Electrics and systems engineering, University of Pennsylvania*, 2014.
- [66] Health protection agency UK. Health effects of exposure to ultrasound and infrasound. *Report of the independent advisory group on non ionising radiation. Document of the health protection agency. Radiation, chemical and enviromental hazards UK.*, (2010).
- [67] Sara De Simone Lucilla Di Marcoberardino, Jaques Marchala Paola Calicchia, and Jaques Marchal. Characterization of a parametric loudspeaker and its application in ndt. *Acoustics 2012, Apr 2012, Nantes, France. 2012*, 2012. Societe Francaise Acoustique.
- [68] Nobuo Tanaka and Motoki Tanaka. Active noise control using a steerable parametric array loudspeaker. *The Journal of the Acoustical Society of America*, 127(6):3526–3537, 2010.
- [69] Yoshinobu Kajikawa Kihiro Tanaka, Chuang Shi. Study on active noise control system using parametric loudspeaker array. *European Acoustics Association, Forum Acusticum, Krakov*, 2014.
- [70] K. Tanaka, C. Shi, and Y. Kajikawa. Study on active noise control system using parametric array loudspeakers. volume 2014-January, 2014. cited By 2.
- [71] Laura. Investigation into the feasibility of using a parametric array control in an active noise control system. *Proceedings of Acoustics, Busselton, Western Australia*, 2005.
- [72] Cristian Fugel. Simultaneous translation of lectures and speeches. *Springer Science+Business Media, Mach Translat* 21(209-252), 2007.
- [73] Olszewski D. Steerable highly directional audio beam loudspeaker. *Interspeech-Eurospeech, 9th European Conference on Speech communication and technology, Lisbon, Portugal*, 2005.
- [74] Kang E. Pampin J., Kollin J. S. Application of ultrasonic sound beams in performance and sound art. *Proceedings of the International Computer Music Conference*, 2007.
- [75] Gerald Oster. Auditory beat in the brain. 1973.

- [76] Emin Gabrielyan. The basics of line moiré patterns and optical speedup. *Switzernet Sàrl, Scientifica park of Swiss federal.*, Institute of Technology, Laussane (EPFL).
- [77] Jensen K. et al. Beat estimation on the beat. *Department of computer science, University of Copenhagen. IEEE Workshop on applications of signal processing to audio and acoustics*, 2003.
- [78] H. Pratt et al. Human brain potential evoked by acoustic beats and binaural beats. *Evoked potentials laboratory. Technion-Israel Institute of Technology and Neurology Research Laboratory, University of California, Irvine*.
- [79] Lord Rayleigh. *Theory of sound*. Dover publications,, 1945 re-issue.
- [80] David Ortiz Puerta O.Quintero. Una aproximación al filtrado adaptativo para la cancelación de ruidos en señales de voz monofónicas. *Congreso Latinoamericano de Control Automatico*, 2014.
- [81] Antonin Novak. *Identification of Nonlinear Systems in Acoustics*. PhD thesis, Université du Maine, Nantes, France, 2009.
- [82] Square D Product Data Bulletin. Power system harmonics causes and effects of variable frequency drives. *Bulletin No. 8803PD9402*, 1994.
- [83] Ee-Leng Tan. Woon Seng Gan. PeiFeng Ji. Jun Yang. Distortion analysis and reduction for the parametric array. *Audio Engineering Society. Convention Paper presented at the 124th Convention. Amsterdam. The Netherlands*, 2008.
- [84] Ying Wang. Min Chen. Hui Li. Zhe Zhou. Defining the parameters of truncated square-rooting dsb for parametric loudspeaker. *Proceedings of the 2007 IEEE. International Conference on Mechatronics and Automation. Harbin. China*, 2007.
- [85] Ee-Leng Tan. Woon Seng Gan. Jun Yang. Preprocessing techniques for parametric loudspeaker. *ICALIP*, 2008.
- [86] Chuang Shi. Yoshinobu Kajikawa. Automatic gain control for parametric array loudspeakers. *Department of Electrical and Electronic Engineering, Kansai University. IEEE*, 2016.
- [87] K. Hausmair, S. Chi, P. Singerl, and C. Vogel. Aliasing-free digital pulse-width modulation for burst-mode rf transmitters. *IEEE Transactions on Circuits and Systems I: Regular Papers*, 60(2):415–427, Feb 2013.
- [88] B. M. Bird S. Bowes. Novel approach to the analysis and synthesis of modulation processes in power converters. *IEEE Proceedings (London), Vol 3 No2 pp 216-223*, 1988.
- [89] Heng Deng Lars Helle Yin Bo Kim B Larsen. A general solution for theoretical harmonic components of carrier based pwm schemes. *Applied Power Electronics Conference and Exposition*, 2009.
- [90] Xavier Lozano Carreras. Análisis del contenido espectral de modulaciones de ancho de pulso para inversores fotovoltaicos multinivel conectados a red. *Ingeniería Eléctrica, proyecto final de carrera.*,
- [91] D. Ikefuji, M. Nakayama, T. Nishiura, and Y. Yamashita. Weighted double sideband modulation toward high quality audible sound on parametric loudspeaker. In *2013 IEEE International Conference on Acoustics, Speech and Signal Processing*, pages 843–847, May 2013.
- [92] NIST/SEMATECH. e-handbook of statistical methods. <http://www.itl.nist.gov/div898/handbook/>, date, 2017.
- [93] Christian Andres Diaz Helmuth Trefftz Olga Lucia Quintero Sakti Srivastava. Collaborative networked virtual surgical simulators (cnvss) implementing hybrid clientserver architecture: Factors affecting collaborative performance. *Presence Teleoperators & Virtual environments 23 (4): 393-409*, 2014.
- [94] Jun Yang Peifeng Ji. A preliminary experimental study of parameters’ effectson parametric loudspeakers. *IEEE International Ultrasonics Symposium Proceedings*, 2016.

- [95] Paquier M Koehl V. Loudspeakers sound quality: comparison of assesment procedures. *Acoustics Euronoise Paris*, 2008.
- [96] Chih Chung Lee Mingsian Bai, Chin Wei Tung. Optimal design of loudspeaker arrays for robust cross-talk cancellation using the taguchi method and the genetic algorithm. *Journal Acoustic Society America Volumen 117(5)*,, 2005.
- [97] George E Box, J Stuart Hunter, and William G. Hunter. *Statistics for experimenters, Design, Innovation, and Discovery*. Wiley, 1993.
- [98] Woon Seng Gan Wei Ji. Identification of a parametric loudspeaker system using an adaptive volterra filter. *Applied Acoustics*, 2012.
- [99] Chuang Shi and Yoshinobu Kajikawa. Identification of the parametric array loudspeaker with a volterra filter using the sparse nlms algorithm. *Department of Electrical and Electronic Engineering, Kansai University. ICASS P 2015 IEEE*, 2015.
- [100] Er MH Lee CM, Yang J. Gan Ws. Modeling nonnonlinearity on air with volterra kernels for use in a parametric array loudspeakers. *112th Convention of the Audio Engineering society*, 2002.
- [101] Y. Mu, P. Ji, W. Ji, M. Wu, and J. Yang. Multipoint linearization of parametric loudspeakers using volterra filters. In *Signal and Information Processing Association Annual Summit and Conference (APSIPA), 2014 Asia-Pacific*, pages 1–6, Dec 2014.
- [102] Yuta Hatano. Chuang Shi. Satoshi Kinoshita. Yoshinobu Kajikawas. A linearization system for parametric array loudspeakers using the parallel cascade volterra filter. *23rd European Signal Processing Conference (EUSIPCO)*, 2015.
- [103] Shohei Masunaga. Daisuke Ikefuji. Masanori Morise. Masato Nakayama. Takanobu Nishiura. Harmonic distortion measurement for a parametric loudspeaker with logarithmic time stretched pulse. *Acoustics Honk Kong*, 2012.
- [104] Young Wook Kim. Sung il Kim. Novel preprocessing technique to improve harmonic distortion parametricarray. *ICSP 02 Proceedings*, 2002.
- [105] Mohammadreza Niknam Hamidabad. Gibbs phenomenon. *Iran University of Science and Technology*, 2015.
- [106] Mark B. Moffett and Robert H. Mellen. Model for parametric acoustic sources. *The Journal of the Acoustical Society of America*, 61(2):325–337, 1977.
- [107] C. Shi and W. S. Gan. A preprocessing method to increase high frequency response of a parametric loudspeaker. In *Signal and Information Processing Association Annual Summit and Conference (APSIPA), 2013 Asia-Pacific*, pages 1–5, Oct 2013.
- [108] Ali Onur Akar. Characteristics and use of a non-linear end fired array for acoustics in air. *Naval Postgraduate School NPS*, 2007.
- [109] Peter W. Alberti. The anatomy and physiology of the ear and hearing. *article on line book chapter Visiting University of Singapore*, University of Toronto Canada.
- [110] T Aoki . Kamakura. Y. KumamotoT. Kamakura. Y. Kumamoto. Parametric loudspeaker: Characteristics of acoustic field and suitable modulation of carrier ultrasound. *Electron Commun Jpn*, 74(9):76–82.
- [111] A. Arevalo, D. Castro, D. Conchouso, J. Kosel, and I. G. Foulds. Mems digital parametric loudspeaker. In *2016 IEEE 29th International Conference on Micro Electro Mechanical Systems (MEMS)*, pages 1098–1101, Jan 2016.
- [112] Audiospotlight. <https://holosonics.com/>.

- [113] Klaus-Jurgen Bathe. *Finite Element Procedures*. Prentice Hall/Massachusetts Institute of Technology, 1996.
- [114] J. L. S. Bellin and R. T. Beyer. Experimental investigation of an end fire array. *The Journal of the Acoustical Society of America*, 34(8):1051–1054, 1962.
- [115] Leo L. Beranek. *Acoustics*. Acoustic Society of America, American Institute of physics, 1954.
- [116] Buro Happold Bill Addis. A brief history of design methods for building acoustics. *Proceedings of the Third International Congress on Construction History*, 2009.
- [117] Yoshinobu Kajikawa Chuang Shi. Synthesis of volterra filters for the parametric array loudspeaker. *ICASSP(2016)*. *IEEE 978-1-4799-9988-0*, 2016.
- [118] *Digital Analysis of geophysical signals and waves*. <http://dagsaw.sdsu.edu/4.5.html>, 2016.
- [119] Paulo Diniz. *Adaptive Filtering and practical implementations*. Springer, 2013.
- [120] Emmanuel C Ifeakor. Berrie W. Jervis. *Digital signal processing a practical approach*. Adison Wesley, 1995.
- [121] Kenneth G. Foote. Parametric acoustic array and p. j. westervelt: A tribute. *The Journal of the Acoustical Society of America*, 119(5):3232–3232, 2006.
- [122] Yang-Sub Lee. Mark F. Hamilton. Time-domain modeling of pulse finite-amplitude sound beams. *Journal Acoustic Society of America* 97, 1995.
- [123] Zbigniew Hanzelka. Andrzej Bien. Power quality application guide. harmonic, interharmonics. *Copper Development Association. IEE Endo*, 2004.
- [124] H. Hobaek. S. Tjøtta. Theory of parametric acoustic arrays. *Journal de physique colloques*, 1979.
- [125] Hypersound.
- [126] D. Ikefuji, M. Nakayama, T. Nishiura, and Y. Yamashita. Robust sound image localization for moving listener with curved-type parametric loudspeaker. In *2015 Asia-Pacific Signal and Information Processing Association Annual Summit and Conference (APSIPA)*, pages 1045–1049, Dec 2015.
- [127] Institute for Information and Austria Communication Technologies Steyrergasse 17 8010 Graz, editors. *Akustische Vermessung parametrischer Lautsprecherarrays im Kontext der Transauraltechnik*, 2014.
- [128] S. Kashiwase and K. Kondo. Towards a parametric speaker system with human head tracking beam control. In *2014 IEEE 3rd Global Conference on Consumer Electronics (GCCE)*, pages 22–23, Oct 2014.
- [129] Jin-Young Kim, Seung-Soo Choi, In-Dong Kim, and Wonkyu Moon. Design of compact and high-efficiency power supply and power amplifier for parametric array transducer. In *Future Energy Electronics Conference (IFEEC), 2015 IEEE 2nd International*, pages 1–5, Nov 2015.
- [130] Mark F. Hamilton Thomas D. Kite, John T. Post. Parametric array in air: Distortion reduction by pre-processing. *ICA/ASA Proceedings, Seattle*, 1998.
- [131] Richard Lyons. Understanding digital signal processing. *Prentice Hall*, 2013.
- [132] Shohei Masunaga. Daisuke Ikefuji. Masanori Morise. Masato Nakayama. Takanobu Nishiura. Steering for listening area of reflective audio spot with parametric loudspeaker array. *Proceedings of Meetings on Acoustics, ICA*, 2013.
- [133] Bernhard Schwarz-Rohr Volker Mellert. The origin in audio signal in a beam of modulated ultrasound in air. *Proceedings of CFA/DAGA'04, Strasbourg, France*, 2004.
- [134] Harold M. Merklinger. Improved efficiency in the parametric transmitting array. *Journal Acoustic Society of America*, 58(4), 1975.

- [135] Meyer Sound. Dsp beam steering with modern line arrays. *Meyer Sound. Technical report*, 2002.
- [136] Y. Mu, P. Ji, W. Ji, M. Wu, and J. Yang. Modeling and compensation for the distortion of parametric loudspeakers using a one-dimension volterra filter. *IEEE/ACM Transactions on Audio, Speech, and Language Processing*, 22(12):2169–2181, Dec 2014.
- [137] D. Olszewski and K. Linhard. 3g-3 optimum array configuration for parametric ultrasound loudspeakers using standard emitters. In *2006 IEEE Ultrasonics Symposium*, pages 657–660, Oct 2006.
- [138] Peifeng Ji. Weinlin Hu. Jun Yang. Development of an acoustic filter for parametric loudspeaker using phononic crystals. *Ultrasonics Elsevier*, 2016.
- [139] Joseph Pompei. The use of airborne ultrasonics for generating audible sound beams. *Journal of Audio Engineering Society. MIT Media Lab Cambridge, MA*, 47:726–731, 1999.
- [140] Raymond van der Rots and Arthur Berkhoff. Directional loudspeaker arrays for acoustic warning systems with minimised noise pollution. *Applied Acoustics*, 2014. <http://dx.doi.org/10.1016/j.apacoust.2014.09.024> 0003-682X/ 2014 Elsevier.
- [141] Alexandre Ritty. Bruno Gazengel. Pierrick Lotton. Pascal Hamery. Improvement of a directional loudspeaker by coupling of a piezoelectric film and acoustic cavities. *19th International Congress on Acoustics, Madrid*, 2007.
- [142] Seongju Chang Seongteak Jang, Dongjun Suh. Shadow sound system embodied with directional ultrasonic speaker. 2013. Dept. of Civil and Environmental Engineering KAIST, Daejeon 305-701, South Korea @kaist.ac.kr.
- [143] Yuta Hatano and Chuang Shi, Satoshi Kinoshita, and Yoshinobu Kajikawa. Linearization of the parametric array loudspeaker upon varying input amplitudes. *Proceedings of APSIPA Annual Summit and Conference 2015*, 2015. Kansai University, Osaka, Japan.
- [144] C. Shi and Y. Kajikawa. A comparative study of preprocessing methods in the parametric loudspeaker. In *Signal and Information Processing Association Annual Summit and Conference (APSIPA), 2014 Asia-Pacific*, pages 1–5, Dec 2014.
- [145] Steven W. Smith. *The scientist and engineers guide to Digital Signal Processing*. <http://www.dspguide.com/> Online book pdf, 1997-1998.
- [146] B.A. Stach. *Clinical Audiology: An Introduction*,. 2010.
- [147] X. Sun and K. Okada. High quality directional audio system. In *2008 Digest of Technical Papers - International Conference on Consumer Electronics*, pages 1–2, Jan 2008.
- [148] Yoshio yamasaki Shigeto Takeoka. Acoustic projector using directivity controllable parametric loudspeaker array. *Proceedings of 20th International Congress on Acoustics, ICA , Sydney, Australia*, 2010.
- [149] Manish Talwar. Removing of harmonics using labview. *International Journal of Advanced Research in Computer Science and Software Engineering*, 2015.
- [150] K. Tanaka, C. Shi, and Y. Kajikawa. Multi-channel active noise control using parametric array loudspeakers. In *Signal and Information Processing Association Annual Summit and Conference (APSIPA), 2014 Asia-Pacific*, pages 1–6, Dec 2014.
- [151] E. L. Tan, W. S. Gan, and C. H. Chen. Spatial sound reproduction using conventional and parametric loudspeakers. In *Signal Information Processing Association Annual Summit and Conference (APSIPA ASC), 2012 Asia-Pacific*, pages 1–9, Dec 2012.
- [152] Kazuo Ikegaya Tomoo Kamakura, Masahide Yoneyama. Developments of parametric loudspeaker for practical use. *10th International Symposium on Nonlinear Acoustics*, 1984.

- [153] Glen Wade. Human uses of ultrasound: ancient and modern. *Ultrasonics, Elsevier*, 38:1–5, 2000.
- [154] Wei Ji. Ee-Leng Tan. Woon Seng Gan. Baseband distortion modeling for a parametric loudspeaker system using volterra kernels. *Digital Signal Processing Laboratory, School of electrical and electronic engineering. Kansai University. Osaka Japan*, 2015.
- [155] Jun Yang, Woon-Seng Gan, Khim-Sia Tan, and Meng-Hwa Er. Acoustic beamforming of a parametric speaker comprising ultrasonic transducers. *Sensors and Actuators A: Physical*, 125(1):91 – 99, 2005.
- [156] K. Yasui, U. Masashi, W. Quan, X. Wu, and H. Furuhashi. One-to-one audio guidance system using human vision, designed for a guide robot. In *2015 International Conference on Computational Science and Computational Intelligence (CSCI)*, pages 841–842, Dec 2015.
- [157] Y. Zhang and L. Tao. Factors analysis of the sound field for audio directional systems. In *Electronic and Mechanical Engineering and Information Technology (EMEIT), 2011 International Conference on*, volume 2, pages 758–761, Aug 2011.
- [158] Lijun Zhu and Dinei Florencio. 3d numerical modeling of parametric speaker using finite-difference time-domain. *internship at Microsoft Research*, 2015.

Appendices

```
#####  
#  
# Design of experiments Plackett Burmann  
# 11 Factors, 2 Levels, 12 runs  
# Andrés Yarce Botero  
#  
# Libraries: BsMD rsm  
#  
#####  
  
library(BsMD)  
  
# Level for each run for each factor  
  
A=c(1,-1,-1,1,-1,-1,-1,1,1,1,-1,1)  
B=c(1,1,-1,-1,1,-1,-1,-1,1,1,1,-1)  
C=c(1,-1,1,-1,-1,1,-1,-1,-1,1,1,1)  
D=c(1,1,-1,1,-1,-1,1,-1,-1,-1,1,1)  
E=c(1,1,1,-1,1,-1,-1,1,-1,-1,1,1)  
F=c(1,1,1,1,-1,1,-1,-1,1,-1,-1,-1)  
G=c(1,-1,1,1,1,-1,1,-1,-1,1,-1,-1)  
H=c(1,-1,-1,1,1,1,-1,1,-1,-1,1,-1)  
I=c(1,-1,-1,-1,1,1,1,-1,1,-1,-1,1)  
J=c(1,1,-1,-1,-1,1,1,1,-1,1,-1,-1)  
K=c(1,-1,1,-1,-1,-1,1,1,1,-1,1,-1)  
  
# Output values THD and Fundamental value  
THD=c(77.17,47.62,54.32,47.16,44.72,66.48,84.23,71.42,58.94,72.13,53.17,67.18)  
  
summary(THD)  
Fundamental=c(49,41,34,43,38,53,38,53,38,57,43,52)  
summary(Fundamental)  
  
# Generate and print the array  
data1=data.frame(A,B,C,D,E,F,G,H,I,J,K,THD,Fundamental)  
print(data1)  
  
# Assign vectors for parts of the array  
X<- as.matrix(data1[,1:11])  
y1<-data1["THD"]  
y2<-data1["Fundamental"]  
  
# Generate Bayesian analysis for the output 1 y1  
data1y1.BsProb <- BsProb(X = X, y = y1, blk = 0, mFac = 11, mInt = 1,p = 0.20, g = 2.49, ng = 1, nMod = 10)  
plot(data1y1.BsProb)  
  
#Generate Bayesian analysis for the output 2 y2  
data1y2.BsProb <- BsProb(X = X, y = y2, blk = 0, mFac = 11, mInt = 1,p = 0.20, g = 2.49, ng = 1, nMod = 10)  
plot(data1y2.BsProb)  
summary(data1y1.BsProb)  
summary(data1y2.BsProb)  
  
# Linearize the two outputs to generate the Daniels plot  
length(y1)  
length(y2)  
  
# Lineal regression  
data1y1.lm <- lm(THD ~ A + B + C + D + E + F + G + H + I + J + K, data = data1)  
summary(data1y1.lm)  
data1y2.lm <- lm(Fundamental ~ A + B + C + D + E + F + G + H + I + J + K, data = data1)  
summary(data1y1.lm)  
print(coef(data1y1.lm))  
print(coef(data1y2.lm))  
  
#Daniel plot for the THD output  
par(mfrow=c(1,3),oma=c(0,0,1,0),pty="s")  
DanielPlot(data1y1.lm, half = TRUE, main = "Half-Normal Plot")  
DanielPlot(data1y1.lm, main = "Normal Plot of Effects")  
DanielPlot(data1y1.lm,faclab = list(idx = c(12,4,13), lab = c(" -H"," VG"," -B")),main = "Active Contrasts")  
  
#Daniel plot for the Fundamental  
par(mfrow=c(1,3),oma=c(0,0,1,0),pty="s")  
DanielPlot(data1y2.lm, half = TRUE, main = "Half-Normal Plot")  
DanielPlot(data1y2.lm, main = "Normal Plot of Effects")  
DanielPlot(data1y2.lm,faclab = list(idx = c(12,4,13), lab = c(" -H"," VG"," -B")),main = "Active Contrasts")  
  
#Lenth plot for both outputs  
LenthPlot(data1y1.lm, main = "Lenth's Plot")  
LenthPlot(data1y2.lm, main = "Lenth's Plot")
```

```
#####
#
# Design of experiments Box-Behnken
# 3 Factors, 3 Levels, 15 Runs
# Andrés Yarce Botero
#
# Libraries:      rsm
#
#####

# rsm packet upload
library(rsm)

# Factor level for each run for the factors per output THD
Gain=c(-1,1,-1,1,-1,1,-1,1,0,0,0,0,0,0,0)
OutLevel=c(-1,-1,1,1,0,0,0,0,-1,1,-1,1,0,0,0)
Comdecay=c(0,0,0,0,-1,-1,1,1,-1,-1,1,1,0,0,0)

# Factor level for each run for the factors per output fundamental
Volume=c(-1,1,-1,1,-1,1,-1,1,0,0,0,0,0,0,0)
Mixer=c(-1,-1,1,1,0,0,0,0,-1,1,-1,1,0,0,0)
Comdecay=c(0,0,0,0,-1,-1,1,1,-1,-1,1,1,0,0,0)

#Output values for the THD and fundamental
THD=c(34.25,45.92,41.2,50.2,37.77,31.48,76.55,91.04,17.7,29.17,78.23,86.65,51.24,49.3,53.51)
summary(THD)
Fundamental=c(-65,-64,-65,-63,-72,-71,-61,-62,-72,-73,-62,-61,-65,-65,-66)
summary(Fundamental)

# Generate and print the data1
data1=data.frame(Gain,OutLevel,Comdecay,THD)
print(data1)
data2=data.frame(Volume, Mixer,Comdecay,Fundamental)
print(data2)

# Second order regrestion for the THD
Data1.lm<-rsm(THD~SO(Gain,OutLevel,Comdecay))
summary(Data1.lm)

# Second order regrestion for the Fundamental
Data2.lm<-rsm(Fundamental~SO(Volume,Mixer,comdecay))
summary(Data2.lm)

# Parity graphics
par(mfrow=c(1,2))
plot(THD,fitted(Data1.lm))
abline(a=0,b=1)
title("Parity")
plot(Fundamental,fitted(Data2.lm))
abline(a=0,b=1)
title("Parity")

# Residual análisis
par(mfrow=c(1,2))
plot(fitted(Data1.lm),residuals(Data1.lm))
title("Residuals")
plot(fitted(Data2.lm),residuals(Data2.lm))
title("Residuals")

# Contour plots
par(mfrow = c(1, 3))
contour (Data1.lm, ~ Gain + OutLevel + comdecay)
contour (Data1.lm, ~
title("Contour")

# Superficie de respuesta
par(mfrow = c(1, 3))
persp (Data1.lm, ~ Gain + OutLevel + comdecay, col = rainbow(50), contours = "colors")
par(mfrow = c(1, 3))
persp (Data2.lm, ~ Volume + Mixer + comdecay, col = rainbow(50), contours = "colors")
```

Figure 7.2: R Code for the Box Behnken Design

```
summary(THD)
  Min. 1st Qu.  Median    Mean 3rd Qu.    Max.
17.70  36.01  49.30  51.61  65.03  91.04

Call:
rsm(formula = THD ~ SO(Gain, OutLevel, Comdecay))

            Estimate Std. Error t value Pr(>|t|)
(Intercept)    51.3500     2.3952  21.4386 4.095e-06 ***
Gain            3.6088     1.4668   2.4603  0.05720 .
OutLevel        3.8900     1.4668   2.6521  0.04531 *
Comdecay       27.0437     1.4668  18.4377 8.633e-06 ***
Gain:OutLevel   -0.6675     2.0743  -0.3218  0.76063
Gain:Comdecay    5.1950     2.0743   2.5044  0.05420 .
OutLevel:Comdecay -0.7625     2.0743  -0.3676  0.72823
Gain^2          -1.0925     2.1590  -0.5060  0.63436
OutLevel^2      -7.3650     2.1590  -3.4113  0.01902 *
Comdecay^2       8.9525     2.1590   4.1466  0.00894 **
---
Signif. codes:  0 '***' 0.001 '**' 0.01 '*' 0.05 '.' 0.1 ' ' 1
```

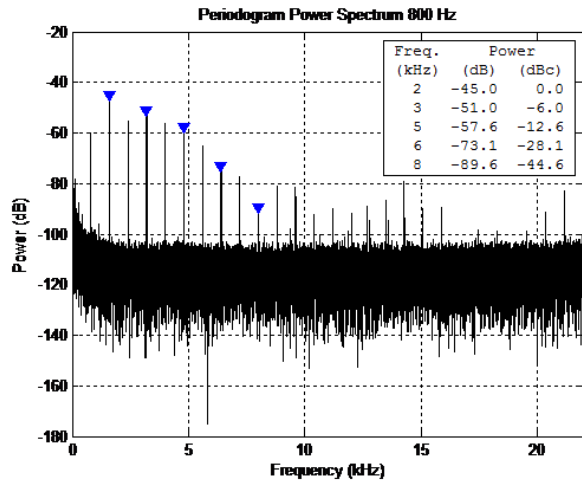
Figure 7.3: Box Behnken THD response Summary R

```
summary(Fundamental)
  Min. 1st Qu.  Median    Mean 3rd Qu.    Max.
-73.0  -68.5  -65.0  -65.8  -62.5  -61.0

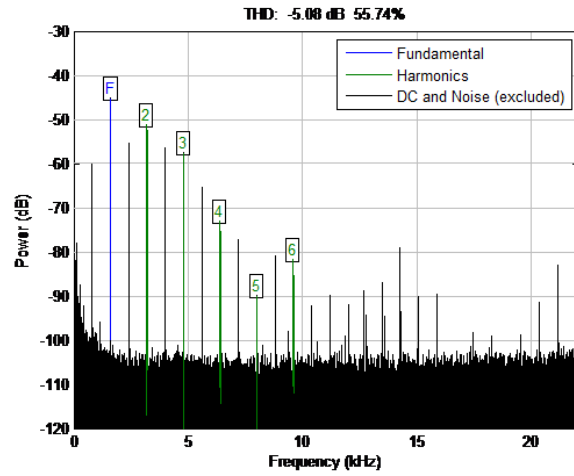
Call:
rsm(formula = Fundamental ~ SO(Volume, Mixer, Comdecay))

            Estimate Std. Error t value Pr(>|t|)
(Intercept)  -65.33333    0.40139 -162.7691 1.661e-10 ***
Volume         0.37500    0.24580   1.5256  0.187618
Mixer          0.12500    0.24580   0.5085  0.632707
Comdecay       5.25000    0.24580  21.3590 4.171e-06 ***
Volume:Mixer    0.25000    0.34761   0.7192  0.504221
Volume:Comdecay -0.50000    0.34761  -1.4384  0.209845
Mixer:Comdecay  0.50000    0.34761   1.4384  0.209845
Volume^2        0.79167    0.36180   2.1881  0.080288 .
Mixer^2         0.29167    0.36180   0.8061  0.456773
Comdecay^2     -1.95833    0.36180  -5.4127  0.002912 **
---
Signif. codes:  0 '***' 0.001 '**' 0.01 '*' 0.05 '.' 0.1 ' ' 1
```

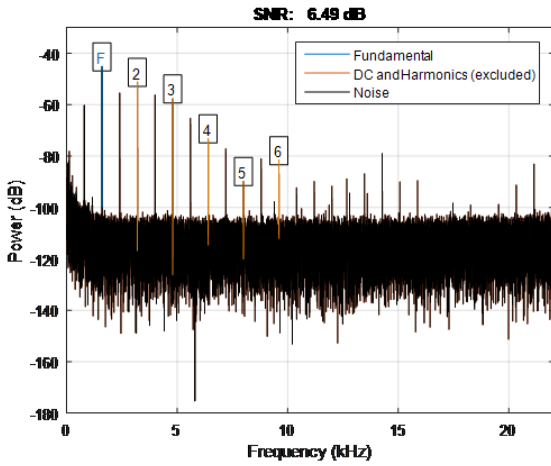
Figure 7.4: Box Behnken Fundamental response Summary R



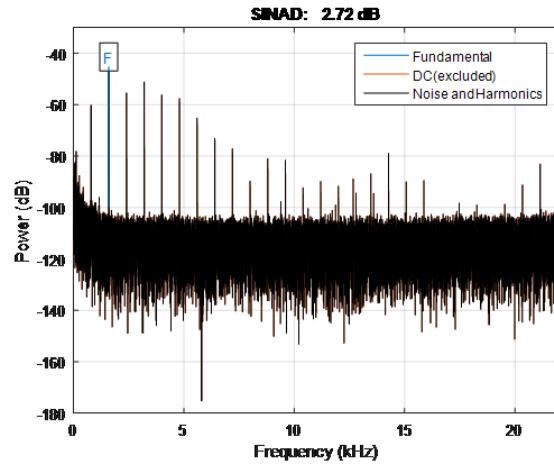
(a)



(b)

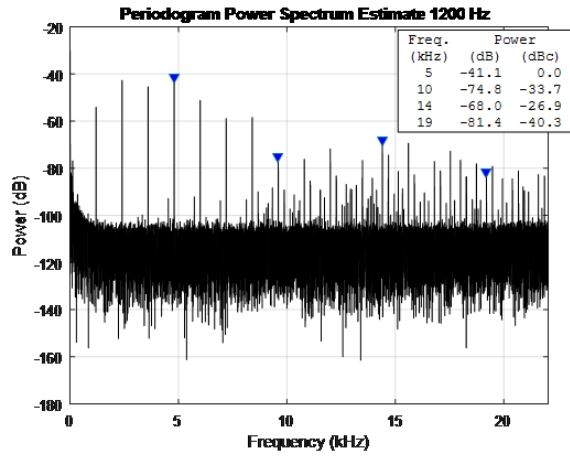


(c)

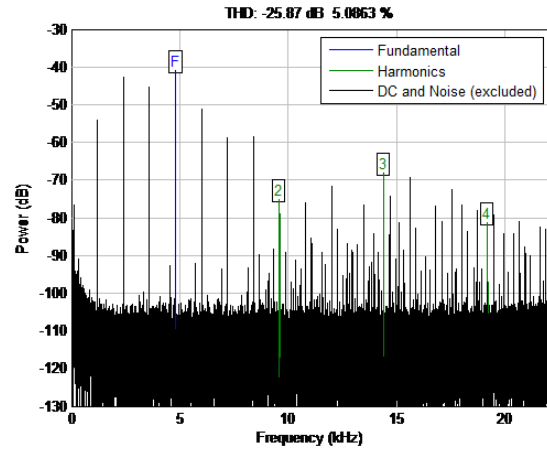


(d)

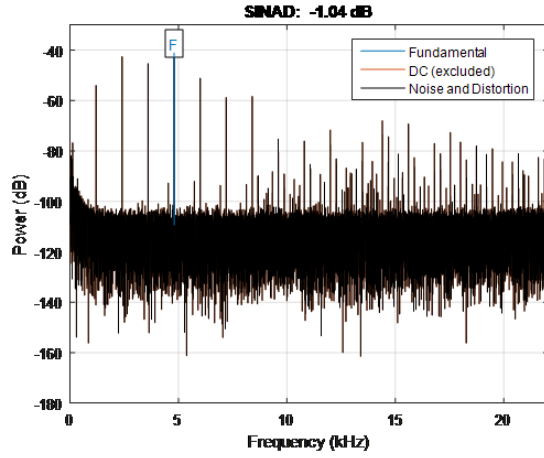
Figure 7.5: Harmonic Distortion 800 Hz signal self-demodulation analysis



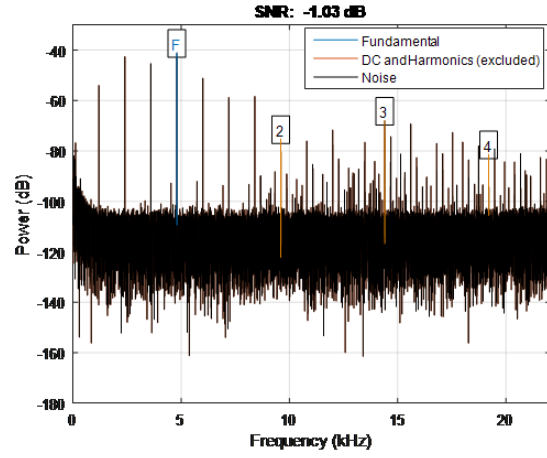
(a)



(b)

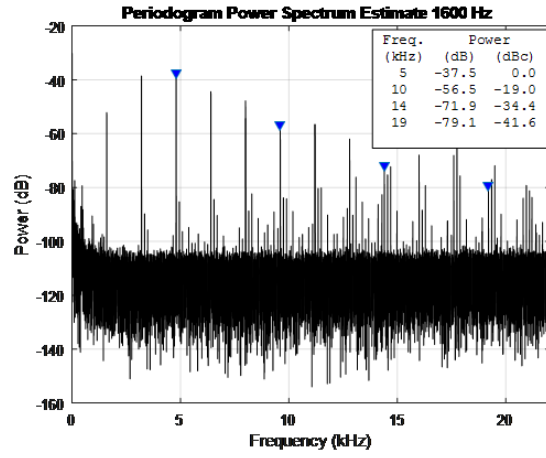


(c)

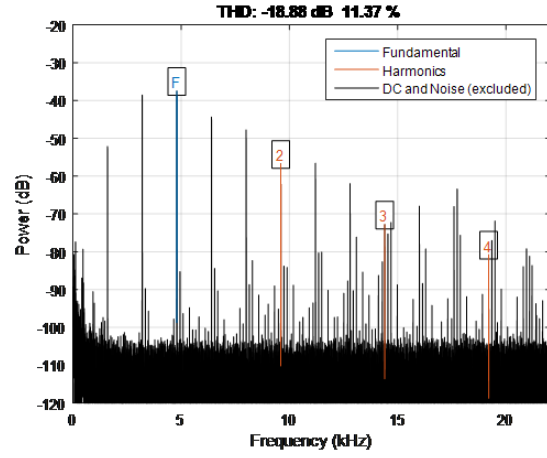


(d)

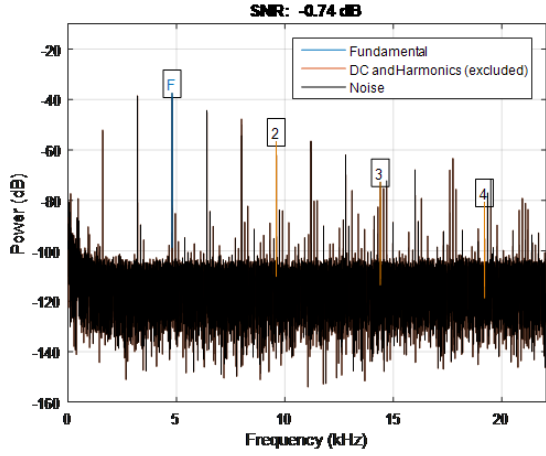
Figure 7.6: Harmonic Distortion 1200 signal Hz self-demodulation analysis



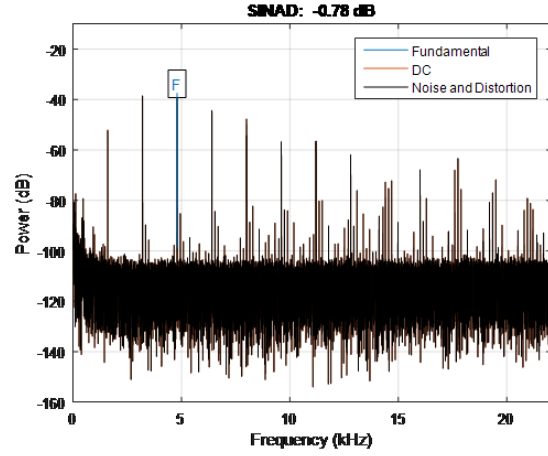
(a)



(b)

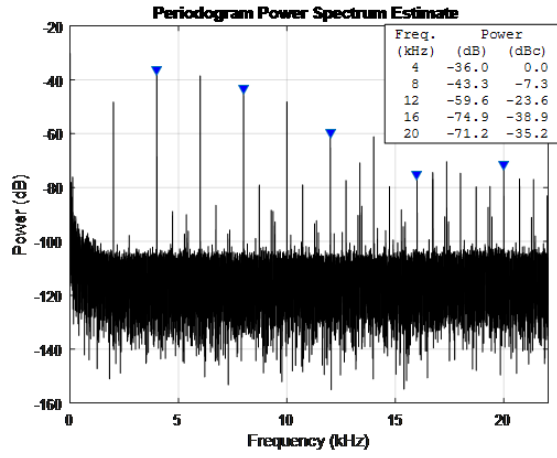


(c)

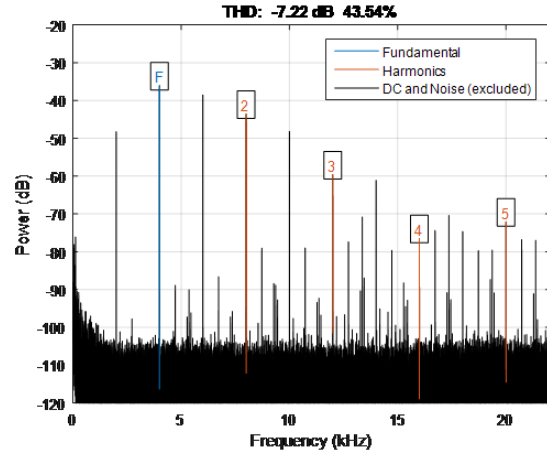


(d)

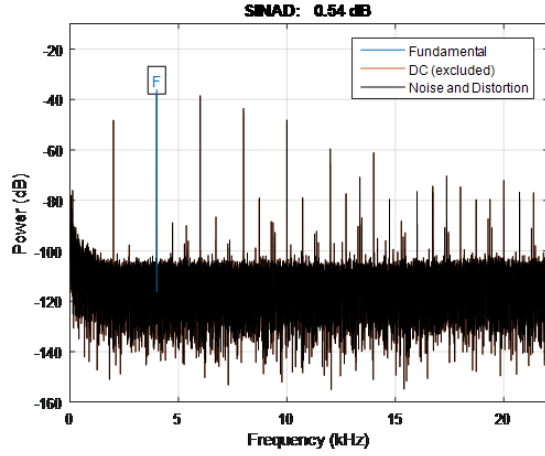
Figure 7.7: Harmonic Distortion 1600 Hz signal self-demodulation analysis



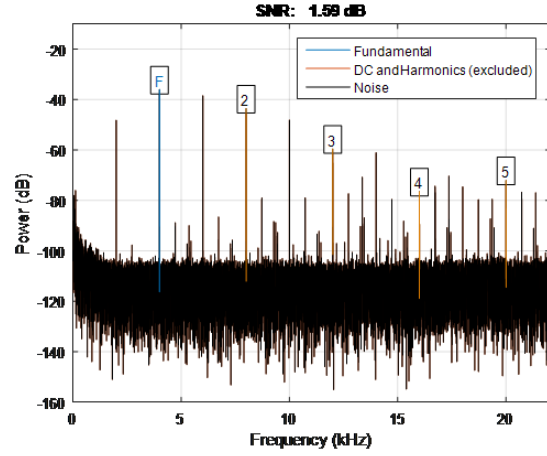
(a)



(b)

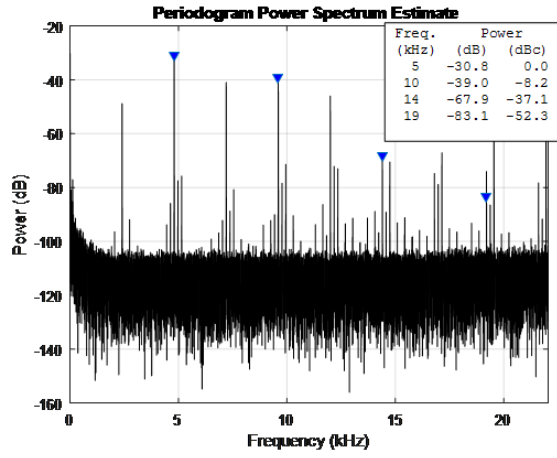


(c)

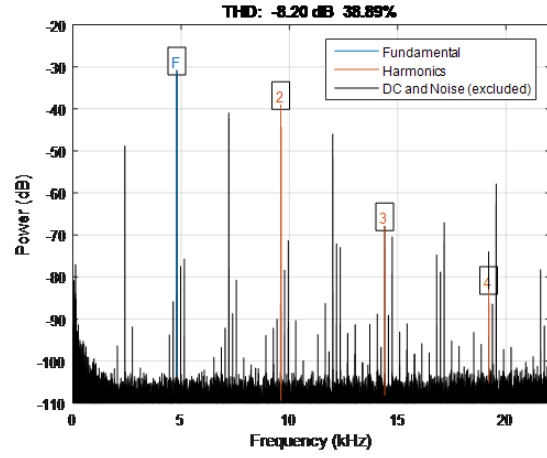


(d)

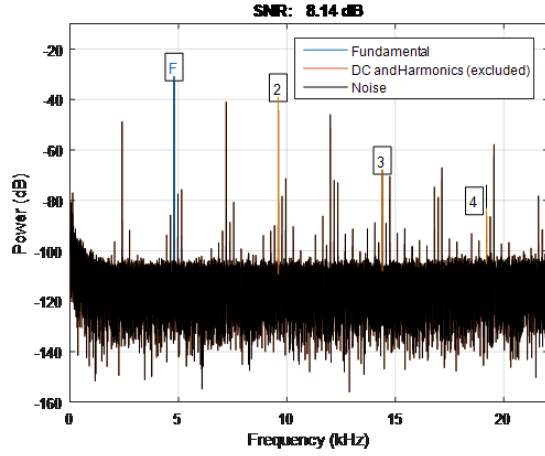
Figure 7.8: Harmonic Distortion 2000 Hz signal self-demodulation analysis



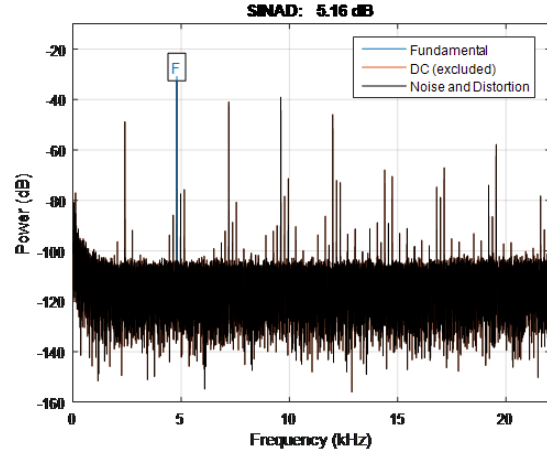
(a)



(b)

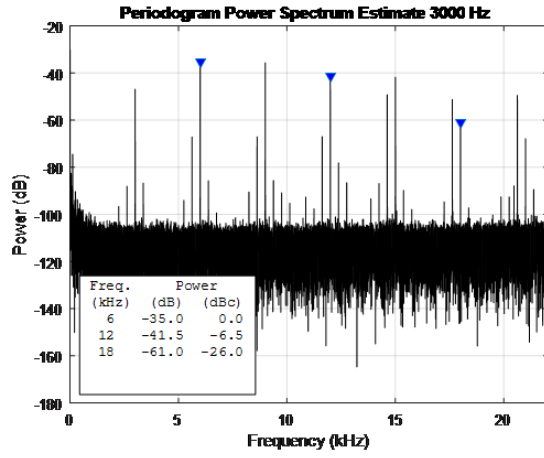


(c)

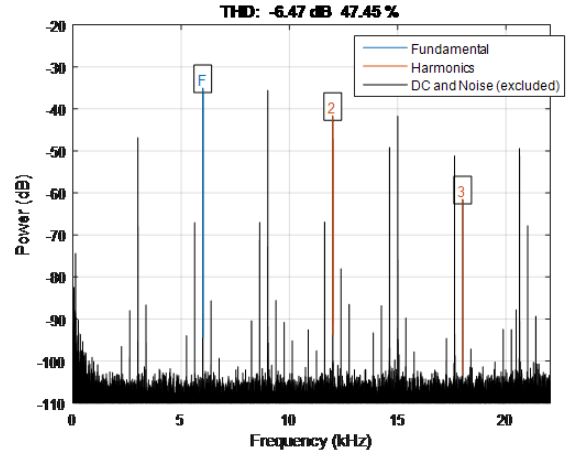


(d)

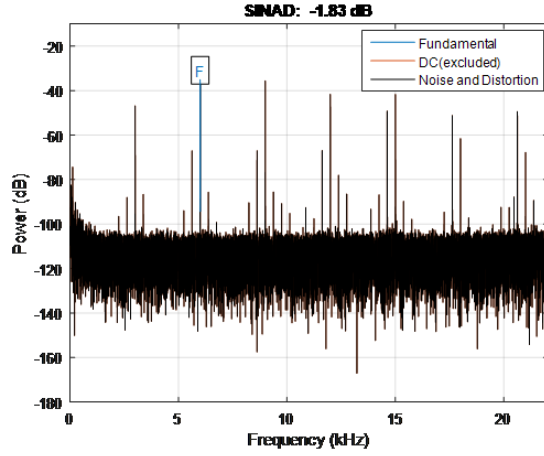
Figure 7.9: Harmonic Distortion 2400 Hz signal self-demodulation analysis



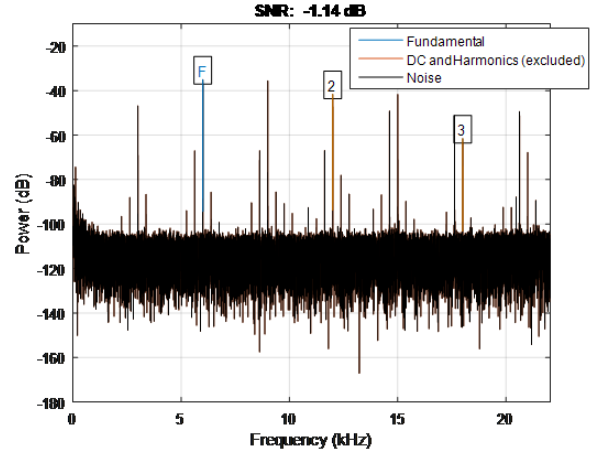
(a)



(b)

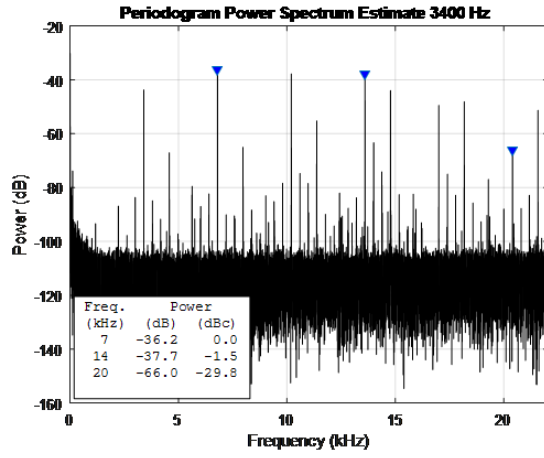


(c)

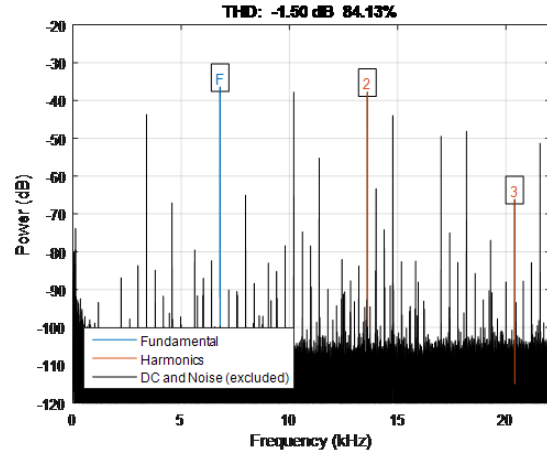


(d)

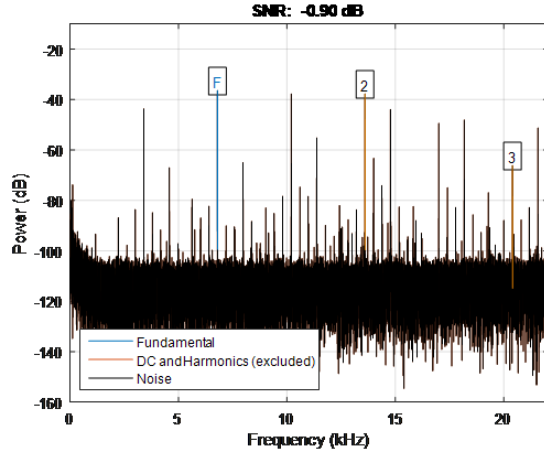
Figure 7.10: Harmonic 3000 Hz Distortion Analysis



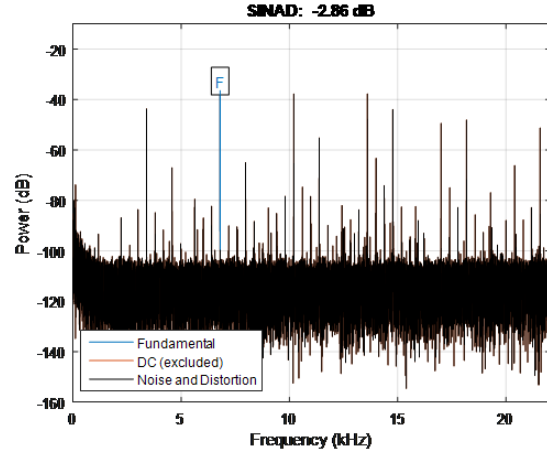
(a)



(b)



(c)



(d)

Figure 7.11: Harmonic 3400 Hz Distortion Analysis